Title
Synthesis of glycopolymers for biomedical applications

Permalink
https://escholarship.org/uc/item/85w3s3xx

Author
Lin, Kenneth

Publication Date
2013

Peer reviewed|Thesis/dissertation

University of California

Los Angeles

Synthesis of glycopolymers
for biomedical applications

A dissertation submitted in partial satisfaction

of the requirements for the degree

Doctor of Philosophy in Biomedical Engineering

by

Kenneth Lin

2013

ABSTRACT OF THE DISSERTATION

Synthesis of glycopolymers for biomedical applications

by

Kenneth Lin

Doctor of Philosophy in Biomedical Engineering

University of California, Los Angeles, 2013

Professor Andrea M Kasko, Chair

Glycopolymers are synthetic analogues of natural polysaccharides that connect saccharides through a synthetic backbone rather than through glycosidic bonds. Current glycopolymerization techniques can be used to create large quantities of material with good control over the saccharide identity and chain length of the polymer, which has allowed structure-property studies of glycopolymer binding with lectins. These studies have shown that structures with longer chain length exhibit greater binding with lectins. However, these studies have not fully addressed the effects of branching or spatial orientation on lectin binding.

Branching architecture affects the biological and physical properties of polysaccharides. Similarly, branching should also affect how glycopolymers interact with their target lectins, yet few reports of branched glycopolymers have been reported. Additionally, there have been no studies on the effect of placing saccharide residues in the polymer backbone and at the branch point. To address this limitation in current synthetic techniques, polymers with branching architecture that incorporate saccharide at the branch point have been synthesized via atom transfer radical polymerization of a saccharide (either mannose or galactose) inimer and mannose monomer. Branching architecture was confirmed through GPC_{PMMA}, GPC_{LS}, and mass spectrometry. These branched glycopolymers more fully recapitulate natural branched polysaccharide structures and were found to interact

more strongly than linear glycopolymers with mannose binding lectin (MBL), an immune complement protein. Most significantly, mannose at the branch point increases the polymer's interaction with MBL compared to similar structures with galactose or no saccharide content at the branch point.

In addition to polysaccharides found throughout living systems, proteins are often post-translationally modified with polysaccharide chains to create glycoproteins. We hypothesized that mimicking the 3D spatial orientation of these glycans through polymerization of glycomonomers from a protein macroinitiator can result in different binding properties of the resulting conjugate. Bovine serum albumin was modified to present multiple initiator groups which initiated the polymerization of mannose and galactose monomers via atom transfer radical polymerization. MBL interaction increases with the number and density of mannose residues attached to the protein. 3D presentation of multiple polymer chains from a protein significantly enhances lectin interaction than compared to linear glycopolymer chains with the same number of mannoses but without 3D presentation.

Structure-property studies have also been hampered by the inherently different distributions in molecular weight between different glycopolymer samples. Post-polymerization modification of pyridyl disulfide polymers with thioglycosides was demonstrated as a route towards creating glycopolymers with pendant glycosides and uniform underlying architecture and polymer chain distribution. These polymers were used to study the effect of glycopolymers on fibroblast adhesion.

We have described synthetic techniques for creating biomimetic glycopolymers that narrow the gap between synthetic structures and natural polysaccharides while still maintaining the high throughput advantage of glycopolymerizations. The structure-property studies have shown how subtle changes in polymer branching architecture and 3D spatial orientation can lead to dramatic enhancements of lectin binding, and can be applied to improved designs of glycomimetic drugs.

The dissertation of Kenneth Lin is approved.

Linda G Baum

Timothy J Deming

Amy Catherine Rowat

Andrea M Kasko, Committee Chair

University of California, Los Angeles

2013

To my parents,

who made sure my bookshelves were always full.

List of Figures

xii

List of Schemes

ACKNOWLEDGMENTS

This dissertation could not have been possible without support from many people in the form of baked goods and words of encouragement and advice.

First, many thanks to my advisor, Professor Andrea Kasko, for her guidance and support through all these years. I have grown extraordinarily as a scientist during my time in the lab and much of that is to her credit.

Thanks to past and present members of the Kasko research group. I've spent way too many hours with you all, but graduate school wouldn't have been anywhere as rewarding without such a talented and friendly group. Special thanks to: Dr. Donald Griffin, my fellow lab warrior, for the company as we fought our battles in the lab. Dr. Darice Wong for keeping all of us sane with her sage advice. Helena Chia for the SEAS runs. Walter Liau for continuing on the sweet side of the lab. Lindsey Sharpe and Jocelyn Bailey, two very capable undergraduates who worked on the galactose hydrogel project described in Chapter 6.

I would also like to thank our collaborators at the Pugh and Wesdemiotis labs at the University of Akron: Cesar Lopez Gonzalez for hosting me and sharing his experience on the other side of this project, Bill Storms for assistance with light scattering, and Lydia Cool and Xiumin Liu for their work with the mass spectrometry of the glycopolymers. I am also grateful for support from the NIH Biotechnology Predoctoral Research Training Program. Chapter 3 is adapted with permission from *Biomacromolecules*, 2013 14 (2), 350-357.

I would be remiss if I did not acknowledge the mentorship I had through the other stages of my education. I was introduced to research by Professor Hai-Quan Mao who was my advisor through my undergraduate and master's years. The knowledge I gained from working with Dr. Xingyu Liu helped me tremendously with the biological experiments of this thesis. Dr. Joyce Lin was a great sounding board as we each made our way through graduate school.

Finally, I am forever indebted to my family for their love and support. My brother, Ben, who has always watched out for his younger brother. My parents, Yen and Su-In, for instilling a love for learning from the beginning.

It has been a great privilege to spend these past several years in the presence of such compassionate people. Thank you.

VITA

2006   B.S. (Materials Science and Engineering)

             Johns Hopkins University.

2007   M.S. (Materials Science and Engineering)

             Johns Hopkins University.

2008-2010   Teaching Assistant (Department of Bioengineering)

             University of California, Los Angeles.

PUBLICATIONS

Kenneth Lin, Kian-Ngiap Chua, Gregory T. Christopherson, Shawn Lim, Hai-Quan Mao. Reducing electrospun nanofiber diameter and variability using cationic amphiphiles. *Polymer*, 2007 48 (21) 6384-6394.

Kenneth Lin and Andrea M. Kasko. Effect of Branching Density on Avidity of Hyperbranched Glycomimetics for Mannose Binding Lectin. *Biomacromolecules*, 2013 14 (2), 350-357

CHAPTER 1

Introduction

1.1   Why glycopolymers?

Glycopolymers are mimics of polysaccharides that connect saccharides through a synthetic backbone rather than through glycosidic bonds. These polymers have been studied for applications ranging from bacterial detection and filtration to tissue engineering to viral inhibition. Their biological function is derived from their biomimicry of natural polysaccharides to promote lectin-saccharide binding.

Synthetic techniques for creating exact replicas of polysaccharides from individual monosaccharides exist, as do techniques for creating mimetics such as glycoclusters or glycodendrimers. However, all of these compounds suffer from drawbacks. Synthetic polysaccharides are notoriously difficult to produce with defined structures due to the chemical similarity of each of the saccharide hydroxyls, and therefore require laborious protection-deprotection chemistry. Techniques such as automated solid phase synthesis and fluorous chemistry have advanced the field, but most syntheses are still limited in their throughput. While these methods produce very well-defined oligosaccharides, relatively short chain lengths are synthesized and small amounts of product are obtained. Other mimetics such as glycoclusters may be relatively easy to synthesize, but depending on the application, may lack the necessary valency to trigger much biological interaction. Glycodendrimers can display a high number of saccharides but require significant purification between each successive generation of dendrimer.

In contrast, glycopolymers are more readily synthesized in large quantities and at higher molecular weight. Some of the first glycopolymers reported were synthesized through post-polymerization modification of an existing polymer backbone with saccharide content. Polymerization of glycomonomers have been reported through many traditional techniques, including ring-opening, cationic, anionic, and radical polymerizations. Many of these techniques allow for good control over the saccharide identity and polymer chain length, which is crucial for structure-property studies.

1.2   Unanswered questions

While a great deal of progress has been made in glycopolymerization, there are still some synthetic shortcomings. Branching has clear effects on the biological and physical properties of polysaccharides and branching most likely also heavily influences the properties of glycopolymers, yet few reports of branched glycopolymers exist in literature.[1–4] Furthermore, no techniques exist to produce branched glycopolymers that contain saccharide residues in the polymer backbone and at the branch point.

In addition to polysaccharides found throughout living systems, proteins are often post-translationally modified with polysaccharide chains to create glycoproteins. Synthetic methods for biomimetics that resemble natural glycoproteins can have many important tissue engineering and immunotherapy applications. Several examples of synthetic protein-glycopolymer conjugates have been described,[5–8] but all were synthesized through a method called "grafting-to". In this method, a glycopolymer is first synthesized, and then attached to a protein. An alternative method, "grafting-from", polymerizes monomers directly from a protein macroinitiator to result in the final protein-glycopolymer conjugate. Each method has its benefits and drawbacks, but no examples of protein-glycopolymers synthesized

through a grafting-from process have been reported. These protein-glycopolymers would distribute polymer chains in a 3D orientation around the protein, which could result in different binding properties.

Structure-property relationships of glycopolymers and their interaction with lectins have been examined previously.[9] However, the effect of branching or 3D spatial presentation of the glycoresidues has not been addressed because synthetic techniques to systematically vary these properties have not been developed.

1.3   Dissertation focus

Overview

The aim of this dissertation is to develop synthetic techniques that narrow the gap between natural polysaccharides and synthetic glycopolymers and examine structure-property relationships between glycopolymers and their protein binding partners. Previous research has thoroughly examined the roles of chain length and saccharide composition, but little research has been conducted on the effects of architecture or spatial orientation. While many glycopolymers have been reported, few have branched architecture and none contain saccharide at the branch point, a property key to truly mimicking natural polysaccharides. Additionally, proteins are often decorated with polysaccharide chains, but few examples of synthetic protein-glycopolymer conjugates exist that allow for the study of multiple chains in a 3D orientation. Finally, structure-property studies of protein-glycopolymer interactions are frustrated by limitations in polymerization techniques that result in batch to batch variability between samples.

Therefore, the specific focus of this dissertation is to develop new techniques to address these synthetic shortcomings and use the resulting glycopolymers to establish more structure-property relationships between glycopolymers and lectins. This focus builds towards our long term goal of using glycopolymers for urgent biomedical problems.

Significance

This dissertation demonstrates synthetic techniques for creating more biomimetic glycan structures. These glycomimetics can be used towards further elucidating polymer structural designs for improved saccharide binding with lectins. The research provides evidence towards the remarkable enhancement of protein binding due to glycopolymer branching architecture and 3D presentation. These results can influence the design principles for glycomimetic drugs that could be used for various biomedical applications.

Outline of chapters

Chapter 2 of this dissertation provides a broad overview of glycopolymer synthesis and applications, particularly for immune modulation. Chapters 3 through 5 describe new techniques that address the limitations of current glycopolymerizations: Chapter 3 details the synthesis of hyperbranched glycopolymers containing saccharide component at the branch point, Chapter 4 details the synthesis of protein-glycopolymer conjugates, and Chapter 5 details the synthesis of branched glycopolymers through post-polymerization modification of pendant pyridyl disulfides with thioglycosides. Chapter 6 examines the biological interactions of the glycopolymers (from Chapters 3 and 4) with mannose binding lectin, a key protein of immune complement, and the ability of glycopolymers (from Chapter 5) to inhibit fibroblast adhesion. Finally, Chapter 7 summarizes the research conclusions and presents possible future directions in the glycopolymer field.

CHAPTER 2

Background

Polysaccharides are polymers with saccharide repeat units connected through glycosidic bonds. As one of the three classes of biopolymers (the others being DNA/RNA and proteins), they make up much of the living world, from our joints and cartilage (hyaluronic acid) to the plant matter we eat and wear (grain as starch and cotton as cellulose). Natural polysaccharides have been adapted for various applications beyond just food and clothing. For example, starches are used to increase the viscosity of liquid solutions without substantially affecting other properties. The pharmaceutical industry uses polysaccharides to package medicine inside capsules as an alternative to gelatin for users with dietary restrictions.

Therapeutic uses of polysaccharides are also widespread. For example heparin (extracted from pig intestine) is used as an anti-coagulant drug, and hyaluronic acid (extracted from rooster combs, animal cartilage, and vitreous humour, or through microbial production by *Streptococcus*) is used as an injectable filler to temporarily remove wrinkles. These polysaccharides are typically obtained from natural sources and suffer from the inherent drawbacks of natural products including batch to batch variability or sourcing limitations. Even more important than the lack of consistency in product quality is the risk of contamination from livestock or the preparation process leading to adverse reactions. In a drastic example, a contamination of heparin with oversulfated chondroitin sulfate in 2008 led to over 200 deaths worldwide and a recall of heparin batches by Baxter.[10] This contamination, combined with the other drawbacks of animal derived products,

highlights the need for synthetic alternatives to replace or even improve on natural polysaccharides.

These synthetic alternatives can be split into two categories: synthetic polysaccharides which connect sugar units through glycosidic bonds, and glycomimetics which connect sugar units together through a synthetic backbone.

2.1 Synthetic polysaccharides

Polysaccharide synthesis involves the repeated formations of glycosidic bonds between the anomeric carbon of one sugar (a glycosyl donor), and a hydroxyl group of another sugar (a glycosyl acceptor). There are many challenges posed by this task: 1. the alcohol functional groups are relatively unreactive and require activation, 2. the chemical reactivities of sugar alcohols within a single ring are very similar so protection/deprotection chemistry is necessary to provide control over regioselectivity and connectivity, and 3. the biological properties of polysaccharides are influenced by the alpha/beta linkage so stereoselective control is required. Polysaccharide synthesis can be generally divided into either chemical or enzymatic routes.

2.1.1 Chemical synthesis

Chemical synthesis of polysaccharides typically relies on modifying the glycosyl donor with an anomeric leaving group for reaction with a nucleophile on a glycosyl acceptor. A balance in terms of reactivity of the leaving group is requred here: the group must be reactive enough to react with the acceptor nucleophile, while also not so reactive as to lose stereoselective control. Common anomeric leaving groups include halides, acetates, thioethers, and imidates. Promoters are also added to assist departure of the leaving group.

Regioselective glycosidic bond formation between desired sugars is controlled by the use of protecting groups. For example, a 1,4 glycosidic bond between the 4-OH of a glycosyl acceptor and the anomeric carbon of a glycosyl donor is assured by protecting every alcohol not participating in the reaction (Scheme 2.1). The choice of protecting groups often revolves around their selective removal in the presence of other protecting groups (orthogonality) so that multiple conjugation steps can occur to extend the oligosaccharide chain or introduce branching sites. Protecting groups can also influence the reactivity of the glycosyl acceptor by preventing self-glycosylation. In Scheme 2.1, the glycosyl acceptor only reacts with the glycosyl donor and not itself due to ester protecting groups that deactivate its own anomeric center. This concept, termed the armed/disarmed approach, is due to the electronic effects of different protecting groups with esters being more electron withdrawing than ethers and preventing stabilization of a reactive anomeric center.[11]
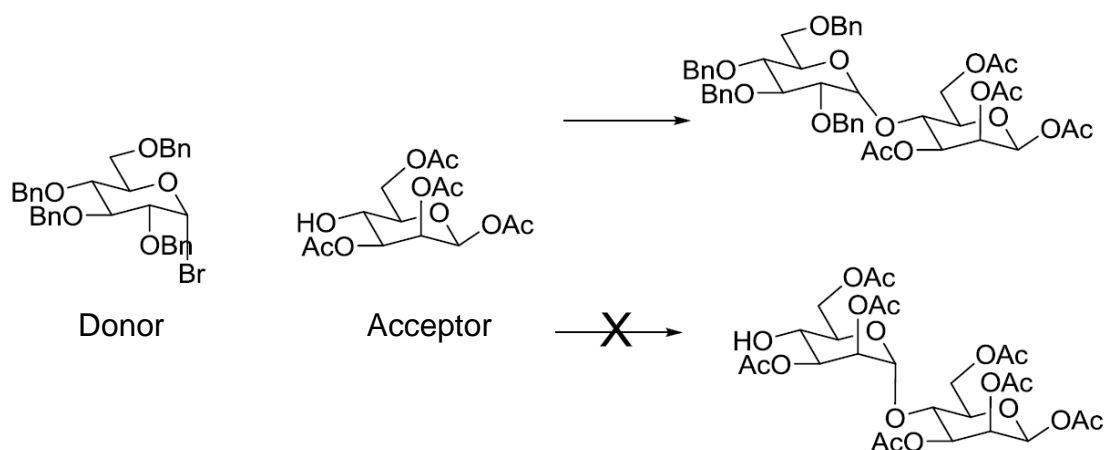
Scheme 2.1: 1,4 regioselectivity is assured by protecting all alcohols except the 4-OH of the glycosyl acceptor. The armed/disarmed approach is also demonstrated where the glycosyl acceptor does not self react due to the use of disarming acetate protecting groups.

Protecting groups are also necessary to control stereochemistry. For example, when reacting a glycoside donor containing an acetate protecting group at the 2-position, an intermediate is formed that blocks attack from the *cis* side so that only *trans* linkages are formed. As shown in Scheme 2.2, only β glucoside linkage is formed as the R-OH nucleophile can only attack from the β side. For mannosides and other sugars with similar 2- OH orientations, the steric situation is reversed and only α linkages form.
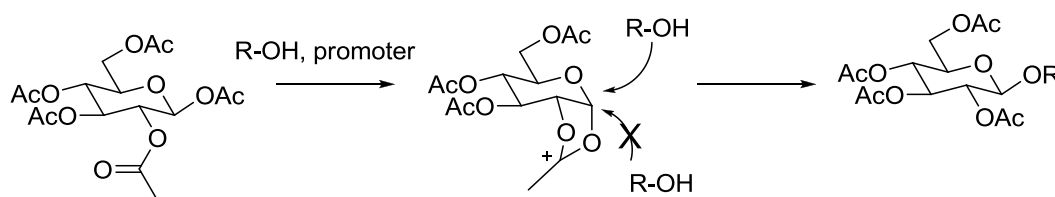
Scheme 2.2: β glucoside linkage of a glucoside is created through an acetoxonium ion intermediate which blocks attack from the α side, resulting in only formation of β linkage.

All these syntheses require a series of protection/deprotection steps for each addition resulting in a tedious and time consuming process. Some of these problems have been addressed by the development of methods that reduce the number of reaction steps and amount of purification required. For example, one pot syntheses of multiple saccharide linkages have been demonstrated where saccharides are protected, linked, and deprotected without workup between steps. In order to prevent the synthesis of undesired products in this one pot system, these syntheses use orthogonal activating groups and nucleophiles that react through different promoters. The armed/disarmed approach is also used so that the most active saccharides are fully consumed before the least active.[12,13]

Seeberger[14] has combined glycoside chemistry with solid phase synthesis (most commonly associated with peptide synthesis) in order to reduce the purification required. In solid phase peptide synthesis, a growing peptide chain attached to a solid support is reacted with an activated amino acid. Likewise, a glycosyl acceptor attached to a solid support is reacted with a glycosyl donor. Subsequent deprotection and washing steps remove excess reagent and byproducts, while the oligosaccharide chain remains on the solid support for further conjugation. When synthesis is complete, the completed chain can be cleaved from the solid support. This method has been used to synthesize long oligosaccharides (30mer)[15] and branched oligosaccharides through the use of orthogonal protecting groups.[16]

Other groups have used a similar concept to isolate the target polysaccharide through fluorous extraction chemistry.[17,18] In this method, fluoro-tagged sacharides are reacted as in typical glycosylation reactions but purified with modified silica that retains fluorous compounds. The desired saccharide is obtained by flushing the column with an eluting mobile solvent and removing the fluorous protecting group. This method's primary advantage over solid phase synthesis is the ability to conduct the reaction entirely in solution and only conducting the purification step on the solid support which leads to faster kinetics and lower quantities of reagents required.

2.1.2   Enzymatic synthesis

The enzymatic method relies on two classes of enzymes to drive the glycosylation: glycosyltransferases or glycosidases (both natural and engineered). Glycosyltransferases are natural proteins used in the biosynthesis of polysaccharides for transferring one phospho-sugar nucleotide donor to another sugar acceptor. Branched amylose has been made using potato phosphorylase to polymerize glucose-1-phosphate into linear amylose with branched points inserted with a glycogen branching enzyme.[19] The same process has also been repeated from a silicon

9

substrate to create an artificial glycocalyx.[20] However, these transferase enzymes and their sugar nucleotide substrates are difficult to obtain.

Glycosidases are more readily accessible but require more experimental determination of the appropriate reaction conditions. In nature, glycosidases catalyze the hydrolysis of glycosidic bonds, but glycosidic bond formation can occur with appropriate reaction conditions. The reaction can be biased towards glycosidic bond formation through either thermodynamic or kinetic control. Thermodynamic control of glycosidases to shift the equilibrium towards the glycoside has limited potential as the process can only generate oligosaccharides, typically with low yields.[21] Kinetic control uses an activated sugar donor to transfer the sugar rather than water, therefore preventing hydrolysis.[22] Yields from kinetic control of glycosidation remain low (10-40%) so glycosidases have been engineered to remove any hydrolase activity by mutating the protein sequence from the original amino acid sequence.[23] These engineered enzymes, or glycosynthases, were first reported by Withers[24] to make oligosaccharides without any hydrolysis. Further work to improve glycosynthases has applied the lessons of solid phase oligosaccharide synthesis by immobilizing the acceptor substrate in order to improve the reaction yield and efficiency.[25]

While both chemical and enzymatic methods have had much success creating well-defined oligosaccharides that can be used to elucidate the bioactivity of saccharide structures, they are not suitable for producing the significant amounts of polysaccharides that would be needed for therapeutic uses. Chemical synthesis methods are hindered by the protection and deprotection steps necessary after each coupling step, while enzymatic synthesis methods are hindered by limited availability and high cost of enzymes and substrates.

2.2 Glycomimetics

Glycomimetics are an alternative to polysaccharides that are significantly easier to synthesize in large quantities and at high molecular weight, while also preserving many of the same biological properties of polysaccharides. However, the ease of synthesis comes at the expense of losing the same structure of polysaccharides. Glycomimetics are multivalent structures of sugars connected through a synthetic backbone rather than the glycosidic bonds seen in oligo- and polysaccharides. These molecules can be as simple as clusters with saccharide groups off a short backbone[26] to more complicated structures based on dendrimers[27] to glycopolymers with a long synthetic backbone decorated with sugar groups (Figure 2.1).

Glycoclusters typically contain only 3 to 5 saccharides arranged around a synthetic scaffold. They derive their biological effect through crosslinking multiple lectins rather than spanning multiple binding sites on a single lectin as seen in larger compounds. However, when the latter type of behavior is required, small glycoclusters are not as capable as other structures with higher valency and larger size. Dendrimers are highly branched structures with perfect symmetry and polydispersity that can satisfy the valency and size requirements. Synthesis is performed in iterative steps, either convergently from the periphery or divergently from the core, with saccharides placed at the periphery of the molecules to form the glycodendrimer. Structures with as many as 128 saccharides from a fifth generation dendrimer have been reported.[28] Thorough reviews of the glycodendrimer field have been written where further information can be found.[29,30]

Although glycodendrimers have useful properties in the glycobiology field, their synthesis is plagued by the same limitations (protection/deprotection requirements, small yields) as synthetic polysaccharides. Glycopolymers, in comparison, are more easily synthesized while still offering a great deal of possible branching and valency. This background will focus on the various methods of synthesizing gly-

copolymers, particularly those polymers synthesized through atom transfer radical polymerization, while also attempting to provide an overview of the applications available with glycopolymers.

Glycocluster
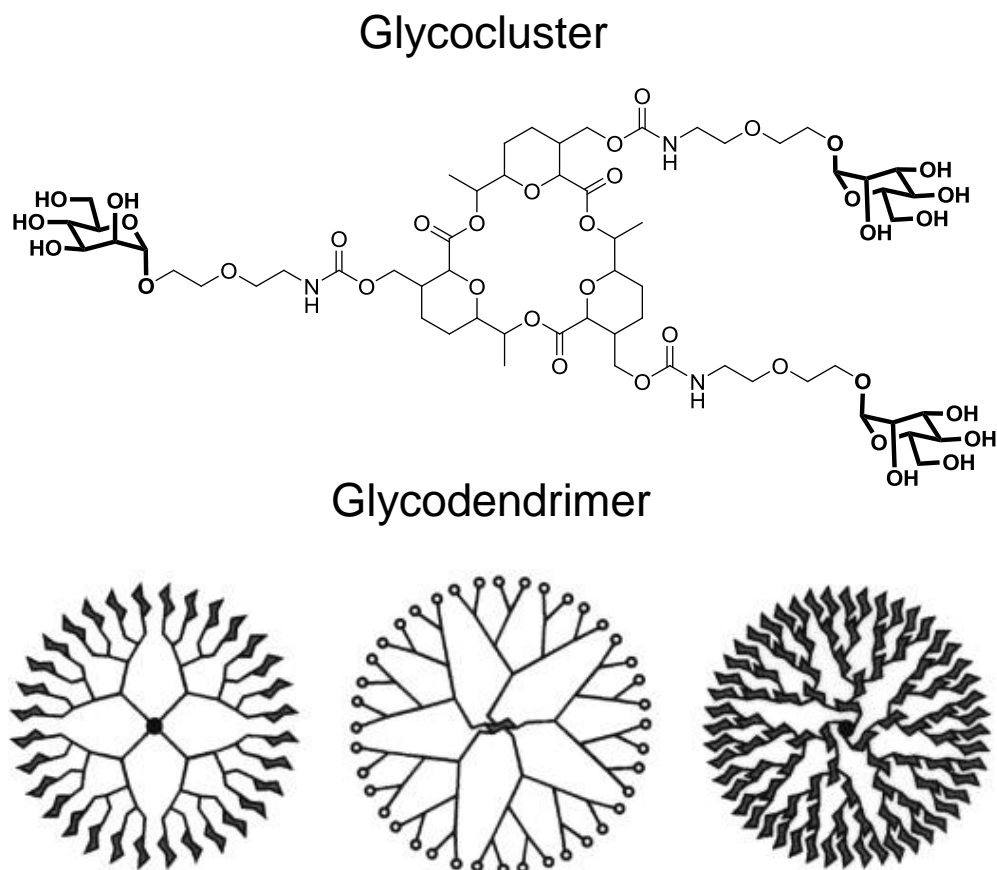
Glycodendrimer

Figure 2.1: Examples of glycocluster with trivalent mannoses[26] and glycodendrimers with exterior or interior saccharides, or composed entirely of saccharide.[29]

2.3 Glycopolymer synthesis

Glycopolymer synthesis can be split into two main branches as seen in Figure 2.2: (1) post-polymerization modification of an existing polymer backbone to bear pendant sugar groups and (2) direct polymerization of sugar monomers containing reactive groups. Both methods have their advantages and disadvantages. Post-polymerization modification allows for easier synthesis and characterization of the polymer backbone without the complicating issues related to side reactions or solubility of the saccharide unit. This method also allows for incorporation of compounds that may be incompatible with a polymerization process. However, it can be difficult to achieve full post-polymerization conjugation of the saccharide. Direct polymerization, on the other hand, does not require an extra conjugation step to add the saccharide component, but synthesis of the glycomonomer may be complicated and polymerization reaction conditions may also be limited.

2.3.1 Post-polymerization modification

Saccharides can be conjugated to a pre-made polymer backbone containing reactive functional groups. The Bertozzi group has formed oxime bonds between aminooxy-GalNac and pendant ketones from a polymer backbone with greater than 70% conjugation.[31] Less active functional groups can also be converted to more reactive intermediates prior to conjugation with a sugar. For example, hydroxyls on poly(vinyl alcohol) were converted to 4-nitrophenyl carbonates and quantitatively reacted with glucosamine.[32] Pendant carboxylic acids from a copolymer of N-isopropylacrylamide and acrylamido n-hexanoic acid were activated with EDC/NHS before reaction with glucosamine to result in a glycopolymer with 85% sugar conjugation.[33]

Post-polymerization modification
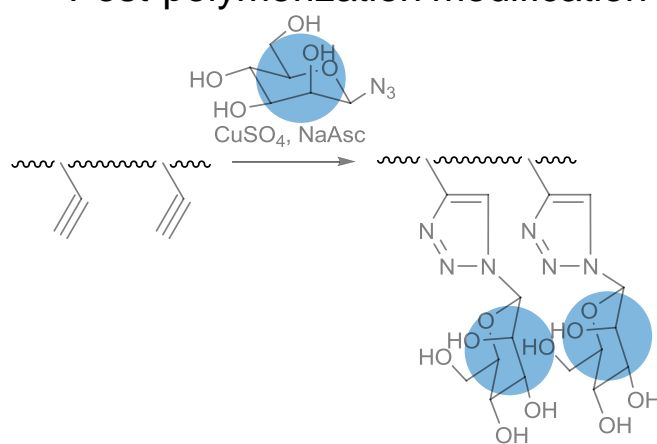
Direct polymerization
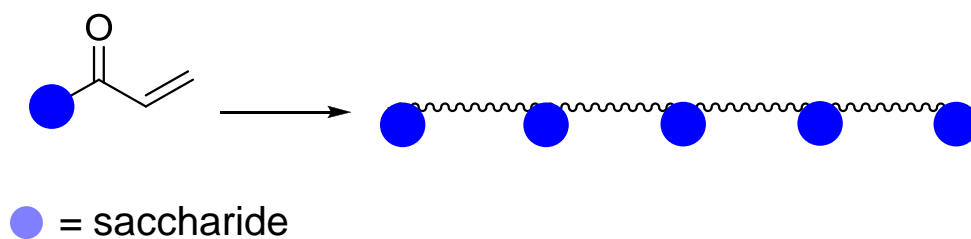
● = saccharide

Figure 2.2: Examples of glycopolymer synthesis: saccharide modification of a polymer backbone and direct polymerization of sugar monomers.

In another approach, click chemistry has been used to incorporate saccharides into a polymer backbone.[34,35] The most prominent method has been copper catalyzed azide-alkyne cycloaddition (CuAAC) where an azide functionalized sugar is reacted with alkynes pendant to the polymer backbone in the presence of a copper catalyst, typically with complete functionalization. The polymer backbone can incorporate alkyne functionality either through the polymerization of protected alkyne-containing monomers or post-polymerization modification of available functional groups with an alkyne. The alkyne-containing polymer reacts with azide-functionalized saccharides with high efficiency to yield a glycopolymer in which sugars are pendant to the backbone. The copper catalysis could be simply removed using alumina or dialysis.

Azide functionality is typically introduced to saccharides through nucleophilic substitution of a leaving group with an azide. At the anomeric position, this is most commonly accomplished by reacting a glycosyl halide with sodium azide at elevated temperatures, although the azide can also be generated directly from the peracetylated sugar as well.[36] Unprotected sugars have also been modified with the azide moiety by selectively activating the anomeric hydroxyl using 2-chloro-1,3-dimethylimidazolinium chloride.[37]

For primary alcohols, tosylation and subsequent reaction with an azide ion will create a primary azide. This method does not require prior protection of the secondary alcohols as tosylation is restricted to primary alcohols. The azide has also been introduced directly from the bare primary hydroxyl through a phosphonium salt intermediate.[38]

One interesting route towards a glycopolymer combines CuAAC and atom transfer radical polymerization for a one-pot reaction where both polymerization and click chemistry can occur due to their common reliance on Cu(I) species.[39] Propargyl methacrylate (alkyne), 2-azidoethyl mannopyranose (azide), an ATRP initiator, and a catalyst/ligand were combined and heated so that CuAAC and

ATRP occurred concurrently to form glycopolymers with PDI = 1.12-1.14. The rates of each of these two reactions could be varied by fine tuning the solvent and catalyst concentration. In most cases, 100% functionalization with saccharide was achieved. It is worthwhile to note that the inspiration for this concurrent one-pot process came from the ability to first polymerize an azide functionalized polymer through ATRP and subsequently perform the cycloaddition with an alkyne in one pot using the same catalyst.[40]

Traditional glycoside chemistry has also been used to conjugate an acetylated glucose to a copolymer of *N*-isopropylacrylamide and hydroxy ethylmethacrylamide. An alcohol off the polymer backbone acts as an acceptor of the glycosyl donor (pentaacetate glucose) with boron trifluoride etherate as activator. This method is a very simple route towards glycopolymer synthesis but results in glycopolymers that are not as well-defined due to incomplete reactivity of saccharides to the backbone with just 32% of possible sites conjugated with a sugar.[33]

Modification of polymer surfaces with glycopolymers has been accomplished photochemically. A poly(propylene) microporous membrane was grafted with sugar content after exposure to UV radiation in the presence of gluconamidoethyl methacrylate and a photoinitiator.[41] In another example, a photoreactive carbohydrate, azidophenyl lactamine, could be grafted onto poly(ethylene terephthalate) fibers without additional photoinitiator.[42] Upon UV exposure, the azidophenyl group converts to phenylnitrene and forms covalent bonds to the PET fibers to create a carbohydrate surface density of 3-67 nmol/cm^2 on the fiber surface.

2.3.2 Direct polymerization of glycomonomers

The glycopolymer field has expanded from the first example of direct polymerizations using uncontrolled free radical polymerization in 1985[43] to include nearly all other conventional polymerization techniques, including anionic and cationic

polymerizations, ring-opening polymerizations, and radical polymerizations. Well-defined glycopolymers have been synthesized via living radical polymerizations such as nitroxide-mediated polymerization (NMP), radical addition-fragmentation chain transfer polymerization (RAFT), and atom transfer radical polymerization (ATRP).[44–48] This background will focus chiefly on the ATRP of glycopolymers.

2.3.2.1 Atom transfer radical polymerization (ATRP)

Living polymerization are polymerizations where termination and transfer of the polymer chain do not occur. Many polymerization techniques, including ATRP, satisfy these two conditions by biasing the reaction equilibrium towards a high concentration of dormant species, and away from a low concentration of propagating chains so that chain-chain termination does not occur.

ATRP requires an initiator with a homolytically cleavable halogen, a vinyl monomer amenable to radical polymerization, and a ligated transition metal. Initiation of radical polymerization begins with the transfer of a halide atom from an initiator to a ligated transition metal compound (typically a copper halide salt), resulting in an active polymer chain that can reversibly deactivate with the metal-halide compound through another halide transfer or propagate with polymerizable monomers (Scheme 2.3). If initiation is fast and quantitative, all the chains will begin growing at the same time and grow for the same average time, producing polymer with characteristics such as defined molecular weights and narrow molecular weight distributions. When polymerization is complete, the polymer chains are capped with a halogen which allows for re-initiation with a comonomer to create a block copolymer, or conjugation to a compound through end group modification.

The mechanism of ATRP differs slightly when using protic solvents which are commonly used when polymerizing unprotected sugar monomers. Disproportionation of the Cu(I) complex into Cu(0) and Cu(II) occurs, along with hydrolysis of the polymer-halide or Cu(II)-halide complex. These mechanistic changes of ATRP in protic media result in faster polymerizations with potentially less control as the concentration of deactivator, Cu(II), is decreased. Polydispersities are generally higher in polymerizations with water due to loss of polymerization control.
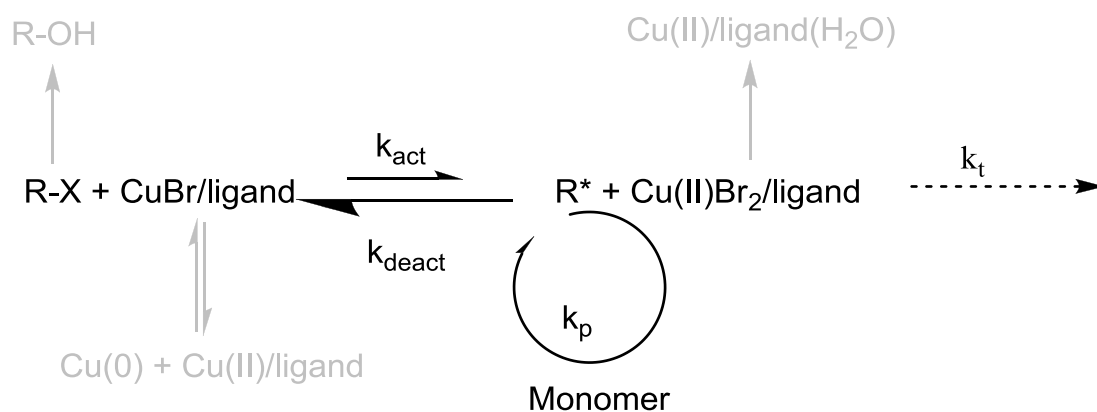
Scheme 2.3: Mechanism of atom transfer radical polymerization. The portion of scheme in grey occurs in protic solvents.

These limitations in aqueous ATRP have been addressed through the development of AGET-ATRP (Activators Generated by Electron Transfer-ATRP).[49] AGET-ATRP utilizes a redox reaction between Cu(II) and a reducing agent (e.g. tin 2-ethylhexanoate, ascorbic acid) to create Cu(I) and induce polymerization. This polymerization route offers greater control over traditional ATRP in aqueous media as it uses an oxidatively stable Cu(II)/ligand precursor to maintain the amount of deactivator throughout the polymerization.

Fukuda and coworkers reported the first ATRP of glycomonomers in 1998 with the homopolymerization of a methacrylated derivative of protected glucofuranose as well as copolymerization with styrene.[50] The first ATRP of unprotected glycomonomers was demonstrated by Narain and Armes in 2002.[51] However, the

glycomonomer used in this case, a ring opened methacrylated gluconolactone, did not present the sugar in its native cyclic form. The glycopolymer synthesized had increased PDIs as water content increased: PDI = 1.19 in methanol, 1.28 in 9:1 methanol/water, 1.48 in 6:4 methanol/water, and finally 1.82 in water. The polymerizations were believed to still be living in nature as chain extension polymerizations were successful. In order to avoid some of these problems of aqueous ATRP, AGET-ATRP of glycomonomers has been used, although primarily with surface initiated polymerizations.[52,53]

In comparison, RAFT polymerizations, which do not rely on redox cycles, are better controlled as water is inert to radicals. In one example, aqueous RAFT polymerizations of an unprotected methacrylated mannose had PDIs below 1.14.[54]

2.3.2.2 Initiators for glycopolymerizations

A wide range of initiators have been used for ATRP of glycopolymers. Functionalization of the initiator with moieties such as activated disulfides,[55] amino acids and peptides,[56] azides,[57] biotin,[58] and N-hydroxysuccinimidyl esters[59] allows for incorporation of these groups into the glycopolymer. Post-polymerization conjugation has been used to tether these glycopolymers with active initiator ends to biologically active compounds such as thiolated siRNA with the pyridyl disulfide[55] or viral coat proteins with the azide polymers.[57] Triblock ABA copolymers have also been synthesized by reacting the NHS ester initiated glycopolymers with aminated poly(ethylene glycol).[59]

Initiators tethered to a surface have also allowed for surface polymerizations of glycopolymers, as first demonstrated by Fukuda.[60] Surface polymerizations of glycomonomers from silsesquioxane nanoparticles[61] and titanium surfaces[62] have also been demonstrated.

2.3.2.3 Glycomonomers

Saccharide monomers for ATRP generally employ protecting groups over their hydroxyls for both ease of synthesis and solubility in organic solvents. These protection schemes have been educated by much of the glycochemistry described earlier in order to provide regio- and stereoselectivity of the saccharide modification. Isopropylidenes are commonly used many saccharides, as their use results in a solitary exposed hydroxyl which can then be conjugated with a polymerizable vinyl group.[63] For example, when galactose and acetone are stirred heterogeneously under acidic conditions, its 1,2 and 3,4 hydroxyls are protected by two isopropylidene groups while the primary 6 alcohol remains free (1,2;3,4 di-*O*-ispropylidene galactopyranose). Muthukrishnan noted that steric hindrance of the bulky isopropylidene-protected monomer may have led to the extremely slow polymerizations of a sugar acrylate,[1] although the slow rate was not seen with the more active methacrylate derivative.[2] Deprotection of the glycomonomer or glycopolymer under mild acidic conditions results in removal of the isopropylidenes while preserving the sugar's attachment to the vinyl group (glycomonomer) or polymer backbone (glycopolymer).

Acetate protection has also been used, mostly when using vinyl compounds that have been attached to the sugar at the anomeric position. Maynard and coworkers reacted a GlcNac derivative with trimethylsilyl trifluoromethanesulfonate to create an activated oxazoline anomeric carbon, which was then conjugated to 2-hydroxyethyl methacrylate in the presence of 10-camphorsulfonic acid.[58] Li et al. synthesized 2-(2',3',4',6'-tetra-*O*-acetyl-β-D-glucopyranosyloxy)ethyl acrylate through bromination at the anomeric position of a pentaacetate glucopyranose, followed by a Helferich reaction with hydroxyl ethyl acrylate in the presence of HgBr$_2$.[64] These cases have in common the activation of the anomeric position followed by conjugation of an alcohol with a promoter.

Basic deprotection conditions remove the acetates; however, the saccharide can be simultaneously cleaved from the polymer backbone. As an alternative to polymerizing protected monomers, controlled polymerization of sugar monomers with exposed hydroxyls has also been demonstrated, allowing for polymerizations in protic media. Narain and Armes demonstrated the first ATRP of unprotected glycopolymers using a ring-opened methacrylate derivative of gluconolactone.[51] The Maynard group deprotected glycomonomers of their acetate protecting groups using sodium methoxide while maintaining the acrylate ester and subsequently polymerized them in a mixture of methanol and water.[55] This method of synthesizing unprotected glycomonomers is not ideal as it results in a mixture of products (partial deprotection) that must be purified by column chromatography due to the similarity between acetate and acrylate esters. A more direct route to a polymerizable glycomonomer is through chemo-enzymatic synthesis.[65, 66] Stenzel used a *Candida antartica* lipase to transesterify completely unprotected mannose with vinyl methacrylate to result in a 6-*O*-methacryloyl mannose monomer.[54] However, the vinyl methacrylate is not commercially available, and the heterogeneous conditions required for monomer synthesis result in slow reaction rates.

2.3.3 Glycopolymer composition

Polymers synthesized from multiple types of monomers are known as copolymers (compared to homopolymers with just one type of monomer). Two common copolymer types are statistical copolymers where the monomer sequence is governed by the mole fraction of monomer and block copolymers where two or more homopolymers are linked covalently.

Copolymers of glycomonomers have been synthesized to create polymers with different saccharide arrangements. Co-glycopolymers are often statistical mixtures of two different saccharides. Kiessling synthesized statistical copolymers with varying ratios of mannose and galactose by controlling the feed ratio of

glycomonomers for ring-opening metathesis polymerization.[67] Haddleton used post-polymerization modification of pendant alkynes with azido mannoses or galactose to synthesize polymers with different ratios of mannose and galactose.[68] Multi-block co-glycopolymers with sequence control over the position of saccharides have also been synthesized by the same research group.[69] In the most extreme case, two equivalents of mannose or glucose monomers to initiator were added sequentially to create alternating $(mannose)_2$-$(glucose)_2$ units.

Amphiphilic block copolymers have also been synthesized with a hydrophobic block and hydrophilic saccharide block. These amphiphilic copolymers could self-assemble into glycomicelles and will have some degree of bioactivity and biocompatibility compared to traditional block copolymer micelles using a wholly synthetic component such as hydroxyethyl acrylate. This bioactivity could involve a targeting effect using, for example, hepatocyte's affinity for galactose. Copolymers of styrene and a glucose acrylate,[64] butyl acrylate and a glucosamine methacrylate,[70] caprolactone and a gluconolactone methacrylate,[71] as well as caprolactone and a galactose methacrylate[72] have been demonstrated. Some of these amphiphilic copolymers were shown to assemble into micelle structures that could interact with lectins.

2.3.4 Glycopolymer architecture

Polymer architecture describes different variations of the same underlying polymer structure (e.g. linear versus branched). Architecture has also been used to distinguish between macromolecules with fundamentally different linkages (e.g. clusters vs. dendrimers vs. polymers) but in this dissertation, architecture solely refers to the underlying polymer structure.

Most glycopolymers described are linear chains where the saccharide residue is pendant off of the backbone. Glycopolymers with different architectural shapes have been synthesized, including star,[61] cylindrical brushes,[73] and hyperbranched glycopolymers.[1,2] Examples of these structures can be found in Figure 2.3

Linear	Star	Brush	Hyperbranched
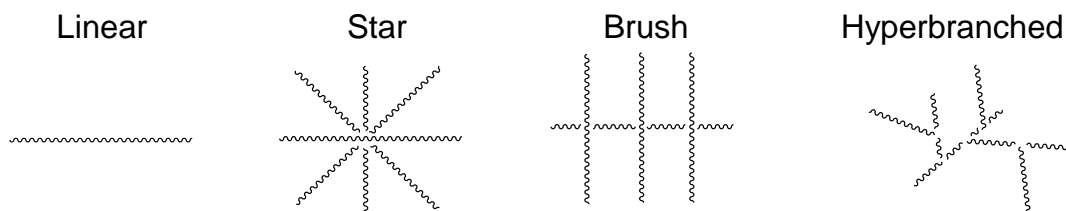
Figure 2.3: Idealized structures of linear, star, brush, and hyperbranched polymers.

The Müller group reported star glycopolymers synthesized from ATRP of methacrylated glucofuranose from a silsesquioxane nanoparticle based macroinitiator with 58 initiating sites.[61] Four armed star glycopolymers of gluconolactone methacrylate from a polypeptide macroinitiator have also been synthesized by another group.[74] This star-shaped co-glycopolymer interacted with lectins and self-assembled into micelles, leading to potential applications as a targeted drug delivery platform. Cylindrical glycobrushes were also made by the Müller group using a "grafting-from" approach[73] where methacrylated glucofuranoses were polymerized from a macroinitiator. Grafting efficiency was estimated between 20 and 40% through cleavage of the glycopolymer side chains. Transmission electron microscopy confirmed the architecture by showing long wormlike cylinders.

The Müller group has also reported the hyperbranched polymerizations of both acrylate[1] and methacrylate[2] sugar monomers by ATRP. Branching units were incorporated through the polymerization of an inimer, either 2-(2-bromopropionyloxy) ethyl acrylate or 2-(2-bromoisobutyryloxy) ethyl methacrylate. The inimer allowed for polymer growth from two active sites (either the vinyl group or the homolytically cleavable halogen), resulting in branching of the polymer. Hyperbranched glycopolymers have also been synthesized using RAFT. Perrier copolymerized

23

a protected alkyne acrylate with ethylene glycol dimethacrylate as a branching monomer. The glycopolymer was created following deprotection of the alkyne and post-polymerization modification with an azido saccharide.[3] Narain copolymerized glucose or lactose derived monomers with *N,N'*-methylenebis(acrylamide) as a branching agent.[4] These examples demonstrate the ability to synthesize glycopolymers with branched architectures, but all are lacking any saccharide content at the branch point.

2.4 Biomedical applications of glycopolymers

Glycopolymers have been studied for applications ranging from immune modulation to bacterial filtration to tissue engineering. Some of the work is highlighted in this section.

2.4.1 Immune

Glycopolymers have been used to modulate both innate and adaptive immunity through two general strategies: binding with immune system proteins to induce a desired response, or competitive binding to prevent infection or block undesired immune activity.

2.4.1.1 Innate immunity applications

Innate immunity is the branch of the immune system that defends against infection through a non-specific manner. It includes cells that release chemical factors or phagocytose unwanted particles and pathogens, as well as mechanisms such as inflammation, coagulation, and complement. Complement is a group of circulating blood proteins that, when activated, cause localized inflammation, recruitment of phagocytes, pathogen opsonization, and lysis of the target cell. When working with

24

implanted biomaterials or extracorporeal blood circuits, complement activation is an unwanted occurrence that leads to inflammation and poor patient prognoses. Materials used in these devices trigger the complement cascade (among other innate immunity reactions) through adsorption of plasma proteins (e.g. antibodies which lead to the classical pathway or C3 which lead to the alternative pathway). Polyethylene glycol and other polymers are often added to resist protein adsorption and thus shield against innate immunity reactions. Carbohydrates, due to their hydrophilicity and general biocompatibility, may also be a good material to resist complement activation. One group synthesized a glycopolymer of pendant ring-opened glucose and lactose derivatives that did not trigger blood coagulation, platelet activation or complement activation, but did cause some cytotoxicity.[4]

Complement activation can also be manipulated as a potential avenue for immunotherapy through the mannose binding lectin pathway. This pathway is activated by the binding of mannose binding lectin (MBL) to sugars such as mannose or *N*-acetylglucosamine commonly found on bacterial membranes.[75] Glycopolymers could serve as biomimetics of bacterial membrane polysaccharides and glycoproteins that can activate complement. The Haddleton group synthesized bovine serum albumin-mannose glycopolymer conjugates via post-polymerization modification of the saccharide component to a polymer backbone, followed by coupling of the glycopolymer to the protein. This protein-polymer bound MBL and resulted in deposition of complement protein C9.[5]

Like complement, macrophages are also sensitive to mannose through the macrophage mannose receptor. This receptor is an attractive target for specifically targeting and delivering a therapeutic through a glycopolymer-drug conjugate. To demonstrate this, mannose, *N*-acetylglucosamine, or galactose derivatives were copolymerized through RAFT with pyridyl disulfide containing monomers.[76] The glycopolymers with mannose or *N*-acetylglucosamine had increased macrophage uptake *in vitro* and *in vivo* compared to galactose containing glycopolymers.

2.4.1.2 Adaptive immunity applications

Adaptive immunity, in contrast to innate immunity, provides specific long-term defense against infection. Long-term defense is provided by immunological memory cells created from B and T lymphocyte activation against infection. Artificial memory can be created safely by vaccinating with antigens that mimic the presence of a pathogen.

Current vaccines against microbial infections such as bacterial meningitis use natural antigens derived from purified extracts of bacterial polysaccharide coats. The extraction of these polysaccharide antigens is an expensive process that still results in a great deal of variability. A lower cost conjugate vaccine against *Haemophilus influenzae* type b (Hib) has been developed consisting of a synthetic polysaccharide antigen (polyribosylribitol phosphate connected through glycosidic bonds) conjugated to tetanus toxoid. While this vaccine is based on a synthetic polysaccharide rather than a glycopolymer, it is worth mentioning because of its immense success: the vaccine triggers long term antibody protection against Hib and is now part of Cuba's vaccination program.[77,78]

Synthetic glycopolymers have also been used for vaccination. Mice were vaccinated against *Candida albicans* using a glycopolymer conjugate made up of mannan trisaccharides pendant to a poly(acrylamide) backbone with chicken serum albumin as the immunogenic carrier protein.[6] The mannan glycopolymer induced a larger immune response compared to a control trisaccharide-tetanus conjugate vaccine, although significant immunogenicity was found against the poly(acrylamide) backbone.

While most other saccharide-based vaccines incorporate protein content, one recently described vaccine has both synthetic antigen and carrier components.[79] A glycopolymer with pendant *N*-acetylgalactosamines (GalNAc, also known as the Tn antigen on tumor cells) was conjugated to a gold nanoparticle in order to

create a mimic of cancer cell surfaces displaying Tn antigen. The glycopolymer-nanoparticle conjugate successfully generated antibodies against the Tn antigen that were also cross-reactive with natural glycoproteins displaying the antigen. However, antibody levels were lower than those generated using a traditional carrier protein. Nevertheless, it is the first example of a glycopolymer based anti-cancer vaccine.

2.4.1.3   Competitive immune inhibitors

Competitive inhibition of pathogen binding to a host cell is a common strategy used to prevent disease. One common example of this strategy is neuraminidase inhibition, which uses sialic acid analogues to bind neuraminidase, a viral protein necessary for escape from the host cell. Since viral entry, replication, and release are all controlled in part by binding of carbohydrates, glycopolymers can also be used to competitively inhibit binding between pathogens and host cells. Sialic acid containing glycopolymers have been synthesized that can disrupt influenza virus binding with sialoglycoproteins on host cells. Inhibitors containing sialyl oligosachharides have been synthesized through post-polymerization modification of poly(acrylamide),[80] poly(acrylic acid),[81] poly(glutamic acid),[82] and poly(styrene) backbones.[83]

Glycopolymers have also been used to prevent entrance of HIV to the immune system by inhibiting binding of HIV envelope glycoprotein gp120 with dendritic cell associated lectin DC-SIGN.[68,69] DC-SIGN binds to mannose containing polysaccharides so glycopolymers with pendant mannoses were synthesized to block possible binding sites on DC-SIGN. Surface plasmon resonance showed that glycopolymers with higher densities of mannose had higher affinity binding with DC-SIGN, although gp120 still had the highest affinity.

Competitive inhibition can also be used to protect xenograft transplants from rejection due to xenoreactive antibodies. One of these antibodies binds to a disaccharide, Galα1-3Gal. Poly(styrene-*co*-maleic acid) was grafted with the disaccharide and the resulting glycopolymer was used to inhibit binding of the anti-Gal antibody with pig endothelial cells.[84] This competitive binding successfully protected the pig cells from the cytotoxic effects of human serum. The authors envision using the glycopolymer as an immunosuppressant drug to prevent transplant rejection by clearing anti-Gal xenoreactive antibodies from plasma.

2.4.2 Surface modification

The surfaces of cells are covered by a dense coat of glycolipids and glycoproteins. This glycan layer, or glycocalyx, functions as a signal for the immune system to distinguish between self and non-self cells as well as a protective barrier for the cell. These functions are important to consider when working with implantable devices and tissue engineered organs where the non-specific adsorption of protein can lead to complications. The Ulbricht group created a glycocalyx mimetic through D-gluconamidoethyl methacrylate grafted via ATRP onto a gold surface plasmon resonance sensor.[85] The high abundance of saccharide hydroxyls provided good hydration and steric repulsion to prevent non-specific protein adsorption resulting in just 0.03% BSA irreversibly adsorbing on the sensor when tested with the densest and longest glycopolymer chains.

The Bertozzi group produced a mucin mimetic glycopolymer end functionalized with hydrophobic domains that could insert into lipid bilayers[86] and live cell membranes.[87] Polymers were first synthesized through the radical copolymerization of isopropenyl methyl ketone or methyl vinyl ketone with *N*-[3-(dimethylamino)propyl]-acrylamide using a phospholipid modified AIBN derivative. Saccharide content was then added through post-polymerization grafting of aminooxy GalNac or LacNac. The inserted glycopolymers could bind to their corresponding lectins and had

similar membrane mobility as natural proteins, demonstrating the preservation of biological activity through the insertion process. The ability to modify a cell surface can be used as a platform to systematically study how glycocalyx structure properties affect cell behavior.

2.4.3 Bacterial detection and filtration

Bacteria use host saccharides to help facilitate cell adhesion. This dependence on saccharides by bacteria can be leveraged for detection and filtration strategies. For example, the Seeberger group developed a fluorescent mannose glycopolymer that would detect *E. coli* by binding to lectins on the bacterial pili.[88] Mannose residues were added via post-polymerization modification to a fluorescent poly(p-phenylene ethynylene) backbone. When the glycopolymer was incubated with *E. coli*, large aggregates of bacteria would form due to the multivalent interaction with the glycopolymer. This method had a detection limit of as little as 10,000 bacteria, similar to the limit of fluorescent antibodies. Similar work for a bacteria sensor has also been accomplished using microarrays,[89] quantum dots,[90] and magnetic nanoparticles functionalized with carbohydrates.[91] These methods did not use glycopolymers but still incorporated multivalency.

Microfiltration membranes have been modified with glycopolymers to capture bacteria. 2-Lactobionamidoethyl methacrylate (LAMA) monomers were grafted from a poly(propylene) microfiltration membrane via UV-induced polymerization.[92] *E. faecalis*, a bacterial strain that recognizes LAMA, would selectively bind to the poly(LAMA) modified surface while *S. maltophili*a, a negative control, had no increase in adhesion compared to an unmodified surface. *E. faecalis* could be subsequently released for future testing through competitive binding with a galactose solution. These results showed the potential for glycopolymers to be used in filtration and sensor systems, provided that different pendant sugar groups are added to capture multiple bacterial strains.

2.4.4 Tissue engineering

Natural polysaccharides such as alginate and chondroitin sulfate have been used as scaffolds in tissue engineering. These polysaccharides can be difficult to isolate in large quantities from their natural sources while also controlling for batch to batch variability. Synthetic versions of natural polysaccharides can prove useful for future tissue engineering applications. Chondroitin sulfate mimetics have been produced through ring-opening metathesis polymerization of the chondroitin sulfate disaccharide unit and were shown to interact with glycoaminoglycan binding proteins.[93] As a major component of the extracellular matrix, notably in cartilage, such chondroitin sulfate mimetics could prove useful as a scaffold for further work.

The Chaikof group reported the synthesis of a series of glycosaminoglycan mimetics through the cyanoxyl mediated copolymerization of acrylamide with nonsulfated or sulfated GlcNac and lactose.[94–97] These polymers were tested for biological function against natural heparin's ability as a chaperone for Fibroblast Growth Factor-2 (FGF-2) and as an anticoagulant. The sulfated polymers were shown to enhance FGF-2 binding to its receptor, as well as modestly prolonging coagulation time. In both cases however, the natural heparin still exhibited significantly higher activity. Later work with a heparin glycomimetic as an FGF-2 chaperone demonstrated that the glycopolymer could stimulate FGF-2 mediated cell proliferation along with protecting the growth factor from proteolytic, acid, and heat induced denaturation.[98]

Much of the tissue engineering work with glycopolymers has been focused on regenerating liver tissue by using hepatocyte asialoglycoprotein receptors (ASGP-R) ability to bind galactose residues. Kim and colleagues have studied this binding with glycopolymers made of galactose and glucose residues. Their glycopolymer promotes adhesion of hepatocytes and induces different morphologies compared to collagen controls,[99] as well as regulates hepatocyte cell growth without involving integrin mediated signaling.[100]

Similar work has been done by the Mao group with galactose grafted onto polymeric films.[101] The sugars were conjugated through surface grafting of a poly(acrylic acid) spacer to the scaffold, followed by covalent binding to the carboxylate with an amine modified galactose. The hepatocytes cultured on galactose modified surfaces maintained better hepatocyte functions of albumin secretion and ammonia removal compared to those cultured on collagen coated and unmodified control surfaces.

2.4.5 Drug and gene delivery

Platforms for drug and gene delivery must protect the payload from the physiological environment, control the release profile for optimal efficacy, and target specific areas of the body or cell surface receptors for localized release. Delivery vehicles that incorporate saccharides would be ideal for this application as sugar-lectin interactions can be used to target the drug to the desired location. The Stenzel group created glycomicelles that were both temperature and pH sensitive with this motivation.[102] A block copolymer of poly(acryloyl glucosamine) and poly(N-isopropylacrylamide) was synthesized that transitioned from fully soluble to micellar as the temperature was raised above poly(NIPAAm)'s LCST. Once the micellar structure was formed, an acid-labile crosslinking agent and an initiator were added to restart RAFT polymerization through the dithioester chain ends. The crosslinked glycomicelles were stable at pH 6 and 8.2, but degraded within 30 minutes at pH 2. This research laid the groundwork for potential targeting and delivery applications.

Suriano targeted self-assembled galactosylated micelles loaded with doxorubicin (DOX) against ASGP-R positive liver cancer cells.[103] Galactose containing micelles effectively delivered DOX to the cancer cells through ASGP-R mediated endocytosis compared to ASGP-R negative HEK293 cells. Cytotoxicity of the ASGP-R positive cells by DOX was higher when exposed to galactose micelles than with glucose micelles and free DOX. In comparison, glucose micelles enter cells through non-specific endocytosis or through glucose transporters while free DOX enters cells through passive diffusion.

Galactose has also been used as a the targeting block of a poly(phosphoramidate) polymer which was used to transfect cells with DNA efficiently, with four times less cytotoxicity than poly(ethyleneimine) (PEI). The galactose component resulted in increased gene expression in hepatocytes compared to HeLa cells, presumably mediated by ASGP-R. However, overall transfection efficiency of the galactosylated DNA nanoparticles was lower due to decreased DNA binding capacity from the galactose modification.[104]

Cationic saccharides have promise as an alternative nontoxic gene delivery agent in comparison to synthetic cationic polymer carriers such as poly(ethyleneimine) which have good delivery efficiency but high cytotoxicity. The role of positively charged sugars has been informed by early work using chitosan, a natural polysaccharide composed chiefly of glucosamine and *N*-acetyl glucosamine.[105] The Reineke group has performed a great deal of gene delivery work using glycopolymers. They have created a library of cationic glycopolymers based off of poly(glycoamidoamine) copolymerized with oligoethyleneamine monomers. This library varies polymer properties in terms of carbohydrate density, hydroxyl content, stereochemistry, and amine density.[106] In general, these glycopolymers led to similar gene expression as PEI with significantly lower toxicity. The cationic saccharide units can complex negatively charged DNA nucleotides through charge interaction, but are also thought to condense DNA through hydrogen bonding with saccharide hydroxyls.[107]

CHAPTER 3

Synthesis of hyperbranched glycopolymers

3.1   Introduction

Controlled polymerization techniques have been used to synthesize many linear glycopolymers with control over the chain length and monomer identity. However, only a few examples of glycopolymers with control over branching have been described. Müller's group uses self-condensing ATRP of a sugar acrylate with an inimer, 2-(2-bromopropionyloxy)ethyl acrylate, to produce hyperbranched polymers containing sugar residues.[1,2] Perrier's group uses RAFT to copolymerize ethylene glycol dimethacrylate (EGDMA) and a silyl protected alkyne-acrylate.[3] After isolation and deprotection, the alkyne was functionalized with azido-ethyl galactose via copper catalyzed azide-alkyne cycloaddition ("click" chemistry) or a radically-catalyzed thiol-yne reaction with glucothiose. Narain also used RAFT to synthesize branched glycopolymers by copolymerizing glucose or lactose monomers with *N,N'*-methylenebis(acrylamide).[4] In these examples of branched glycomimetic polymers, the saccharide residue is pendant to the polymer backbone and the branching repeat units do not contain a saccharide residue.

In order to closely replicate and control the interaction of glycomimetics with naturally occurring lectins, as well as fully explore structure-property relationships of saccharide-lectin binding, efficient synthetic techniques are needed to produce both short and long chain glycomimetics with well-defined structures that incorporate branching as well as saccharide content at the branch point. In this chapter, I describe the synthesis of branched mannose polymers that place the mannose residues at the branch points (Figure 3.1).

Saccharide branch points are created by the incorporation of a mannose inimer with two reactive sites, a polymerizable vinyl group and a homolytically cleavable halogen. The inimer can be copolymerized with other sugar acrylates to yield polymers with varying degrees of branching and carbohydrate composition. This method creates glycopolymers that more directly mimic structures found in natural polysaccharides, in contrast to previous branched glycopolymers that have no saccharide content at the branch point. For comparison, linear mannose polymers as well as branched mannose polymers that lack mannose content at the branch point are also synthesized.

We are specifically interested in creating mannose polymers as it plays an important role in innate immunity. Mannose binding lectin (MBL) of the innate immunity complement system binds to mannose and other saccharides with similar configurations. Biological studies with MBL using these glycopolymers will be discussed in Chapter 6.
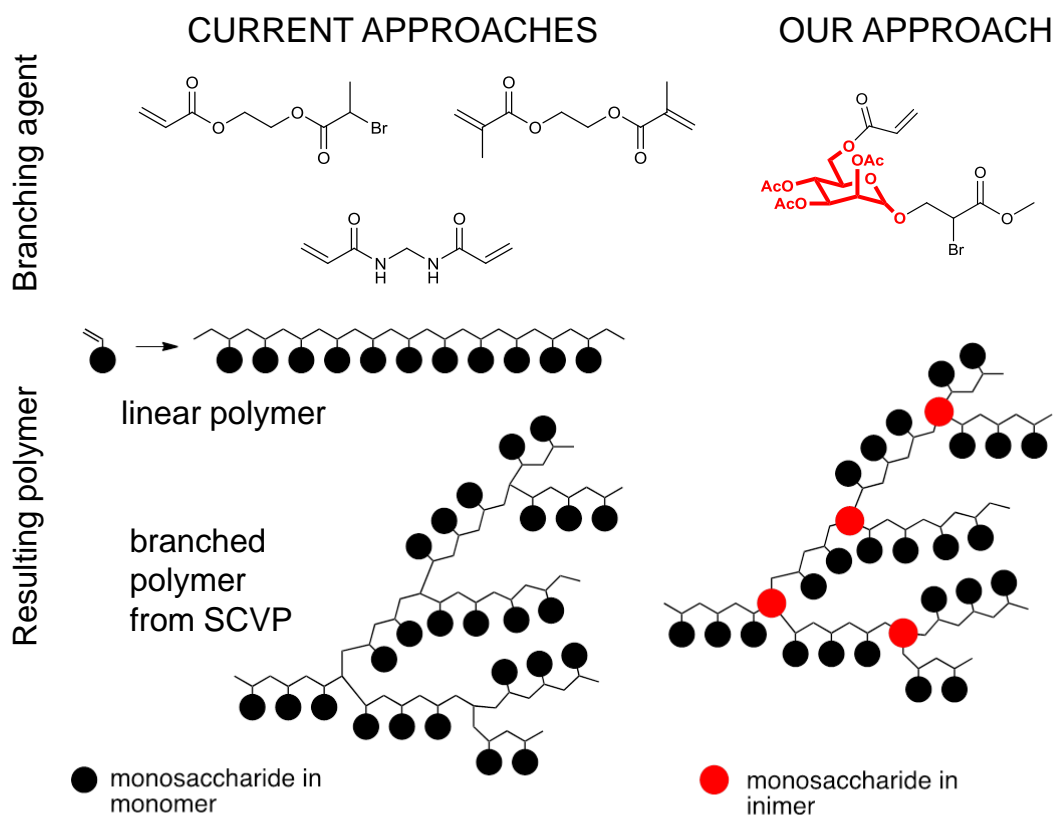
Figure 3.1: A new class of hyperbranched glycopolymer which incorporates the saccharide residues at the branch point, in contrast to current approaches that lack saccharide residues at the branch point due differences in the branching agent (Current approach structures from references,[1],[3] and[4]).

3.2 Synthesis of glycomonomers, glycoinitiators, and glycoinimers

The mannose-based glycomonomer, 6-acryloxy-1,2,3,4-tetraacetate-β-mannopyranose, was prepared in three steps from the beginning saccharide as shown in Scheme 3.1. The primary alcohol was selectively protected at the six position with triphenylmethyl chloride at 0 °C and the remaining alcohols subsequently protected with acetic anhydride at room temperature in a one-pot reaction. The coupling of the trityl group to the primary alcohol was conducted at elevated temperature to bias the carbohydrate ring towards the beta conformation. Acidic deprotection of the trityl group from sugar with alpha anomer was found to result in partial migration of an acetate from the four position to the six position. This hurdle was overcome by selectively crystallizing the beta anomer with diethyl ether and using only the beta anomer for subsequent reactions. This anomer selection is the cause of the low yield in the first protection step. Whereas the anomer identity is important for some lectin interactions, our target lectin binds to the 3- and 4- hydroxyls[75] so we do not expect a difference in biological activity due to the anomer choice. Following the trityl deprotection, the unprotected primary alcohol was acrylated with acryloyl chloride to obtain the glycomonomer, 6-acryloxy-1,2,3,4-tetraacetate β-mannopyranose.

The mannose-based inimer, methyl 2-bromo-3-(6-acryloxy-2,3,4-triacetate mannopyranosyl) propionate, was prepared from the glycosylation of methyl 2-bromo-3-hydroxypropionate[108] with 6-acryloxy-1,2,3,4-tetraacetate β-mannopyranose using boron trifluoride etherate as activator.

The mannose based initiator, methyl 2-bromo-3-(2,3,4,6-tetraacetate mannopyranosyl) propionate, was prepared in a similar manner from methyl 2-bromo-3-hydroxypropionate and pentaacetate mannopyranose.

A galactose version of the glycoinimer was also synthesized as shown in Scheme 3.2. Galactose was first protected with isopropylidenes to leave the primary alcohol open for acrylation with acryloyl chloride. The isopropylidenes were removed with acetic acid and replaced with acetate protecting groups to create an analogous galactose monomer, 6-acryloxy-1,2,3,4-tetraacetate β-galactopyranose. Methyl 2-bromo-3-hydroxypropionate was then attached to the sugar to produce the galactose inimer, methyl 2-bromo-3-(6-acryloxy-2,3,4-triacetate galactopyranosyl) propionate.
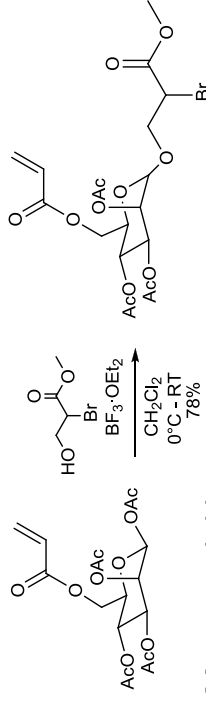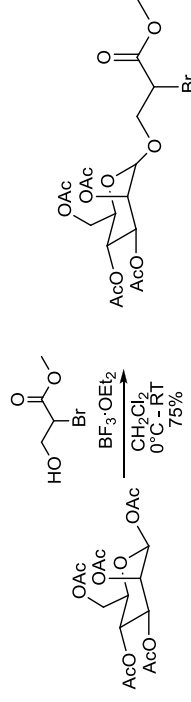
Scheme 3.1: Synthesis of 6-acryloxy-1,2,3,4-tetraacetate β-mannopyranose (mannose monomer), methyl 2-bromo-3-(6-acryloxy-2,3,4-triacetate mannopyranosyl) propionate (mannose inimer), and methyl 2-bromo-3-(2,3,4,6-tetraacetate mannopyranosyl) propionate (mannose initiator).

Galactose inimer
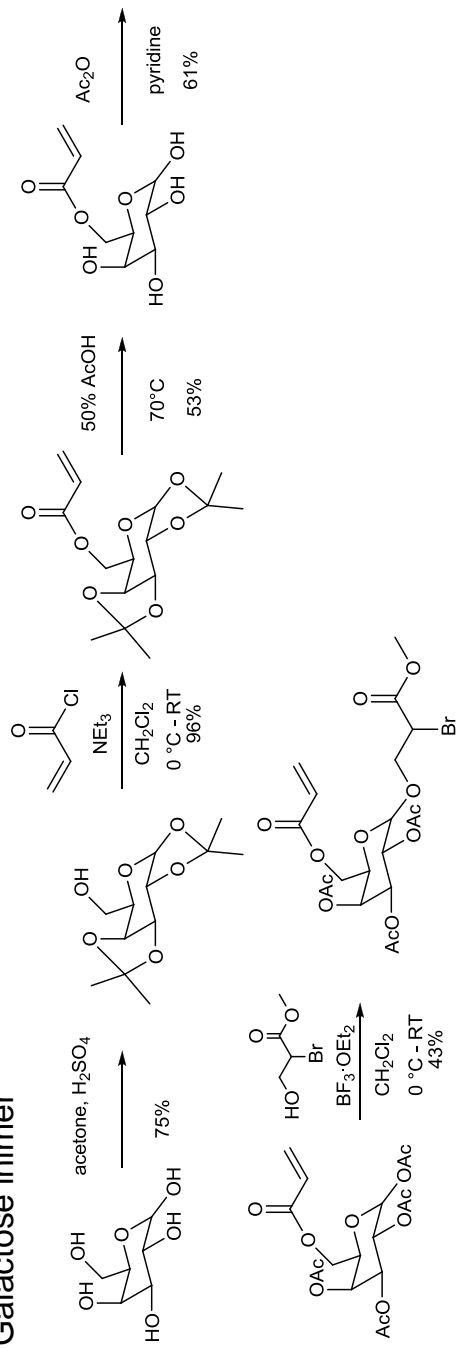
Scheme 3.2: Synthesis of methyl 2-bromo-3-(6-acryloxy-2,3,4-triacetate galactopyranosyl) propionate (galactose inimer).

3.3 Synthesis of linear and branched glycopolymers

Linear and branched glycopolymers were synthesized by ATRP in ethyl acetate using CuBr as catalyst and Me_6Tren as ligand (Scheme 3.3). In order to elucidate the importance of incorporating the saccharide unit in the branch point, branched polymers were synthesized using either an inimer incorporating mannose or an inimer with no mannose. The resultant polymers were characterized by GPC relative to poly(methyl methacrylate) standards with polymerization results listed in Table 3.1.

Linear glycopolymers with 14-75 repeat units were obtained from ATRP of the mannose glycomonomer using the mannose glycoinitiator and varying the $[M]_0:[I]_0$ from 25:1 to 100:1. Branched polymers with mannose at the branch point (# mannose = 8-42) were synthesized via copolymerization of the mannose glycomonomer and mannose glycoinimer. Apparent branching density was controlled by varying $[M]_0:[Mannose\ inimer]_0$ from 1:1 to 10:1; homopolymerizations of the glycoinimer were unsuccessful. The Pugh group previously reported homopolymerization of an inimer with a structurally similar reactive site to create hyperbranched polyacrylates.[108,109] Their inimer incorporated alkyl, perfluoroalkyl, siloxane, oligooxyethylene, and mesogenic side groups, whereas the inimer here had methyl ester side groups and incorporates mannose within its backbone and the backbone of the resultant polymers (Figure 3.2). The presence of the saccharide unit in our glycoinimer may be preventing homopolymerization, possibly due to steric effects.

Saccharide inimer

Inimer (Pugh)

R =
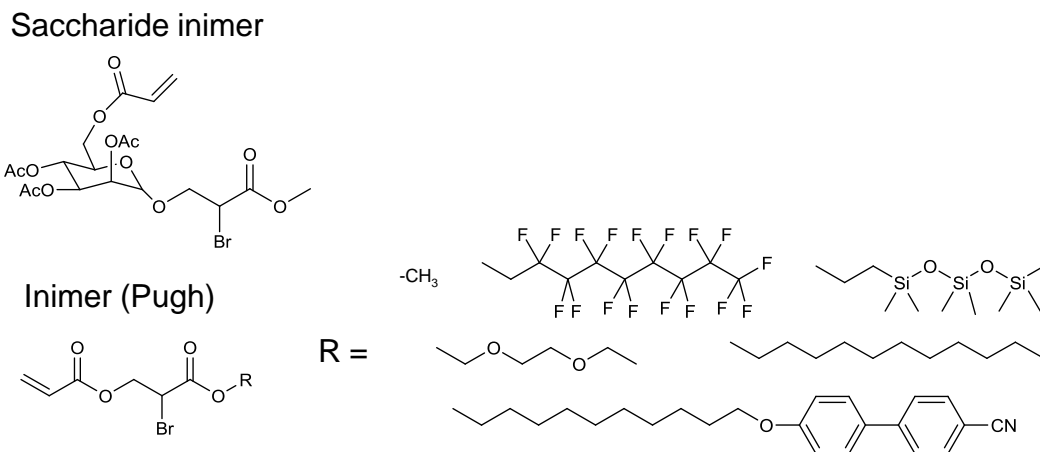
Figure 3.2: Our inimer places a saccharide in the branch point, while having a pendant methyl side group. The Pugh inimer[108,109] incorporates a variety of side groups but has no saccharide component.

Branched polymers with no mannose in the branching repeat unit were synthesized by copolymerizing mannose acrylate with (2-bromo-2-methoxycarbonyl)ethyl acrylate.[108] $[M]_0 : [Inimer]_0$ was varied from 1:1 to 5:1 to obtain samples with different branching densities. Finally, branched polymers with galactose at the branch point were synthesized by copolymerizing the mannose glycomonomer with the galactose glycoinimer with a 1:1 $[M]_0 : [Galactose inimer]_0$ ratio.
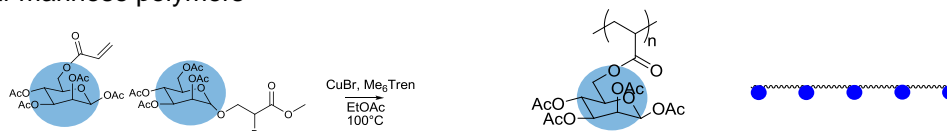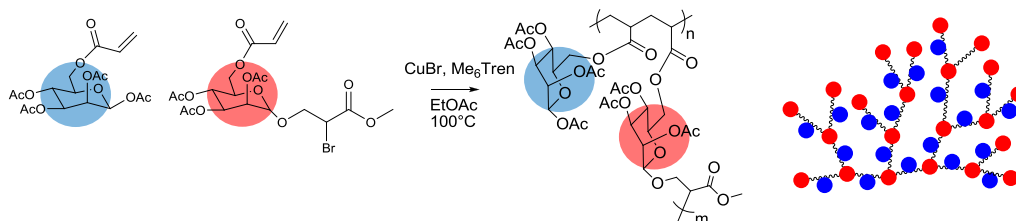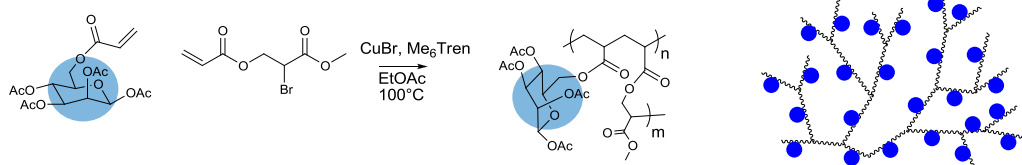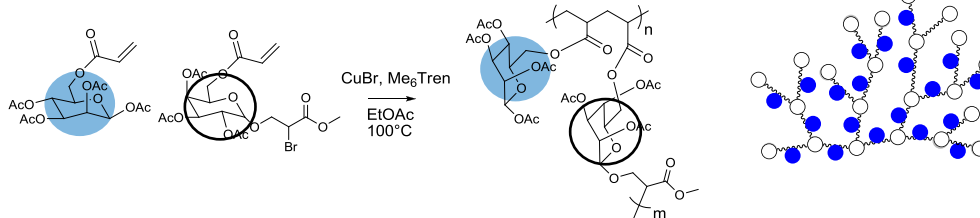
Scheme 3.3: Synthesis of linear and branched (with mannose, without saccha-ride, and with galactose at the branch point) glycopolymers by ATRP of 6-acryloxy-1,2,3,4-tetraacetate β-mannopyranose, methyl 2-bromo-3-(6-acryloxy-2,3,4-triacetate mannopyranosyl) propionate, (2-bromo-2-methoxycarbonyl)ethyl acrylate, and methyl 2-bromo-3-(6-acryloxy-2,3,4-triacetate galactopyranosyl) pro-pionate.

Table 3.1: Summary of GPC_{PMMA} data for linear and branched (with mannose, without saccharide, and with galactose at the branch point) glycopolymers synthesized by ATRP.

Linear mannose polymers

$[M]_0$:[Mannose initiator]$_0$:[CuBr]:[Me$_6$Tren]	M_w	M_n	# mannose	PDI
25:1:1:1	6990	5770	14	1.21
50:1:1:1	20480	16820	42	1.22
100:1:1:1	37600	30310	75	1.24

Branched glycopolymers with mannose at branch point

$[M]_0$:[Mannose inimer]$_0$:[CuBr]:[Me$_6$Tren]	M_w	M_n	# mannose	PDI
25:25:1:1	8600	5750	14	1.5
50:25:1:1[a]	15610	5980	14	2.61
50:25:1:1[b]	37920	17640	42	2.15
50:10:1:1	4670	3240	8	1.44
125:25:1:1	5780	4050	10	1.43
100:10:1:1	6230	4590	11	1.36

Branched glycopolymers without saccharide at branch point

$[M]_0$:[Inimer]$_0$:[CuBr]:[Me$_6$Tren]	M_w	M_n	# mannose	PDI
25:25:1:1	10280	5360	10	1.92
50:25:1:1	36380	8440	18	3.12
125:25:1:1	8680	5150	12	1.67

Branched glycopolymers with galactose at branch point

$[M]_0$:[Galactose inimer]$_0$:[CuBr]:[Me$_6$Tren]	M_w	M_n	# mannose	PDI
25:25:1:1	6320	3690	4	1.71
50:50:1:1	17110	11260	13	1.52
50:25:1:1	6150	3250	5	1.89

a: 56% conversion, b: 99% conversion

3.4 Branching characterization of glycopolymers

To confirm glycoinimer incorporation into the polymer chain, which will result in a branched sample with saccharide at the branch point, we initially characterized the protected polymers by NMR and GPC_{PMMA}. NMR of the protected polymers showed peaks corresponding to the inimer; however, the inimer could be incorporated solely through the acrylate resulting in a linear polymer. GPC_{PMMA} of samples synthesized with an inimer showed broader polydispersities, compared with the more narrow distributions exhibited by the linear polymers. GPC_{PMMA} provides a relative molecular weight through calibration of polymer elution times with known molecular weight standards so these measurements alone do not give any direct information about branching (Figure 3.3a). Nevertheless, the broad PDIs are a good indication of branching architecture because hyperbranched polymers are theorized to have broad molecular weight distributions.[110]

The glycopolymers were deprotected with sodium methoxide in methanol and chloroform for additional GPC characterization, NMR characterization, and further lectin binding studies (in Chapter 6). The deprotected polymers became insoluble in THF and acetone but were soluble in water. ^{1}H NMR spectra of the deprotected polymers were inconclusive. Although the spectra were clearer due to removal of peaks corresponding to the acetate protecting groups, the branch point fragment still could not be identified due to overlap with the protons of the mannose ring (Figure 3.4). Further COSY NMR experiments also failed to identify the branch point with no cross-peaks between OCH_2 and CH of the branching unit (Figure 3.5).

a.

Branched, PDI = 2.15

Linear, PDI = 1.22

16   20   24   28   32   36
minutes

b.

30000

2.8

20000

1.6

10000

• Linear polymers
○ Branched polymers

0

0   5000   10000   15000   20000

Expected M_n
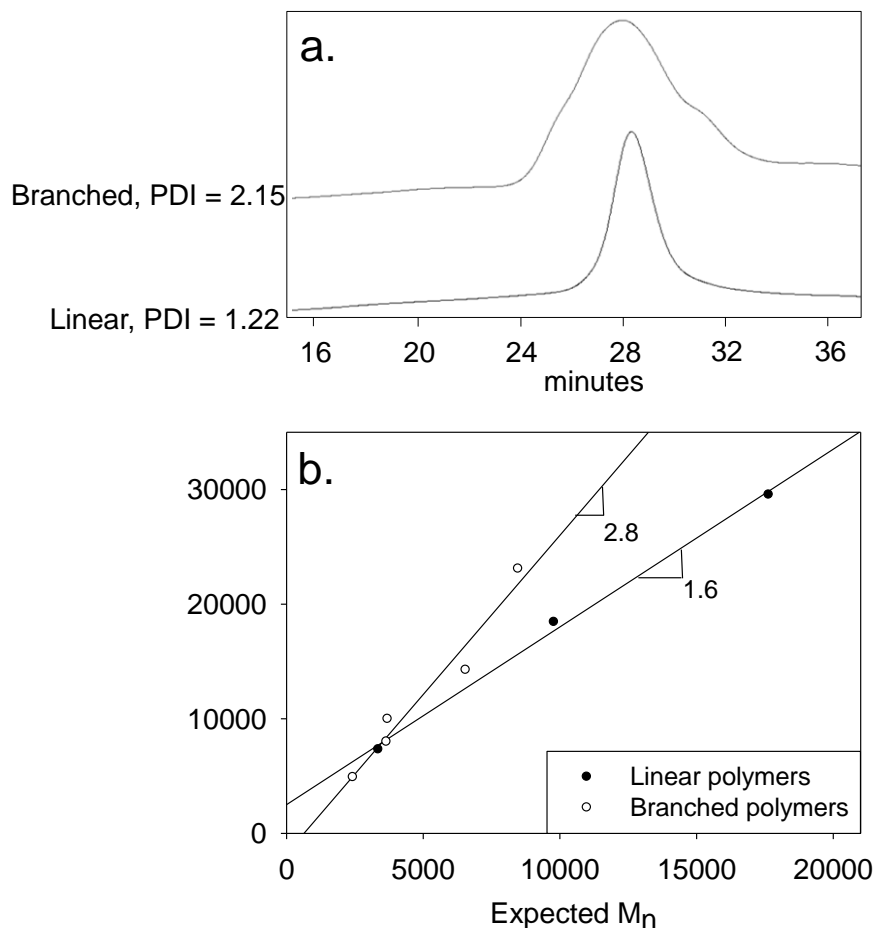
Figure 3.3: Evidence of branching architecture of polymers from GPC_{PMMA}. (a) GPC chromatogram of a linear and branched glycopolymer conducted in THF showing higher polydispersity for branched polymers (b) Linear and branched glycopolymers have a different relationship between expected molecular weights (calculated from values obtained in THF) and measured molecular weights (obtained in DMF), indicating the polymers have different architectures.

Figure 3.3b plots the expected molecular weights for the linear and branched polymers with sugar at the branch point (calculated from the values obtained in THF) compared with the measured molecular weights of the deprotected polymers in DMF. If all of the polymers have the same architecture, then we expect all of the data would fall along a single line. However, the linear polymers clearly have a different relationship between molecular weight and hydrodynamic volume (slope = 1.6) than those samples synthesized using an inimer (slope = 2.8), indirectly indicating that these samples have a different molecular architecture. Branched polymers have a more compact shape than linear polymers of the same molecular weight.[111] Because GPC separates on the basis of hydrodynamic volume, molecular weights are typically underestimated for branched polymers compared to their linear analogues. These two results, the broad polydispersity and the difference in the relationship between molecular weight and hydrodynamic volume, strongly suggest a branched architecture.
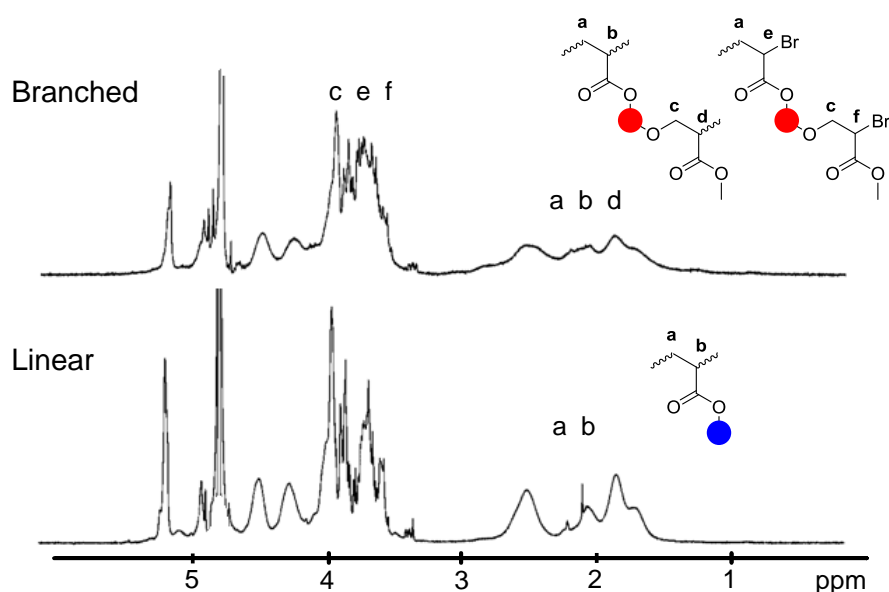
Figure 3.4: ^{1}H NMR spectra of deprotected branched and linear polymers cannot identify branch point fragment. Sugar ring proton peaks overlapped with those from expected branch point peaks (c, e, f).
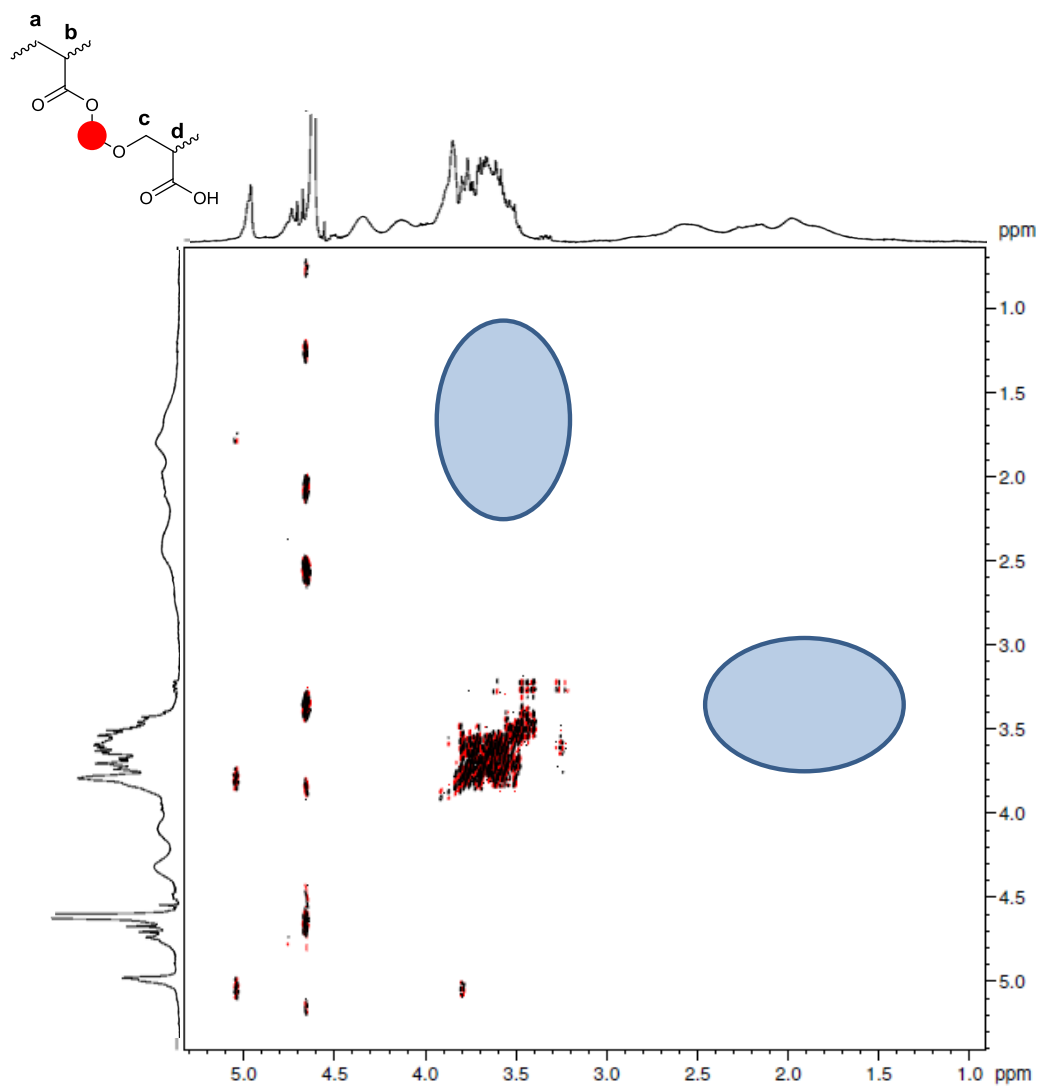
Figure 3.5: Expanded region of the ^{1}H-^{1}H COSY-NMR spectrum of a hyper-branched glycopolymer synthesized from copolymerization of glycomonomer and glycoinimer in a one to one ratio. No cross peaks are observed between protons from c and d.

To further confirm the branched architecture, gel permeation chromatography with an in-line light scattering detector (GPC_{LS}) was performed on linear protected glycopolymers and (presumably) branched protected glycopolymers to find absolute molecular weight values (Table 3.2). Some very high molecular weight aggregates were detected; these aggregates were not included in the GPC_{LS} analysis. For all linear and branched polymers, absolute molecular weight was higher than the relative molecular weight determined by GPC_{PMMA} indicating that the PMMA standard calibration consistently underestimated the molecular weight of the glycopolymers.

However, the ratio of absolute molecular weight to relative molecular weight is higher for polymers synthesized from the glycoinimer. When the absolute molecular weight (GPC_{LS}) is plotted versus the relative molecular weight (GPC_{PMMA}) as a measure of the error in GPC-determined molecular weight introduced through architecture, different slopes are found for linear and presumably branched glycopolymers (Figure 3.6). This finding is consistent with a branched architecture due to polymerization of the glycoinimer. The different slopes indicate that the linear polymers have larger hydrodynamic volumes at equivalent molecular weights than presumably branched polymers synthesized from the glycoinimer. These results also correlate well with those seen with linear polyacrylates[112,113] and hyperbranched polyacrylates from a chloroinimer (Table 3.3).[109] Linear polyacrylates had a slope of m = 1.46 compared to our linear glycopolymers with a slope of m = 1.51. Hyperbranched polyacrylates had a slope of m = 1.69 (m = 2.76 when higher molecular weight portions were fractionated and tested) compared to our presumably branched glycopolymers with a slope of m = 2.21. The effect of the degree of branching was not studied because there was not enough variation in samples to draw any conclusions.

Table 3.2: Comparison of GPC$_{PMMA}$ and GPC$_{LS}$ data for linear and branched glycopolymers synthesized by ATRP.

Linear mannose polymers

[M]$_0$:[Mannose initiator]$_0$: [CuBr]:[Me$_6$Tren]	M$_{w,PMMA}$	M$_{n,PMMA}$	M$_{w,LS}$	M$_{n,LS}$
10:1:1:1	15460	9540	11890	11050
50:1:1:1	20480	16820	34590	31470
100:1:1:1	37600	30310	73250	44420

Branched mannose polymers with saccharide at branch point

[M]$_0$:[Mannose inimer]$_0$: [CuBr]:[Me$_6$Tren]	M$_{w,PMMA}$	M$_{n,PMMA}$	M$_{w,LS}$	M$_{n,LS}$
10:10:1:1	15040	10920	33540	28180
100:50:1:1	11310	6080	27590	20850
20:10:1:1	28800	13690	72150	48410
50:25:1:1	37920	17650	77690	46420
50:10:1:1	4670	3240	25180	17070
100:10:1:1	6230	4590	19970	17380
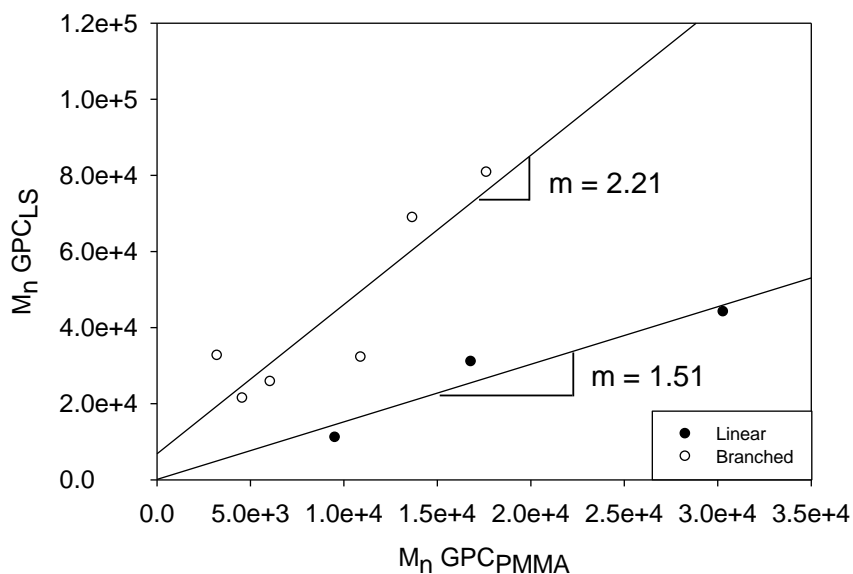
Figure 3.6: The error in GPC-determined molecular weight introduced through architecture is shown by plotting absolute molecular weight (GPC$_{LS}$) versus the relative molecular weight (GPC$_{PMMA}$). Linear and branched glycopolymers exhibit different slopes.

Table 3.3: Slope and intercept values from the linear equation [$M_{n,LS} = m(M_{n,GPC}) + b$] derived from plotting absolute versus relative M_n for polymers of different architectures.

Architecture	m, slope	b, intercept	r[a]
Linear polyacrylate[b]	1.46	-2920	0.985
Linear glycopolymer	1.51	-380	0.909
Hyperbranched polyacrylate[b]	1.69	3730	0.983
Hyperbranched polyacrylate, fractionated[b]	2.76	-7540	0.996
Hyperbranched glycopolymer	2.21	9270	0.859

a: linear correlation coefficient, b: adapted with permission from[109]

GPC_{LS} can also provide the root mean square (rms) radius of gyration through the angular dependence of scattered light (the slope of $K^*c/R(\theta)$ versus $\sin^2(\theta/2)$ gives R_{rms}^2). Molecular conformation can then be found through plotting log(rms) versus log(MW) ($R_g \propto M^\upsilon$) where if $\upsilon = 0.33$, 0.5, or 1, the polymer is a sphere, random coil, or rod respectively. These calculations are only valid when rms >10 nm so that molecular weight and rms radius can be measured simultaneously.

Only a few of the chromatographed polymers could be analyzed for their molecular conformations. Many polymers were excluded from analysis because of their low signal to noise ratio due to uncertainties generated from the use of a triple-angle light scattering detector rather than a more robust 18 angle detector, as well as the small polymer size which resulted in lower light scattering response ($\propto c_i M_i$). The smaller polymers also mean that fewer of the chains in the polymer population have rms >10 nm. Nevertheless, strong conclusions can be made from these data.

Table 3.4 summarizes the υ values found for the glycopolymers of different architectures. Plots of molecular weight versus elution time, rms radius versus elution time, and log(rms radius) versus log (molecular weight) are shown in Figure 3.7. The log-log plot does not contain data from the high molecular weight extremity or data with log(rms) <1. Only one linear glycopolymer could be analyzed for molecular conformation with $\upsilon = 0.67$. In comparison, υ decreased to on average 0.46 for branched glycopolymers with $[M]_0$:[Mannose inimer]$_0 = 2$:1 . The smaller scaling coefficient indicates that the polymers are more compact and likely more branched.

These two light scattering conclusions, the error in GPC-determined molecular weight and the lower molecular conformation scaling coefficient, further confirm a branched architecture.
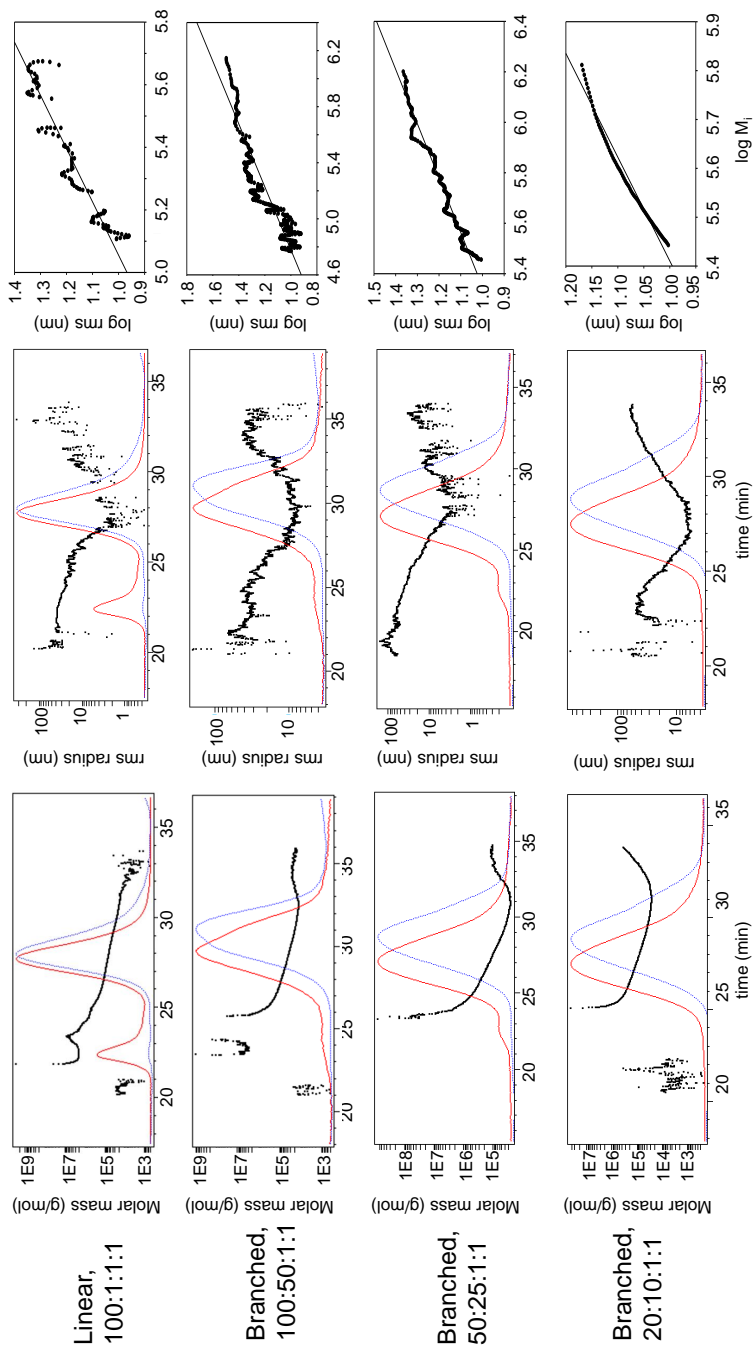
Figure 3.7: Plots of molecular weight versus elution time, rms radius versus elution time, and log(rms) versus log (molecular weight). Numbers indicate $[M]_0:[Mannose\ initiator]_0:[CuBr]:[Me_6Tren]$ or $[M]_0:[Mannose\ inimer]_0:[CuBr]:[Me_6Tren]$.

Table 3.4: Summary of molecular conformation, v.

Architecture	$M_{n,LS}$	v
Linear	44420	0.67
Branched[a]	20850	0.45
Branched[a]	46420	0.46
Branched[a]	48410	0.47

a: $[M]_0$:[Mannose inimer]$_0$ = 2:1

The glycopolymers are also being analyzed by tandem mass spectrometry (MS-MS) by Professor Wesdemiotis' lab at the University of Akron. MS-MS had been used previously to characterize hyperbranched polyacrylates by fragmenting a single oligomer chain using matrix assisted laser desorption/ionization-collisionally activated dissociation (MALDI-CAD) to reveal different fragmentation patterns.[114] In their work, molecular weights corresponding to branched structures were found, confirming the hyperbranched architecture of polyacrylates synthesized from a chloroinimer.

Currently, the glycopolymers have only been analyzed by MALDI (Figure 3.8) but not by MALDI-CAD. MALDI shows incorporation of multiple mannose inimer units with retention of the bromide chain ends. While it is possible that the polymer chain is only initiating from one glycoinimer and incorporating both glycomonomer and glycoinimer only along the acrylate creating a linear polymer, this would be an unlikely occurrence for multiple glycoinimers. It is more likely that the polymer chain grows from both the acrylate and the halogen creating a branch point as depicted in Figure 3.8d. Polymers with branching ratios $[M]_0$:[Mannose inimer]$_0$ = 2:1 and 5:1 showed significant glycoinimer incorporation by MALDI, compared to 10:1 with little glycoinimer content. However, these results have one caveat: the molecular weight averages reported by mass spectrometry may be skewed because the heavier polymer chains are not ionized as readily and are not detected, resulting in reported molecular weights lower than those determined by GPC.
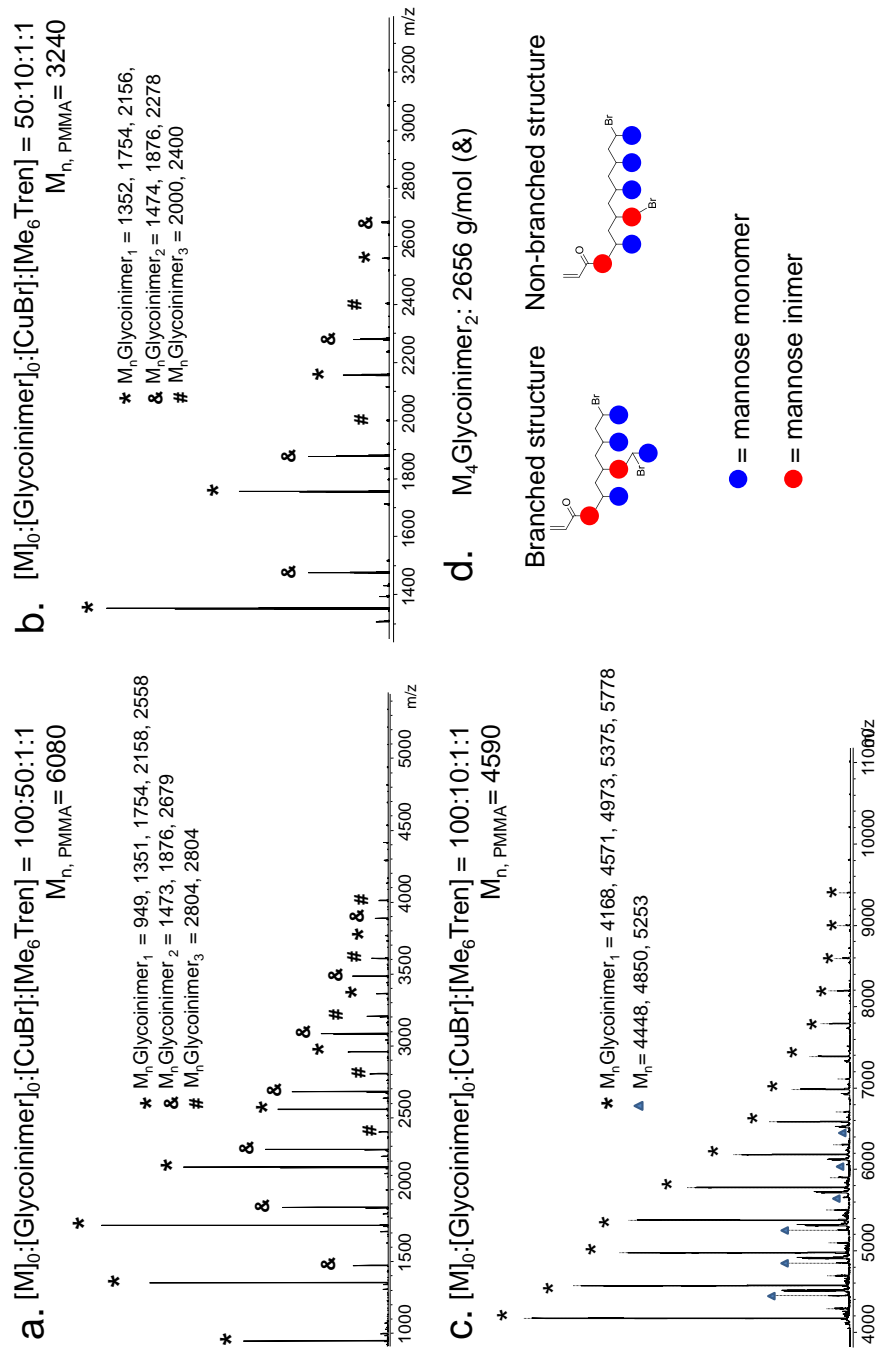
Figure 3.8: MALDI spectra of branched glycopolymers with (a)$[M]_0$:[Mannose inimer]$_0$ = 2:1, (b)$[M]_0$:[Mannose inimer]$_0$ = 5:1, and (c)$[M]_0$:[Mannose inimer]$_0$ = 10:1. (d) Idealized branched and linear structure of M_4:Mannose inimer$_2$ with equivalent molecular weight, 2656 g/mol. m/z of selected peaks are shown.

3.5 Conclusions

In this chapter, I described the synthesis of a reactive inimer incorporating mannose, its copolymerization with mannose acrylate to produce glycomimetic polymers with different branching densities, and the confirmation of branching architecture through GPC_{PMMA}, GPC_{LS}, and mass spectrometry. These branched glycopolymers more fully recapitulate natural polysaccharide structures through the controlled radical copolymerization of glycomonomers and glycoinimers in which the saccharide residues can be incorporated not only pendant to the polymer backbone, but also within the polymer chain in their native ring form (Figure 3.1). This method of incorporating saccharide into the branch point narrows the gap between synthetic glycopolymers and natural polysaccharides and can result in glycopolymers with improved bioactivity. Furthermore, by using a saccharide inimer, the effect of branching density on bioactivity can be studied while maintaining the same overall saccharide content. This advantage is in contrast to previously reported branched glycopolymers that do not allow for changing branching density independently of saccharide content. In Chapter 6, bioactivity of these glycopolymers will be tested with mannose binding lectin, an immune system protein.

3.6 Experimentals

3.6.1 Materials

Acetic acid (Mallinckrodt, ACS grade), acetic anhydride (Fisher, ACS grade), acetone (Fisher, ACS grade), boron trifluoride etherate (Acros, 48%), galactose (Fisher, off white to white powder), mannose (Amresco, high purity grade), pyridine (J.T. Baker, ACS grade), and triphenylmethyl chloride (Acros, 98%) were used as received. Copper bromide (Acros, 98%) was purified by stirring in glacial acetic acid and then rinsing with ethanol. Acryloyl chloride (Alfa Aesar, 96%), dichloromethane (EMD, ACS grade), ethyl acetate (Macron, ACS grade), and triethylamine (Alfa Aesar, 99%) were distilled before use. Tris(2-aminoethyl)amine (Me_6Tren) was synthesized according to a published procedure.[115]

3.6.2 Analytical Techniques

^{1}H NMR spectra (δ ppm) were recorded on Bruker Biospin Ultrashield 300 MHz or 500 MHz NMR spectrometers. Gel permeation chromatography relative to linear poly(methyl methacrylate) standards(GPC_{PMMA}) was conducted on a Waters system equipped with UV/vis absorbance and refractive index detectors and four Waters styragel columns (100-5K, 500-30K, 50-100K, 5K-600K). *N,N*-dimethylformamide (DMF) with 0.01 M lithium bromide or tetrahydrofuran (THF) with a flow rate of 1.0 mL/min was used. Gel permeation chromatography that provided absolute molecular weights (GPC_{LS}) was conducted on four Waters styragel columns (100-5K, 500-30K, 50-100K, 5K-600K) in-line with a Wyatt triple-angle light scattering detector (miniDAWN) and refractive index detector (Optilab rEX). THF with a flow rate of 1.0 mL/min was used. dn/dc values of the glycopolymers (linear or branched) were calculated in batch mode through the Optilab rEX. The Zimm formalism was used for calculating molecular weight due to the small RMS radii of the polymers. Matrix assisted laser desorption/ionization (MALDI) was

performed by Professor Wesdemiotis' lab at the University of Akron. MALDI was conducted in linear mode with *trans*-2-[3-(4-tert-Butylphenyl)-2-methyl-2-propenylidene]malononitrile as matrix.

3.6.3   6-Trityl-1,2,3,4-tetraacetate β-mannopyranose

Mannose (20.0 g, 111 mmol) was added to pyridine (200 mL) and stirred until dissolved. Triphenylmethyl chloride (32.5 g, 117 mmol) was then added and the solution heated to 50 °C for four hours. Without workup, acetic anhydride (103 mL, 1.08 mole) was then added and stirred overnight at room temperature. Pyridine was removed on a rotary evaporator until the solution was concentrated to a brown viscous liquid. The viscous liquid was dissolved in a minimal amount of ethanol, and then precipitated into rapidly stirring ice cold water. The white crystals were collected and washed thoroughly with water. β-mannose was isolated by precipitation in ether to yield 24 g (36%) of a white powder.

^{1}H NMR (300 MHz, CDCl$_3$): δ5.89 (d, H-1), 5.55 (dd, H-2), 5.41 (t, H-4), 5.11 (dd, H-3), 3.69 (m, H-5), 3.38 (dd, H-6a), 3.21 (dd, H-6b), 2.28, 2.17, 2.01, 1.79 (s, 12H, 4 CH$_3$).

3.6.4   1,2,3,4-Tetraacetate β-mannopyranose

6-Trityl-1,2,3,4-tetraacetate β-mannose (24.0 g, 40.6 mmol) was dissolved in glacial acetic acid (96 mL) and water (40 mL) and heated to 60 °C for 5 minutes. The solution was diluted into ice cold brine. The trityl groups precipitated and were removed by filtration. The solution was extracted with dichloromethane (50 mL, 4×). The dichloromethane was washed with brine (50 mL, 2×) then saturated sodium bicarbonate solution (50 mL, 2×), dried over Na$_2$SO$_4$, and concentrated to a yellow viscous liquid. The viscous liquid was mixed with ether and product crystallized out to yield 10.7 g (76%) of a fine white powder.

^{1}H NMR (300 MHz, CDCl$_3$): δ5.91 (d, H-1), 5.53 (dd, H-2), 5.30 (t, H-4), 5.18 (dd, H-3), 3.81 (m, 1H, H-5), 3.67 (m, 2H, H-6a,b), 2.25, 2.14, 2.05 (s, 12H, 4 CH$_3$).

3.6.5   6-Acryloxy-1,2,3,4-tetraacetate β-mannopyranose

1,2,3,4-Tetraacetate β-mannose (4.27 g, 12.2 mmol) was dissolved in dichloromethane (42 mL). The solution was deoxygenated with bubbling nitrogen gas before adding triethylamine (3.42 mL, 24.4 mmol). The solution was cooled in an ice bath before acryloyl chloride (1.86 mL, 22.9 mmol) in dichloromethane (8 mL) was added dropwise. The solution was stirred overnight and then filtered to remove triethylamine salts. The dichloromethane solution was washed with brine (50 mL, 3×) and dried over Na$_2$SO$_4$. The solution was stirred with activated carbon, filtered, and concentrated to a yellow viscous liquid. The product was then precipitated from ether. The product was further purified by dissolving in a minimal amount of dichloromethane and precipitating from ether to yield 3.2 g (65%) of a white powder.

^{1}H NMR (300 MHz, CDCl$_3$): δ6.51 (d, 1H, C**H**$_2$=CH), 6.20 (m, CH$_2$=C**H**), 5.93 (d, 1H, C**H**$_2$=CH), 5.93 (d, H-1), 5.53 (dd, H-2), 5.36 (t, H-4), 5.18 (dd, H-3), 4.35 (d, 2H, H-6a,b), 3.9 (m, H-5), 2.25, 2.15, 2.10, 2.05 (s, 12H, 4 CH$_3$).

3.6.6 Methyl 2-bromo-3-(6-acryloxy-2,3,4-triacetate mannopyranosyl) propionate

6-Acryloxy-1,2,3,4-tetraacetate β-mannose (0.38 g, 0.94 mmol) and methyl 2-bromo-3-hydroxypropionate[108] (0.31 g, 1.74 mmol) were dissolved in dichlomethane (6 mL) and cooled in an ice bath before adding boron trifluoride etherate (380 μL, 2.82 mmol). The solution was stirred overnight and then washed with brine (25 mL, 2$\times$) and saturated sodium bicarbonate solution (25 mL), dried over Na_2SO_4, and concentrated to a viscous liquid. Product was then purified with dry column vacuum chromatography (0-85% EtOAc, hexanes). Fractions with $R_f = 0.48$ in 50% EtOAc/hexanes were combined and concentrated to yield 0.39 g (78%) of a clear viscous liquid which was a mixture of 95% β anomer and 5% α anomer. The NMR assignments are for the β anomer.

^{1}H NMR (300 MHz, CDCl$_3$): δ6.49 (d, 1H, C**H**$_2$=CH), 6.19 (m,CH$_2$=C**H**), 5.91 (d, 1H, C**H**$_2$=CH), 5.30 (m, 3H, H-2, H-3, H-4), 4.78 (d, H-1), 4.43 (t, CHBr), 4.37 (dd, CH**H**$_2$O), 3.96 (m, 3H, H-5, H-6a,b), 3.87 (s, CH$_3$), 1.98-2.2 (s, 12H, 4 CH$_3$).

3.6.7 Methyl 2-bromo-3-(2,3,4,6-tetraacetate mannopyranosyl) propionate

Mannose pentaacetate (1.12 g, 2.87 mmol) and methyl 2-bromo-3-hydroxypropionate (0.63 g, 3.44 mmol) was dissolved in dichloromethane (10 mL) and cooled in an ice bath before adding boron trifluoride etherate (1.05 mL, 5.74 mmol). The solution was stirred overnight and then washed with brine (25 mL, 2×) and saturated sodium bicarbonate solution (25 mL), dried over Na_2SO_4, and concentrated to a viscous liquid. Product was then purified with dry column vacuum chromatography (0-85% EtOAc, hexanes). Fractions with $R_f = 0.53$ in 50% EtOAc/hexanes were combined and concentrated to yield 1.11g (75%) of a clear viscous liquid.

^{1}H NMR (300 MHz, CDCl$_3$): δ5.15 (m, 3H, H-2, H-3, H-4), 4.67 (d, H-1), 4.25 (t, CHBr), 4.1 (dd, CH$_2$O), 3.9 (m, 3H, H-5, H-6a,b), 3.6 (s, CH$_3$), 1.98-2.2 (s, 12H, 4 CH$_3$).

3.6.8 1,2;3,4-Di-isopropylidene galactopyranose

A heterogeneous mixture of galactose (5 g, 27.7 mmol), acetone (50 mL), and sulfuric acid (0.25 mL) was stirred for one day. Unreacted galactose (4.3g) was filtered off and recycled. The filtrate was neutralized with sodium bicarbonate and then concentrated to a brown syrup, taken up in dichloromethane (50 mL), and washed with saturated sodium bicarbonate solution (50 mL, 2×) and brine (50 mL, 2×). The dichloromethane solution was concentrated to yield 0.72g (75% of reacted starting material) as a yellow syrup. The reaction was repeated multiple times, combined, and further purified by vacuum distillation (135 °C at full vacuum) to yield a colorless syrup.

^{1}H NMR (300 MHz, CDCl$_3$): δ5.56 (d, H-1), 4.65 (dd, H-3), 4.37 (dd, H-2), 4.26 (dd, H-4), 3.91 (m, 2H, H-6a,b), 3.8 (m, H-5), 1.3-1.57(s, 12H, 4 CH$_3$).

3.6.9   6-Acryloxy-1,2;3,4-di-isopropylidene galactopyranose

1,2;3,4-Di-isopropylidene-galactopyranose (11.7 g, 45.2 mmol) was dissolved in dichloromethane (120 mL). The solution was deoxygenated with bubbling nitrogen gas before adding triethylamine (11.3 mL, 81.4 mmol). The solution was cooled in an ice bath before acryloyl chloride (5.5 mL, 67.8 mmol) in dichloromethane (20 mL) was added dropwise. The solution was stirred overnight and then filtered of triethylamine hydrochloride salts. The dichloromethane solution was washed with saturated sodium bicarbonate solution (50 mL) and then brine(50 mL, 2×), dried over Na_2SO_4, and concentrated to a yellow syrup. Product was then purified with dry column vacuum chromatography (0-50% EtOAc, hexanes) to 13.6g (96%) of a pale yellow syrup.

^{1}H NMR (300 MHz, CDCl$_3$): δ6.48 (d, 1H, C**H**$_2$=CH), 6.20 (m, CH$_2$=C**H**), 5.83 (d, 1H, C**H**$_2$=CH), 5.58 (d, H-1), 4.67 (dd, H-3), 4.46 (m, 4H, H-4, H-5, H-6,b), 4.23 (dd, H-2), 1.28-1.6 (s, 12H, 4 CH$_3$).

3.6.10   6-Acryloxy galactopyranose

6-Acryloxy-1,2;3,4-di-isopropylidene galactopyranose (21 g, 66.8 mmol) was dissolved in acetic acid (100 mL) followed by slow addition of water (100 mL)and heated to 80 °C for six hours. Acetic acid and water were then removed through rotary evaporation and the remaining pale yellow solid taken up in acetone. The precipitate was collected and recrystallized in methanol to yield 8.3 g (53%) of a white powder.

^{1}H NMR (300 MHz, D$_2$O): δ6.34 (d, 1H,C**H**$_2$=CH), 6.09 (m,CH$_2$=C**H**), 5.88 (d, 1H, C**H**$_2$=CH), 5.13 (d, H-1), 4.20 (m, 3H, H-5, H-6a,b), 3.92 (dd,H-4), 3.71 (o, 2H, H-2, H-3).

3.6.11   6-Acryloxy-1,2,3,4-tetraacetate galactopyranose

6-Acryloxy galactopyranose (1.36 g, 5.8 mmol) was dissolved in pyridine (20 mL) and acetic anhydride (3.2 mL, 33.4 mmol) and stirred overnight. The solution was concentrated by rotary evaporation to a brown syrup. The syrup was taken up in dichloromethane (20 mL) and washed with saturated sodium bicarbonate solution (20 mL, 2×) and brine (20 mL, 2×), dried over Na_2SO_4, and concentrated to yield 1.39 g (61%) of a yellow syrup which was a mixture of 80% α anomer and 20% β anomer. The NMR assignments are for the α anomer.

^{1}H NMR (300 MHz, CDCl$_3$): δ6.34 (d, 2H,C**H**$_2$=CH), 6.31 (s, 1H, H-1), 6.02 (m, CH$_2$=C**H**), 5.79 (d, 1H, C**H**$_2$=CH), 5.46 (s, 1H, H-3), 5.27 (m, 2H, H-2, H-4), 4.32 (t, H-5), 4.12 (m, H-6ab), 1.9-2.08 (s, 12H, CH$_3$)

3.6.12   Methyl 2-bromo-3-(6-acryloxy-2,3,4-triacetate galactopyranosyl) propionate

6-Acryloxy-1,2,3,4-tetraacetate galactopyranose (2.84 g, 7.1 mmol) and methyl 2-bromo-3-hydroxypropionate (1.55 g, 8.5 mmol) were dissolved in dichlomethane (30 mL) and cooled in an ice bath before adding boron trifluoride etherate (1 mL, 21 mmol). The solution was stirred overnight and then washed with brine (30 mL, 2×) and saturated sodium bicarbonate solution (30 mL), dried over Na_2SO_4, and concentrated to a viscous syrup. Product was then purified with dry column vacuum chromatography (0-50% EtOAc, hexanes) to yield 1.56 g (43%) of a clear viscous liquid.

^{1}H NMR (500 MHz, CDCl$_3$): δ6.40 (d, 1H, C**H**$_2$=CH), 6.08 (m, CH$_2$=C**H**), 5.84 (d, 1H, C**H**$_2$=CH), 5.43 (dd, 1H, H-4), 5.31 (H-3β), 5.26 (H-1β), 5.12 (H-2α), 5.05 (H-2β), 5.01 (H-3α), 4.52 (t, H-1α), 4.31 (CHBr), 4.08 (CH$_2$, H-6a,b), 3.89 (CH$_3$), 1.8-2.2 (s, 12H, 4 CH$_3$).

3.6.13 Example linear polymerization

Linear polymers were synthesized as described in the following example. CuBr (3.6 mg, 0.025 mmol) and mannose monomer (0.5 g, 1.2 mmol) were placed in a reaction flask, degassed, and backfilled with nitrogen. Me$_6$Tren (7.2 μL, 0.025 mmol) was added and the contents stirred under nitrogen for 45 minutes. Mannose initiator (12.7 mg, 0.025 mmol) in 1 mL ethyl acetate was added via syringe. The flask contents were degassed through five freeze-pump-thaw cycles and stirred at 100 °C for 70 hours. Contents were passed through an alumina plug and then precipitated into cold methanol to result in 0.28 g (55%) of a fine white powder. The ratio of mannose monomer to mannose initiator was varied between 25 and 100 to create the linear polymers.

3.6.14 Example branched polymerization

Hyperbranched polymers were synthesized as described in the following example. CuBr (5 mg, 0.035 mmol) and mannose monomer (0.31 g, 0.77 mmol) were placed in a reaction flask, degassed and backfilled with nitrogen. Me$_6$Tren (10 μL, 0.035 mmol) was added and the contents stirred under nitrogen for 45 minutes. Mannose inimer (0.203 g, 0.38 mmol) in 0.81 mL ethyl acetate was added. The flask contents were degassed through five freeze-pump-thaw cycles and stirred at 100 °C for 70 hours. Contents were passed through an alumina plug and then precipitated into cold methanol to result in 0.27 g (53%) of a fine white powder. The ratio of mannose monomer to mannose inimer was varied between 1:1 and 10:1 to vary the apparent branching density.

3.6.15 Example polymer deprotection

Polymers were deprotected as described in the following example. 50 mg of a linear mannose polymer with 42 repeat units was dissolved in 5 mL chloroform and 5 mL methanol. Deprotected polymer began to precipitate after adding sodium methoxide (5.5 μL of 5.4 M solution, 0.03 mmol). After five minutes, the solution was centrifuged to collect the precipitate. The precipitate was washed with chloroform and centrifuged again before decanting the supernatant and drying the polymer to collect 24 mg (83%) of a pale yellow powder.

CHAPTER 4

Synthesis of protein-glycopolymers

Pathogen associated glycoproteins contain foreign glycans that are targeted by the host immune system.[116] Synthetic mimics of these pathogenic glycoproteins are potential immune modulators to activate innate immunity or vaccinate against a target glycan. Glycopolymers can be used as mimics of the glycan component. These glycopolymers can incorporate a protein component through two synthetic routes: "grafting-to" where a pre-made polymer is conjugated to an amino acid through a covalent bond, or "grafting-from" where monomers are polymerized directly from a protein macroinitiator.

All previously described protein-glycopolymers have been synthesized through the grafting-to route. Haddleton and coworkers grafted mannose glycopolymers to bovine serum albumin at Cys34 through a maleimide chain end.[5] The BSA-mannose glycopolymer bound mannose binding lectin of immune complement and could activate complement cascade. Another group synthesized a glycopolymer with pendant mannan trisaccharides that was grafted to chicken serum albumin through azide-alkyne click chemistry and used to vaccinate against Candida albicans.[6]

Protein-glycopolymers for applications beyond immune modulation have also been described. Proteins were stabilized with a trehalose glycopolymer through disulfide exchange with pyridyl disulfide chain ends. Trehalose is a disaccharide that helps microorganisms resist desiccation and temperature stresses, and in this case, provides excellent stability for proteins against dehydration and heat.[8] In another example, glycopolymers polymerized from a biotinylated ATRP initiator

were bound with streptavidin to create streptavidin conjugated glycopolymer.[7] With all these cases, post-conjugation purification is required to remove unreacted polymer or protein. Purification can be a relatively simple process by using differences in affinity, molecular weight, or solubility to isolate the protein-polymer; otherwise, fractionation via size exclusion chromatography is necessary.

An alternative is a grafting-from approach where the protein is modified as a macroinitiator for direct polymerization of monomers. If no residual unmodified protein is present, facile purification through dialysis or centrifugal filtration can be used to remove low molecular weight monomer and polymerization byproducts rather than using costly chromatography techniques. Maynard has previously reported the polymerization of a *N*-acetyl glucosamine derived monomer from a peptide initiator[56] but no examples of glycopolymerizations from proteins exist in literature to my knowledge.

In this chapter, I describe a grafting-from approach to polymerize glycomonomers from multiple sites of a protein macroinitiator (mannose and/or galactose from bovine serum albumin). To my knowledge, this is the first report of glycopolymers grafted from a protein. Polymers of different lengths and saccharide composition were synthesized and then characterized for their carbohydrate content and polymer size. Mannose content of the glycopolymers was varied either through polymerization of different mannose chain lengths or by copolymerization with galactose to reduce the density of mannose. These compounds can serve as glycomimetics of natural glycoproteins with applications in tissue engineering, or as activators of innate or adaptive immunity. Furthermore, the design of the polymer-protein conjugate allows us to determine the effect of multivalent spatial orientation on lectin binding in Chapter 6.

4.1 Synthesis of mannose and galactose monomers

Mannose and galactose were chosen as the polymerizable saccharides for this study because mannose is generally reactive with immune system proteins (mannose binding lectin, macrophage mannose receptor) while galactose is not. The mannose-based glycomonomer, 6-acryloxy mannopyranose, was synthesized by removing acetates from 6-acryloxy-1,2,3,4-tetraacetate β-mannopyranose with sodium methoxide. Exposure of the sugar to the basic deprotection conditions was limited to four minutes to minimize cleavage of the acrylate group. The galactose based glycomonomer, 6-acryloxy galactopyranose, was prepared from the original saccharide in three steps. The 1,2- and 3,4- hydroxyls were first protected with isopropylidene groups by stirring galactose in acetone with sulfuric acid, leaving the 6- position available for acrylation with acryloyl chloride. The isopropylidene protecting groups were then removed with acetic acid (Scheme 4.1)
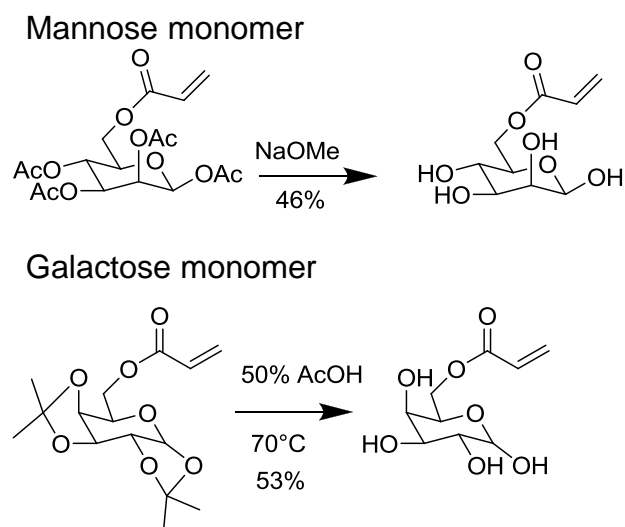
Scheme 4.1: Synthesis of 6-acryloxy mannopyranose and 6-acryloxy galactopyranose.

4.2 Synthesis of initiators

Bovine serum albumin (BSA) is an inexpensive model protein that has been used for previous protein-polymer conjugates, typically using BSA's single free thiol as the polymer attachment site.[40, 117, 118] While this method results in a single polymer chain at a known location, it also requires separation of unreacted protein as only half of the BSA molecules have a free thiol available for conjugation.[119] Instead of attaching the initiator through the thiol, BSA was transformed into a protein macroinitiator through reaction of lysine amines with 2-bromopropionic N-hydroxysuccinimide ester (Scheme 4.2). Another group has formed a protein macroinitiator by modifying a single lysine residue,[120] but we chose to react multiple lysines. This choice sacrifices some uniformity of the resulting protein-polymer conjugates, but allows us to grow multiple polymer chains and explore the effect of 3D spatial orientation of glycopolymer chains on lectin binding. MALDI-TOF confirmed conjugation of the initiator group with disappearance of the original BSA peak at 66.4 kDa and appearance of a peak centered at 69.4 kDa, which corresponds to 22 initiating sites per BSA (Figure 4.1).

ATRP of glycomonomers from the protein macroinitiator alone were unsuccessful. Addition of soluble ethyl bromopropionate as a sacrificial initiator allowed for full initiation of the macroinitiator. Sacrificial initiators have been used during surface polymerizations[121] as well as protein polymerizations.[122] Resin-bound sacrificial initiator, synthesized through reaction of 2-bromopropionyl bromide with Wang resin (Scheme 4.2), was used so that polymer grown from the sacrificial initiator could be easily removed through filtration or centrifugation.

Bovine serum albumin macroinitiator
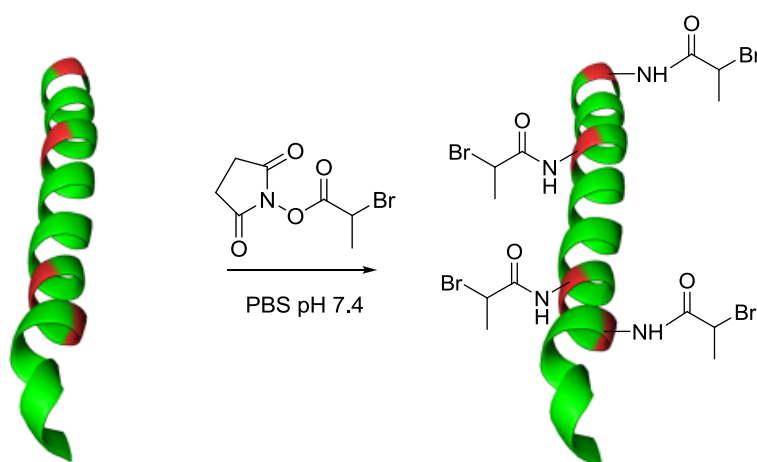
Resin based sacrificial initiator
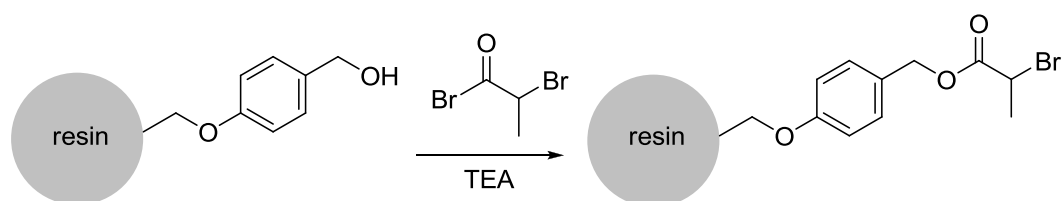
Scheme 4.2: Synthesis of bovine serum albumin macroinitiator (fragment shown here) and resin based sacrificial initiator.
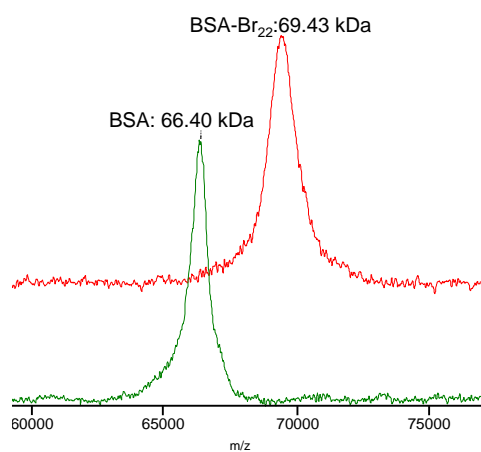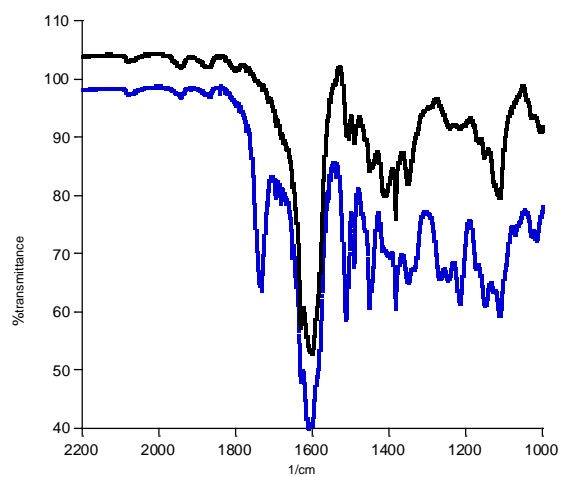
Figure 4.1: (a) MALDI-TOF of BSA-macroinitiator (with peak at 69.4 kDa) versus BSA (with peak at 66.4 kDa) and (b) IR of resin sacrificial initiator (with ester peak at 1730 cm^{-1}) versus Wang resin.

4.3 Synthesis of protein-glycopolymers

Mannose and galactose glycomonomers were homopolymerized separately or copoly-merized together from the BSA macroinitiator in the presence of the resin-bound sacrificial initiator. Polymerization was started by transferring a degassed solution of CuBr/PMDETA and monomer via cannula into a degassed flask containing resin-bound sacrificial initiator (Scheme 4.3). The sacrificial initiator was neces-sary to generate sufficient Cu(II) to control the atom transfer equilibrium. After stirring the solution for ten minutes, a degassed solution of protein macroinitiator and monomer was transferred through a cannula. The solution was stirred for four hours before stopping the polymerization. We adjusted the feed ratio of glycomonomer to initiator (M1200, M600, M150, G600, G300, G150) to elucidate the effect of glycopolymer length and saccharide identity on MBL binding, and copolymerized mannose and galactose together (MG300300, MG150150, MG7575) to elucidate the effect of mannose density.

The resin-bound polymer was removed through centrifugation. The supernatant of the initial centrifugation was then placed in an Amicon centrifugal filtration device and centrifuged again to concentrate the protein-glycopolymer and remove any compounds with molecular weight below 3,000 Da (unreacted monomer, copper). No further purification techniques such as chromatography were necessary.
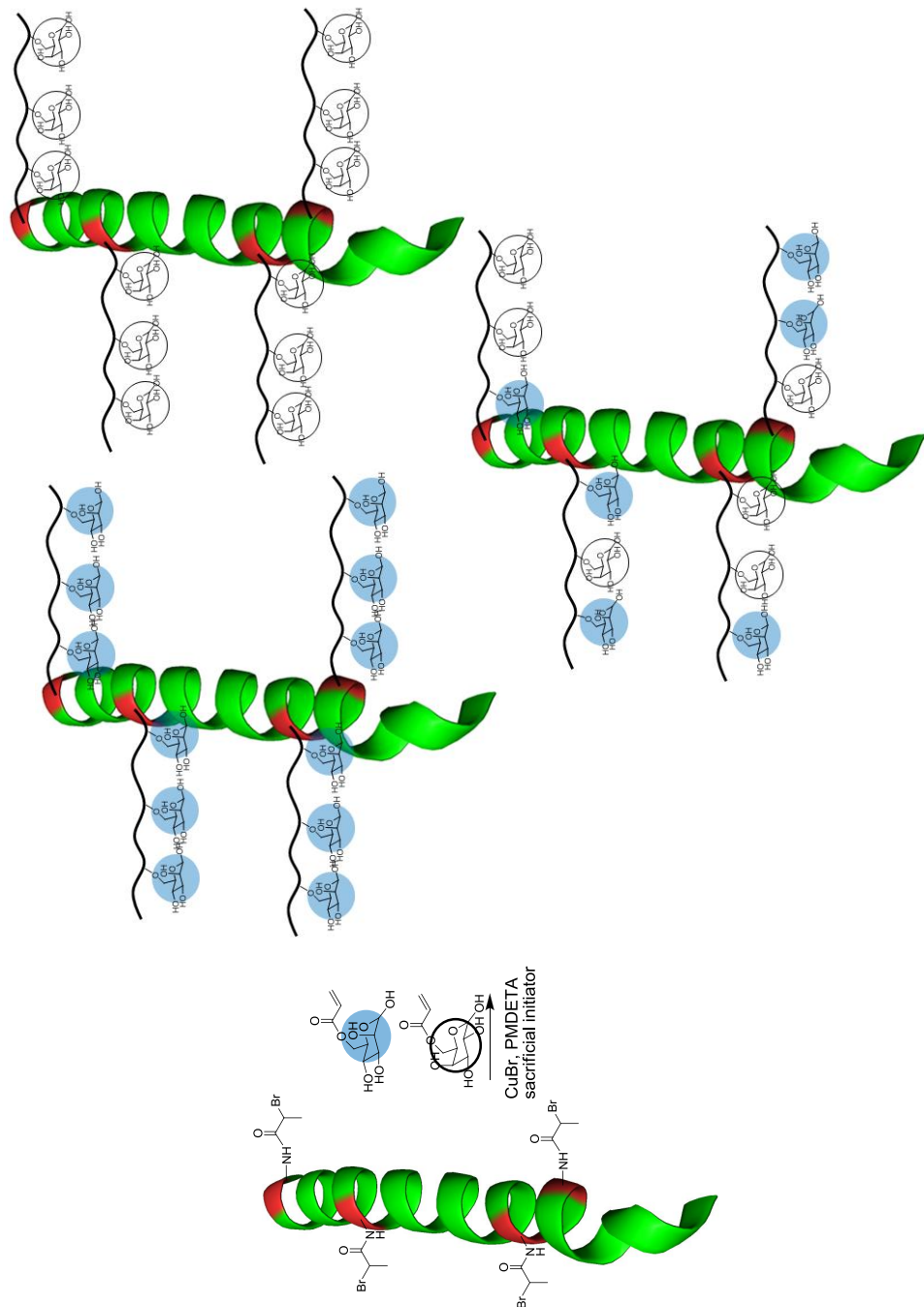
Scheme 4.3: Glycopolymerizations of mannose/galactose acrylate from BSA macroinitiator (fragment shown here) to form homopolymers or copolymers.

4.4 Characterization of glycopolymers

The protein-glycopolymers were characterized with aqueous GPC and SDS-PAGE (Figure 4.2, Table 4.1). GPC curves showed decreasing elution time and increasing curve width as the feed ratio of monomer was increased. These results suggest that molecular weight and polydispersity of the protein-polymer increase with the feed ratio, although no definite numbers can be assigned due to the lack of comparable standards. SDS-PAGE showed similar results with a decrease in migration distance and larger bands with increasing feed ratio. The large bands and presumably high polydispersity can be due to the variable number of polymer chains growing from each protein macroinitiator, but has also been attributed to increased friction between the protein-glycopolymer and the acrylamide gel.[123] It is also important to note that SDS-PAGE showed full conversion of the BSA macroinitiator in all polymerizations so that no separation of unreacted protein was required.

The number of saccharides per protein was determined with bicinchoninic acid assay and phenol-sulfuric acid assay (Table 4.1).[124] The glycopolymers contained from 70 to 360 saccharides. This number was higher than expected, indicating that the resin-bound initiator had lower initiation efficiency than the protein macroinitiator or that the resin-bound chains terminated prematurely. Saccharide content of the copolymers was assumed to be evenly divided between mannose and galactose given the similar structure and presumably reactivity of the two monomers.
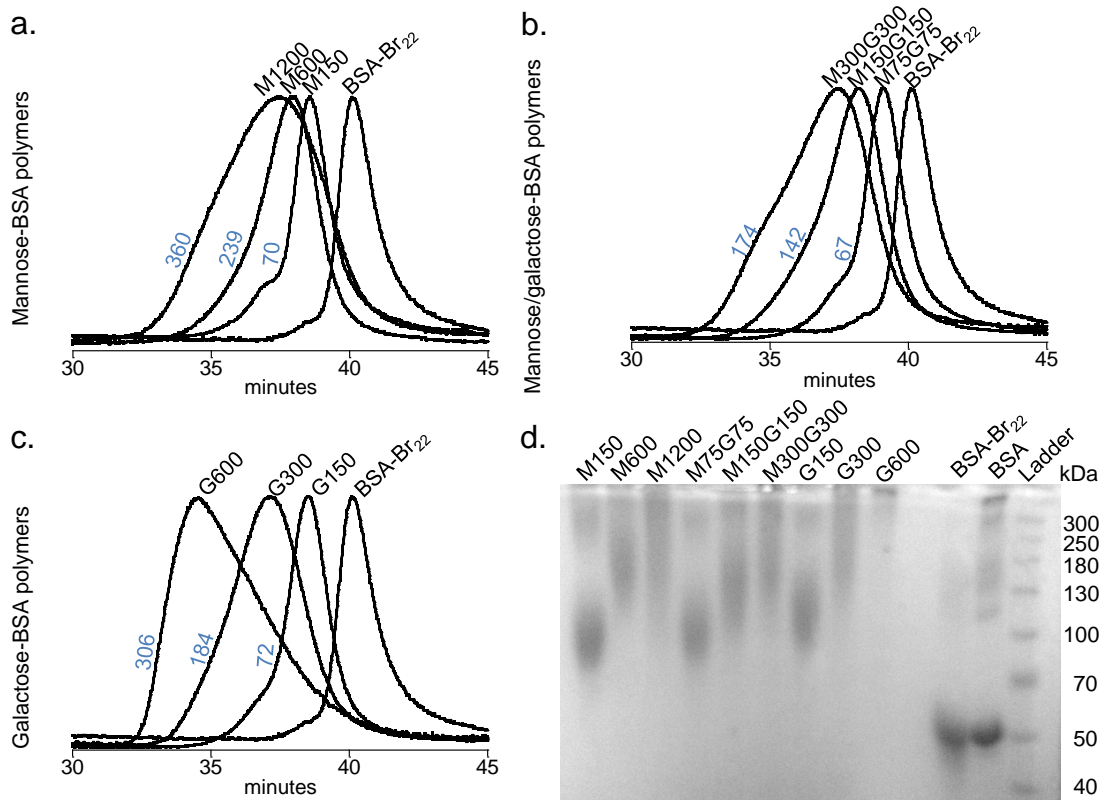
Figure 4.2: GPC traces of (a) mannose-BSA polymers, (b) mannose/galactose-BSA polymers, and (c) galactose-BSA polymers, and (d) SDS-PAGE of all glycopolymers and starting material proteins.

Table 4.1: Elution time and number of saccharides of each protein-glycopolymer.

Entry	[Mannose]:[Galactose]: [Resin-Br]:[BSA-Br$_{22}$]: [CuBr]:[PMDETA]	Peak elution time (min)	# saccharides
M1200	1200:0:3:1:30:30	37.4	360 ± 35
M600	600:0:3:1:30:30	38.0	239 ± 21
M150	150:0:3:1:30:30	38.6	70 ± 19
MG300300	300:300:3:1:30:30	37.5	174 ± 17
MG150150	150:150:3:1:30:30	38.2	142 ± 13
MG7575	75:75:3:1:30:30	39.1	67 ± 3
G600	0:600:3:1:30:30	34.6	306 ± 76
G300	0:300:3:1:30:30	37.1	184 ± 43
G150	0:150:3:1:30:30	38.5	72 ± 4

If we assume the glycopolymers grew evenly between all 22 initiating sites of the protein macroinitiator, each polymer chain statistically would have degrees of polymerization from 3 to 16. To validate this assumption, we characterized the glycopolymer conjugates through a variety of assays. FT-IR, NMR, BSA esterase, and tryptic digest were used to attempt to identify any unreacted initator groups. If a significant amount of unreacted initiator group was found, the polymer chains would be much longer than the current assumption.

The protein-glycopolymers were also hydrolyzed to their component amino acids, saccharides, and poly(acrylic acid) backbones and characterized with GPC and NMR to determine the size of the polymer chains. If polymerization was initiated from just a few sites, the polymer would be long. Conversely, if most of the initiating sites were active, each polymer chain would be short.
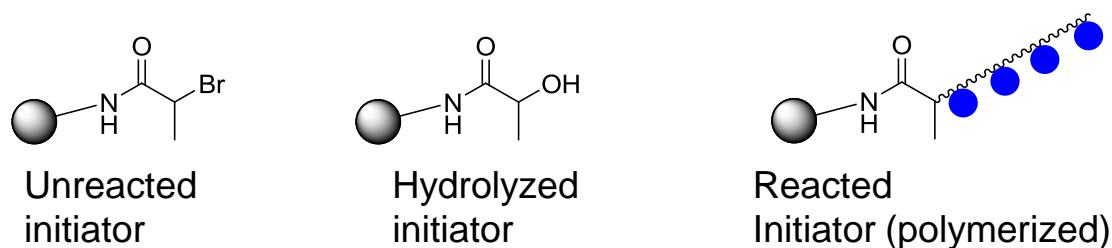
Figure 4.3: Potential structures of initiator post-polymerization: unreacted initiator, hydrolyzed initiator, and reacted initiator.

The lysine modified with an initiator group could have three general structures post-polymerization: unreacted initiator, hydrolyzed initiator, and reacted initiator (Figure 4.3). FT-IR of glycopolymers and starting material proteins did not reveal any peaks that could distinguish between the amide from peptide bonds and the amide from the three structures (Figure 4.4). When comparing BSA starting material to the other samples, there was a decrease in transmittance at 1650 cm^{-1} correlating to an amide bond from any of the three structures; however, differences between the three possible structures could not determined. There was also a

decrease in transmittance at 2900 cm^{-1} in the BSA-Br$_{22}$ sample correlating to the methyl. As the feed ratio of galactose to initiator increased, the peak shape changed slightly which could point to some differences in initiator structure, but this analysis is complicated by C-H absorption in the same region from the saccharide or polymer backbone. FT-IR thus did not provide any further information on the structure of the initiator.

FT-IR did show that saccharide content increased from G150 to G600 as seen by the larger decrease in transmittance at 3400 cm^{-1} and 1730 cm^{-1} which were from saccharide hydroxyls and esters from the polymer respectively.

NMR analysis of the protein samples, shown in Figure 4.5, also failed to identify any of the three general structures in Figure 4.3. It was hoped that peaks from the conjugated initiator would appear as sharp peaks compared to the broader protein resonances. While there were differences between BSA, BSA-Br$_{22}$, and M150 as well as peaks that could correspond to the initiator group, the peaks were obscured by the polymer backbone and amino acid side chains so no definitive conclusion could be made. However, NMR was able to identify the saccharide component of the glycopolymerizations (anomeric proton at 5.1 ppm, broad peaks 3-4.5 ppm).
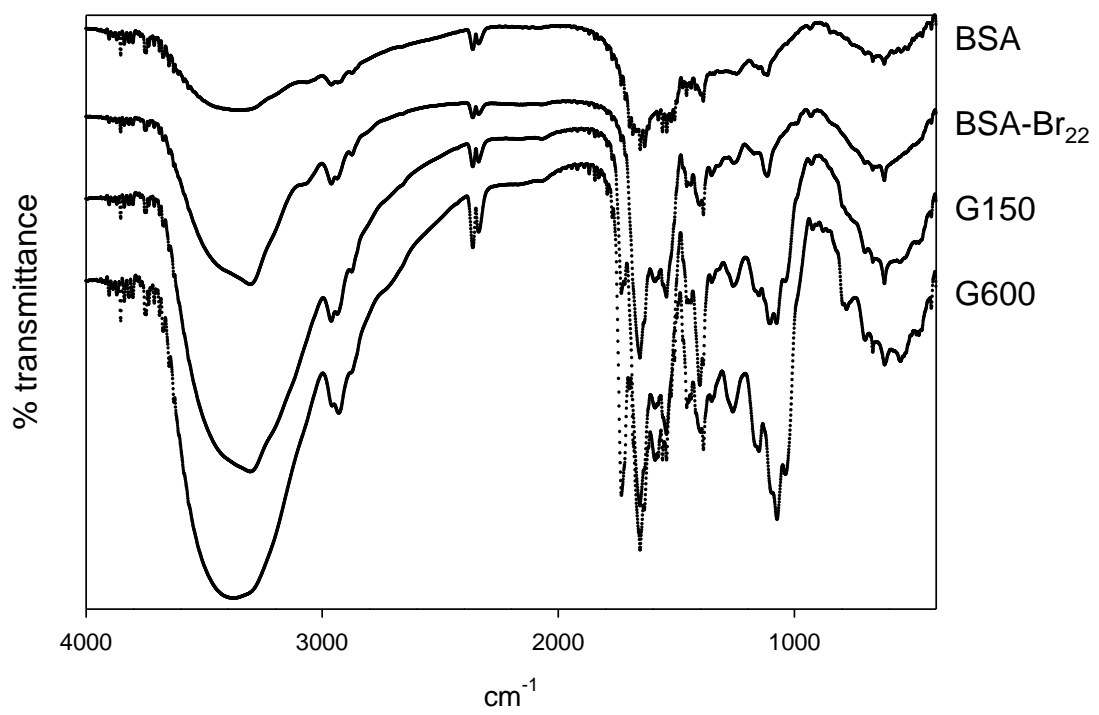
Figure 4.4: Overlaid FT-IR spectra of BSA, BSA-Br$_{22}$, G150, and G600.
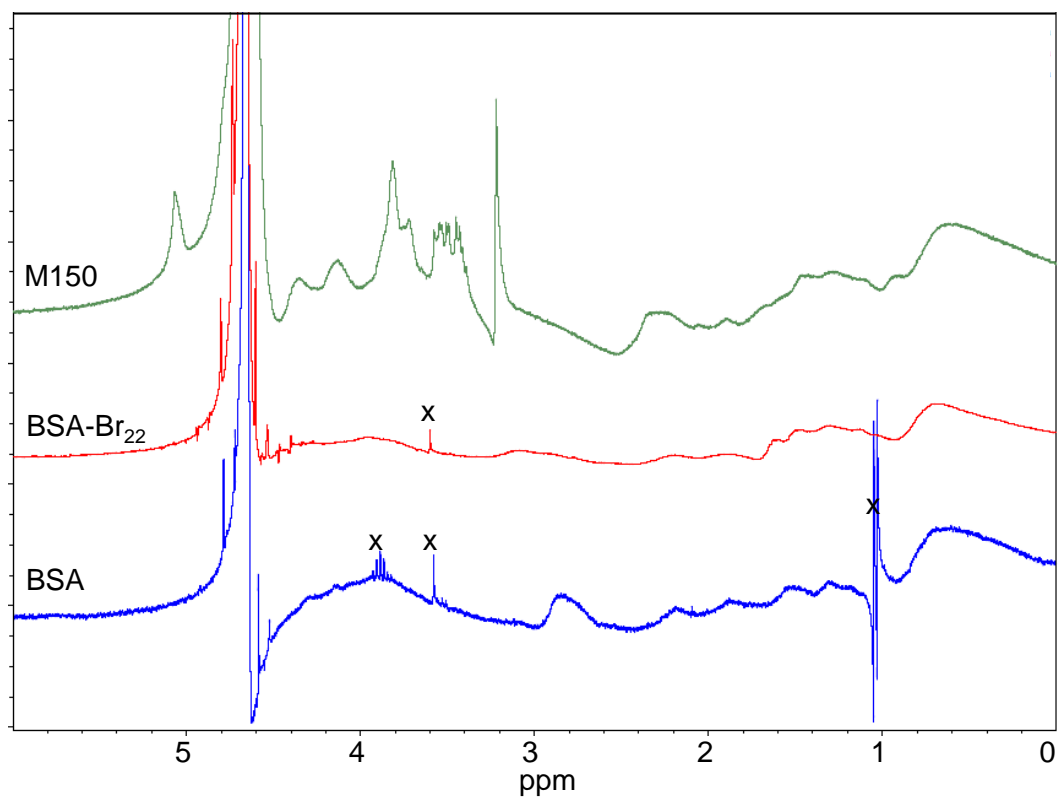
Figure 4.5: Overlaid ^{1}H NMR spectra of BSA, BSA-Br$_{22}$, and M150.

Albumins have pseudo-enzymatic activity through the cleavage of esters, amides, and other bonds. The enzyme-like activity is from irreversible chemical modifications of the protein rather than catalytic activity at an active site.[125] Amino acids such as aspartic acid, lysine, and tyrosine are susceptible to this reaction. This activity is most easily tested through the hydrolysis of p-nitrophenyl acetate (PNA) by BSA to form p-nitrophenol which could be monitored at 410 nm. Differences between the hydrolysis rates by protein-polymers could indicate differences in coverage of the initiator or steric hindrance of the polymer.

Figure 4.6 shows that while modified BSA retains some pseudo-enzymatic activity (all curves are corrected to remove the effect of PNA's hydrolysis in water), native BSA exhibits much higher activity. These results are not surprising as the pseudo-enzymatic activity is from the acetylation of lysines. The BSA macroinitiator scheme reacts many of the available amines with the initiator group so that fewer amines are available to hydrolyze PNA. The protein-polymers have higher rates of hydrolysis due to hydrolysis of PNA by saccharide hydroxyls. Unfortunately, these BSA-esterase results do not provide any further information on the location or size of the individual polymer chains.

Tryptic digests have been used previously with protein-polymer conjugates to discover the site of initiator conjugation.[120, 122] Trypsin cuts proteins into peptides following lysines or, to a lesser extent, arginines. Modifications of the lysines or arginines will hinder cleavage by trypsin and result in a different digest pattern. However, our BSA-macroinitiator contains many initiating sites so identifying the specific modified amino acids would be extraordinarily complex. In our case, tryptic digest can provide some information on whether all initiating sites are active and whether the polymer chains can sterically hinder trypsin activity.

BSA, BSA-Br$_{22}$, G600, G300, and G150 were cleaved with trypsin, and the resulting peptides were characterized by MALDI-TOF (Figure 4.7). The predominant peptide fragment after digestion of BSA was a peak at 1568 m/z which

corresponds to peptide sequence DAFLGSFLYEYSR. This peak was present in all other samples as well and was used to normalize the results. Digestion of BSA-Br$_{22}$ and the galactose conjugates resulted in a peptide fragment at 1731 and 1777 m/z that was present across all the modified samples. Conjugation of the initiator to an amine results in a mass increase of 135 Da. This increase matches exactly with the peptide sequence HPEYAVSVLLRLAK with a modified lysine (1596 + 135 = 1731). A disodium adduct (+46) results in the 1777 m/z peak. Identification of a peptide fragment that contains an uninitiated bromide shows that at least one initiating site does not have polymer.

The tryptic digest results also provide more information on the steric nature of the glycopolymer chains. As the polymer length increases, the ratio of peak height of 1568 and 1731 decreases (Figure 4.7f). The polymer chains sterically hinder trypsin from cutting the peptide fragment at 1731 (as well as 1777). The HPEYAVSVLLRLAK sequence is flanked by lysines 12 and 15 residues away (Lys346 and Lys386). While there is no information on whether there are initiating groups or polymer chains at those amino acids, it is a reasonable assumption that one or both of those sites have polymer that are large enough to disrupt trypsin from interacting with the protein, resulting in the decrease in tryptic activity as polymer length increases.

The protein-glycopolymers were heated with 6 M hydrochloric acid to cleave all amide and ester bonds, resulting in the protein-polymer being hydrolyzed to its amino acids, saccharides, and poly(acrylic acid) backbones. If the poly(acrylic acid) chain length could be determined, the number of saccharides per polymer can also be calculated.

NMR of the cleaved protein-polymer samples showed resonances from amino acids, saccharides, and potentially the poly(acrylic acid) backbone (Figure 4.8). Qualitatively, the integration of the ppm region corresponding to the poly(acrylic acid) backbone increased as monomer feed ratio increased, when normalized to a

peak in the aromatic region. The aromatic peak was chosen as each sample should have the same concentration of amino acids containing aromatics (phenylalanine, tyrosine, tryptophan). However, the overlap of peaks between amino acids and the polymer backbone and chain end combined with the low concentration of polymer prevented any quantification of the polymer's NMR derived molecular weight.

GPC of the hydrolyzed protein samples, shown in Figure 4.9, separated the poly(acrylic acid) backbone from the amino acids and saccharides. If the polymer only grew from a few initiator sites and were therefore high molecular weight, a polymer peak that elutes at a much earlier time would be expected. Instead, the GPC traces showed the elution of presumably poly(acrylic acid) chains (highlighted) followed very closely by the hydrolyzed amino acids and saccharides. This elution behavior is consistent with shorter polymer chains grown from most initiation sites.

When coupled with the tryptic digest experiments, this result shows that while the protein-glycopolymers are not initiated at every site, sufficient polymer chains are grown to result in relatively short chains. While quantifying the polymer length would be ideal, efforts to do so were unsuccessful. Poly(acrylic acid) standards were not available to measure the molecular weight through GPC, and efforts to quantify the molecular weight via MALDI were complicated by the high concentration of other compounds, combined with the expected small molecular weight of the polymers. Nevertheless, we can assume that a close approximation of the number of saccharides per polymer chain can be deduced from # of saccharides per protein/# of initiator sites.
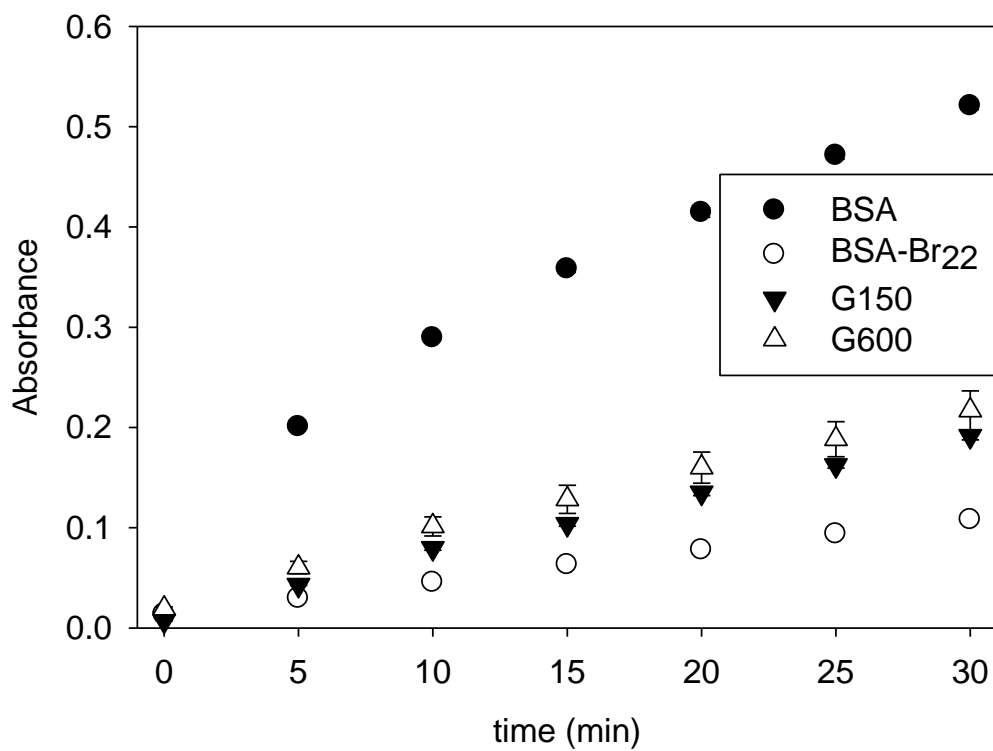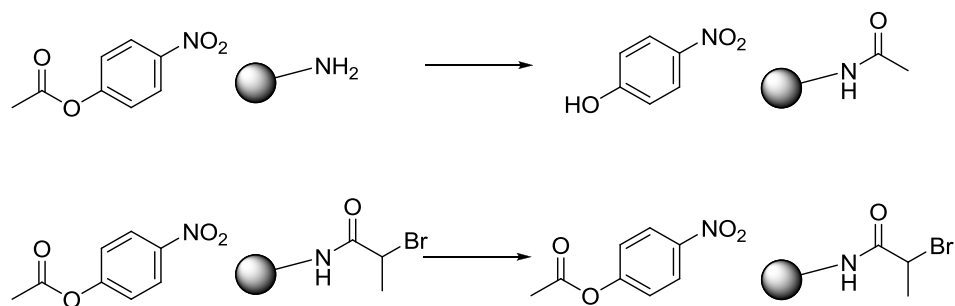
Figure 4.6: Hydrolysis of p-nitrophenyl acetate by BSA, BSA-Br$_{22}$, G150, and G600. Curves are corrected to remove PNA's hydrolysis in water.
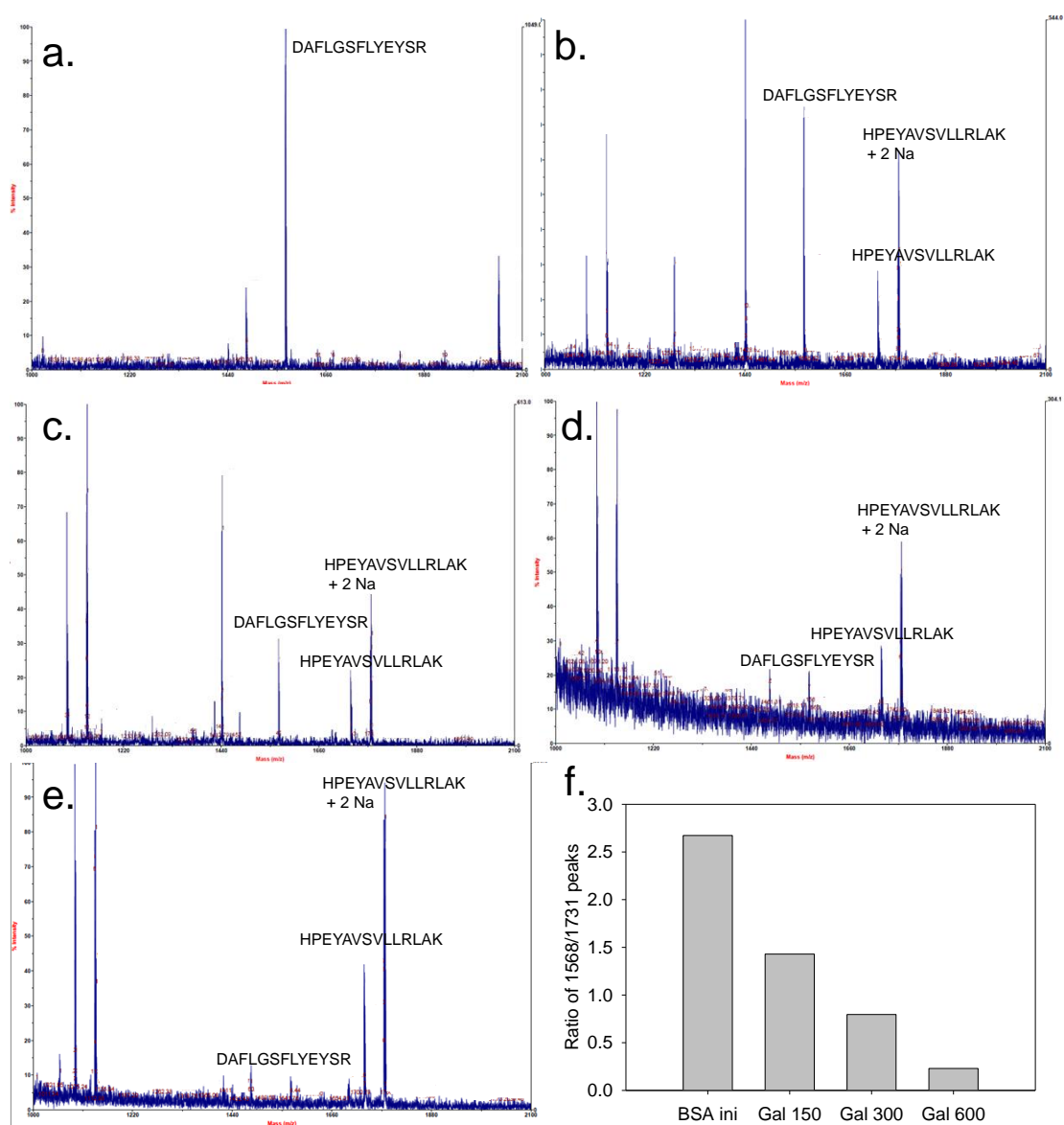
Figure 4.7: MALDI spectra of tryptic digest of (a) BSA, (b) BSA macroinitiator, (c) G150, (d) G300, (e) G600. (f) The ratio of peak heights changes as polymer length increases. The peak at 1568 m/z is found in all samples and is treated as a normalizing peak, and corresponds to peptide sequence DAFLGSFLYEYSR. The peak at 1731 m/z is found only in the BSA macroinitiator and glycopolymer samples, and corresponds to peptide sequence HPEYAVSVLLRLAK with an unreacted initiator group.

86
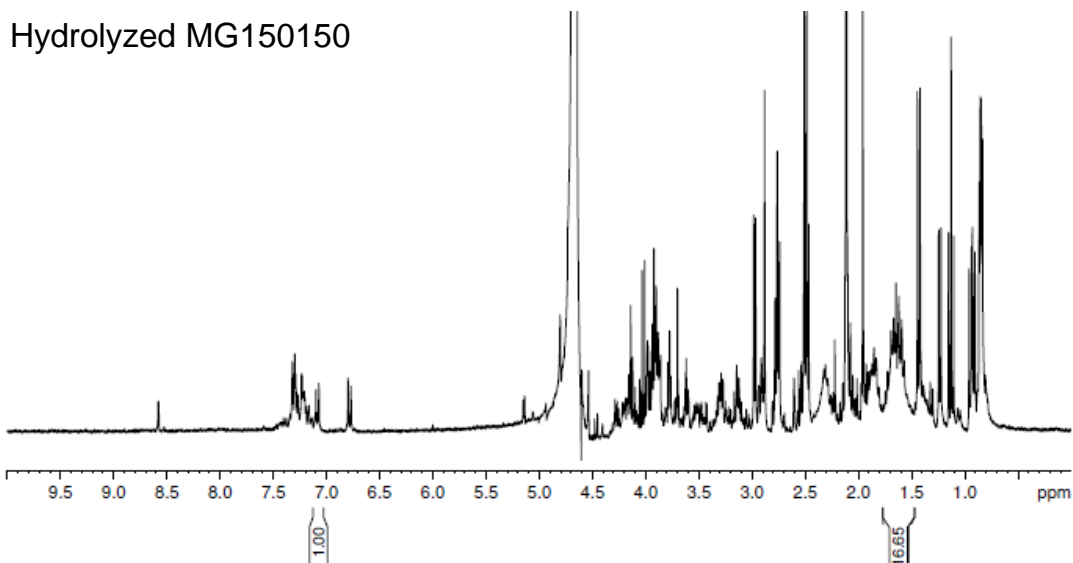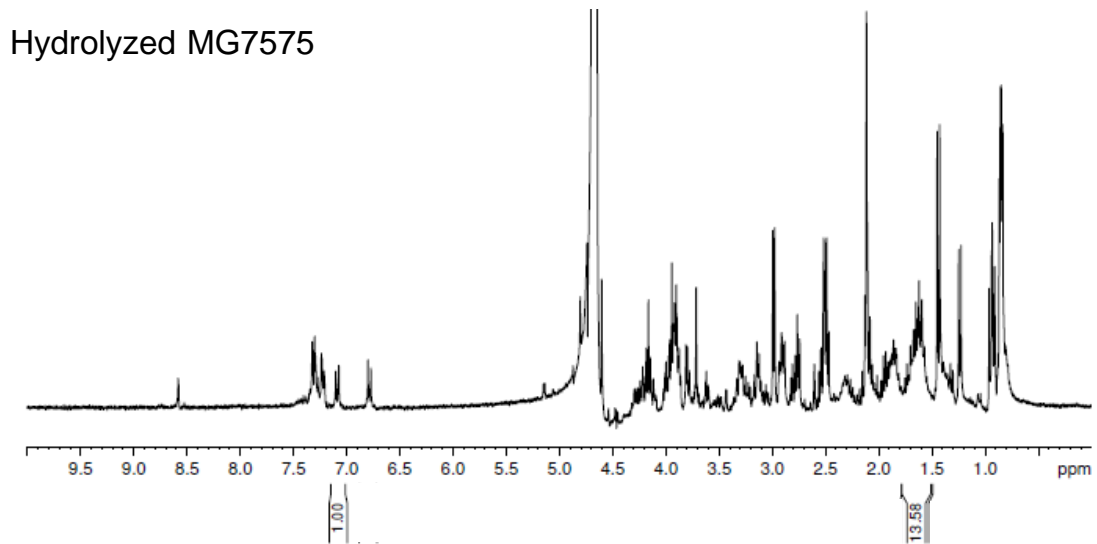
Figure 4.8: ^{1}H NMR spectra of hydrolyzed MG7575 and MG150150. Integration of poly(acrylic acid) backbone increases with feed ratio.
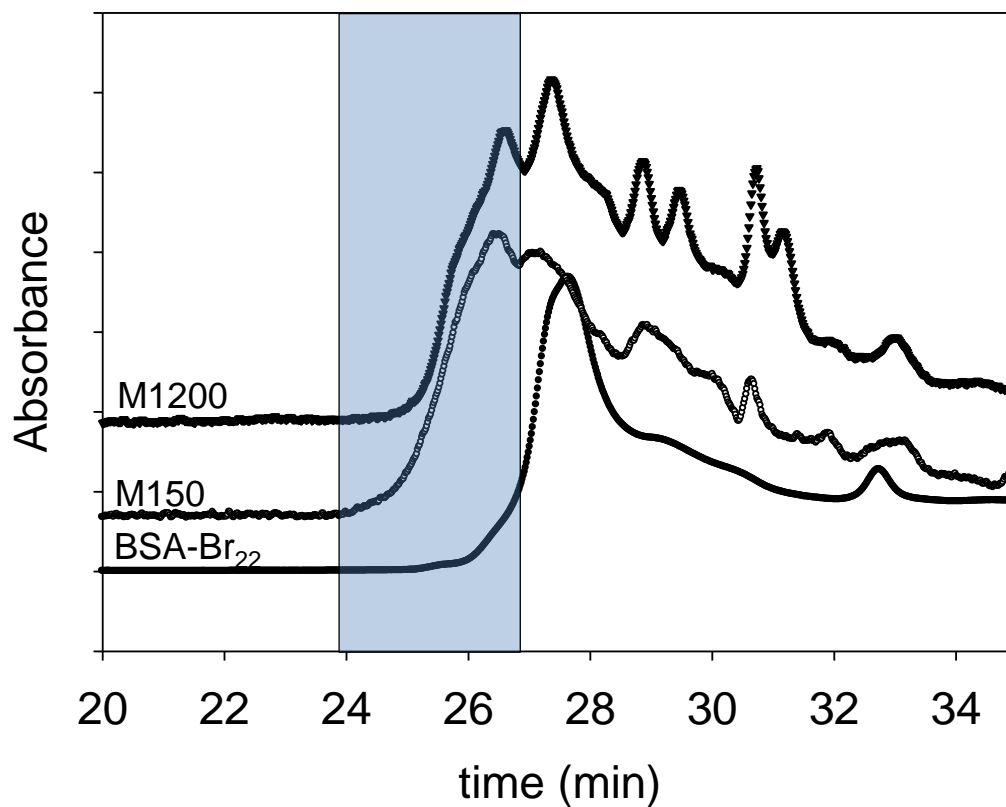
Figure 4.9: Overlaid GPC traces of hydrolyzed BSA-Br$_{22}$, M150, and M1200. Highlighted region shows presumably poly(acrylic acid) chains, separate from lower molecular weight amino acids and saccharides.

4.5 Conclusions

In this chapter, I described the synthesis of water soluble mannose and galactose monomers that were polymerized directly from a bovine serum albumin macroinitiator in the presence of a resin-bound sacrificial initiator. These polymers are the first example of glycopolymer polymerized directly from a protein in a grafting-from method. These protein-glycopolymers did not require chromatographic purification to remove unreacted macroinitiator or unattached glycopolymer chains, an improvement over other polymerization methods which require costly purification. The protein-polymers were characterized by GPC and phenol-sulfuric acid assay to determine the total conjugate size and carbohydrate content. A number of other experiments (NMR, FT-IR, BSA-esterase, tryptic digest, acid hydrolysis) were conducted to determine the number of saccharides per polymer chain. The immune applications of these protein-glycopolymers will be tested in Chapter 6 for their interaction with mannose binding lectin and their ability to activate complement.

4.6 Experimentals

4.6.1 Materials

Acetic acid (Mallinckrodt, ACS grade), bovine serum albumin (Fisher, biotechnology grade), 2-bromopropionic acid (TCI, 98%), 2-bromopropionyl bromide (Alfa Aesar, 97%), dimethyl sulfoxide (Fisher, ACS grade), Dowex 50WX8 ion exchange resin (Aldrich, 200-400 mesh), 1-ethyl-3-(3-dimethylaminopropyl)carbodiimide hydrochloride (Advanced Chem Tech, 98%), hydrochloric acid (Fisher, ACS grade), N-hydroxysuccinimide (Alfa Aesar, 98+%), methanol (EMD, Drisolv), sodium methoxide (Acros, 30wt% in methanol), and trypsin (Thermo Scientific, MS grade) and Wang resin (ChemPep, loading 1 mmol/g) were used as received. 6-Acryloxy-1,2,3,4-tetraacetate β-mannopyranose and 6-acryloxy-1,2;3,4-

di-isopropylidene galactopyranose were synthesized as described in Chapter 3. Copper bromide (Acros, 98%) was purified by stirring in glacial acetic acid and then rinsing with ethanol. N,N,N',N'',N''-pentamethyldiethylenetriamine (Pfaltz and Bauer, 99%) was distilled from CaH_2. Dialysis tubing with 1000 MWCO (Spectrum Labs) and centrifugal filter units with 3000 MWCO (Amicon Ultra) were used for protein purification.

4.6.2 Analytical Techniques

^{1}H NMR spectra (δ ppm) were recorded on Bruker Biospin Ultrashield 300 MHz or 500 MHz NMR Spectrometers. Gel permeation chromatography (GPC) was conducted on a Waters system equipped with UV/vis absorbance and refractive index detectors and four Waters ultrahydrogel columns (100-5K, 1K-80K, 10K-400K, 2K-4M, 500-10M). Phosphate buffer with 10 mM PBS and 0.3 M NaCl at pH 6.6 was used a eluent with a flow rate of 1.0 mL/min. Matrix-assisted laser desorption/ionization (MALDI) was conducted on an Applied Biosystems Voyager-DE-STR MALDI-TOF using sinapic acid as matrix. FT-IR was conducted on a Jasco Model 420.

4.6.3 6-Acryloxy mannopyranose

Sodium methoxide (23 μL of a 5.4 M solution, 0.12 mmol) was added to 5 mL methanol. 6-acryloxy-1,2,3,4-tetraacetate β-mannopyranose (0.5 g, 1.2 mmol) was dissolved in 5 mL dichloromethane. The two solutions were combined and stirred for four minutes before adding Dowex 50WX8 200-400 mesh ion exchange resin. The resin was stirred with the solution for 30 minutes and then filtered out. Product was then purified with dry column vacuum chromatography (0-40% methanol/DCM). Fractions at $R_f = 0.2$ in 25% methanol/DCM were combined and concentrated to yield 0.14 g (46%) of a clear syrup. Fractions at higher R_f with uncleaved acetates were also collected and could be rereacted with sodium methoxide.

^{1}H NMR (500 MHz, D$_2$O): δ6.37(d, 1H, C**H**$_2$=CH), 6.13 (m, CH$_2$=C**H**), 5.89 (d, C**H**$_2$=CH), 5.03 (s, H-1), 4.32 (o, 2H, H-6a,b), 3.91 (q, 1H, H-4), 3.81 (d, 1H, H-2), 3.73 (dd, 1H, H-5), 3.62 (t, 1H, H-3).

4.6.4 6-Acryloxy galactopyranose

6-Acryloxy-1,2;3,4-di-isopropylidene galactopyranose (21 g, 66.8 mmol) was dissolved in acetic acid (100 mL) followed by slow addition of water (100 mL)and heated to 80 °C for six hours. Acetic acid and water were then removed through rotary evaporation and the remaining pale yellow solid taken up in acetone. The precipitate was collected and recrystallized in methanol to yield 8.3 g (53%) of a white powder.

^{1}H NMR (300 MHz, D$_2$O): δ6.34 (d, 1H,C**H**$_2$=CH), 6.09 (m,CH$_2$=C**H**), 5.88 (d, 1H, C**H**$_2$=CH), 5.13 (d, H-1), 4.20 (m, 3H, H-5, H-6a,b), 3.92 (dd,H-4), 3.71 (o, 2H, H-2, H-3).

4.6.5 NHS 2-bromopropionate

2-Bromopropionic acid (1 g, 6.5 mmol), N-hydroxysuccinimide (1.12 g, 9.8 mmol), and 1-ethyl-3-(3-dimethylaminopropyl)carbodiimide hydrochloride (EDC) (2 g, 10.4 mmol) were dissolved in 30 mL dichloromethane and stirred for 4 hours. The organic solution was then washed with brine (20 mL, 3×), dried over Na_2SO_4, and then concentrated by rotary evaporation to 1.6 g (92%) of a colorless syrup. Product was partially hydrolyzed (<10%) and was used immediately for the synthesis of the BSA macroinitiator.

^{1}H NMR (300 MHz, CDCl$_3$): δ4.61 (q, 1H, CHBr), 2.85 (s, 4H, C$_2$H$_4$), 1.95 (d, 3H, CH$_3$).

4.6.6 Bovine serum albumin macroinitiator

NHS 2-bromopropionate (1.6 g, 6.5 mmol) was dissolved in 3.2 mL dimethylsulfoxide and added dropwise to bovine serum albumin (2.3 g, 1.15 mmol lysine) in phosphate buffer (400 mL, 0.1 M, pH 7.5). The solution was stirred overnight, and then dialyzed in 1000 MWCO tubing against water. Protein concentration was determined by bicinchoninic acid assay.

MALDI-TOF: Peak at 69.4 kDa.

4.6.7   Resin sacrificial initiator

Wang resin (0.15 g, 0.15 mmol OH functionality) and triethylamine (62 μL, 0.45 mmol) was added to 5 mL dichloromethane. 2-Bromopropionyl bromide (34 μL, 0.38 mmol) in 5 mL dichloromethane was added dropwise and the heterogeneous solution was stirred overnight. The resin was filtered and rinsed with methanol and water and dried under vacuum to collect a quantitative yield.

Initiator conjugation was confirmed by IR spectroscopy with appearance of an ester peak (1730 cm^{-1}).

4.6.8   Example polymerization

Protein-glycopolymers were synthesized as described in the following example. Resin sacrificial initiator (3.5 mg, 3.5 μmol Br) was added to reaction flask 1. CuBr (5.1 mg, 35 μmol), PMDETA (7.3 μL, 35 μmol), mannose acrylate (21 mg, 89 μmol), galactose acrylate (21 mg, 89 μmol), and water (826 μL) were added to reaction flask 2. BSA macroinitiator solution (8.72 mL, 1.2 μmol Br), mannose acrylate (62 mg, 265 μmol), and galactose acrylate (62 mg, 265 μmol) were added to reaction flask 3. The three flasks were degassed through four freeze-pump-thaw cycles. The contents of flask 2 were added to flask 1 through cannula and the solution stirred. After 10 minutes, the contents of flask 3 were added to flask 1 through cannula and the solution stirred for 4 hours.

The resin sacrificial initiator was then removed through centrifugation. The supernatant was centrifuged again through an Amicon centrifugal filter device with 3,000 Da cutoff. Saturated ammonium chloride solution was added to help solubilize and remove copper. Two rounds of centrifugation with saturated ammonium chloride followed by two rounds of centrifugation with water were performed to collect a viscous liquid that was later characterized by bicinchoninic acid assay and phenol-sulfuric acid assay[124] to determine the protein and saccharide concentration.

Starting ratios of mannose acrylate and/or galactose acrylate to initiator were varied to synthesize other protein-polymers.

4.6.9 BSA esterase assay

Protein sample was added to 50 mM, pH 8.5 PBS buffer to make a 1 mL solution with 10 μM protein. p-nitrophenyl acetate was dissolved in acetonitrile to make a 10 mM stock solution. 10 μL of the PNA stock solution was added to the protein solution. Absorbance at 405 nm was recorded every 5 minutes for 30 minutes.

4.6.10 Tryptic digest

Protein sample was added to a 20 μg/mL trypsin solution to make 2 mg/mL final concentration of protein-polymer. The solution was heated in a 37 °C water bath for 15 hours before characterizing by MALDI.

4.6.11 Protein acid hydrolysis

2 mg of protein or potein-polymer sample was added to 10 mL 6 M hydrochloric acid, sealed in a reaction flask, and heated to 110 °C for 24 hours. Hydrochloric acid and water were removed by rotary evaporation before characterization by GPC, NMR, or MALDI.

CHAPTER 5

Synthesis of glycopolymers through post-polymerization modification of pyridyl disulfide polymers

5.1   Introduction

The previous examples of glycopolymers have been synthesized by directly polymerizing glycomonomers. Another route towards glycopolymers is post-polymerization modification with saccharide content. One of the largest challenges in using polymerization techniques to produce biomimetic structures is the inherent distribution in molecular weight, and potentially architecture, that results. Since any polymer is inherently a mixture of different chain lengths, two different batches of polymerizations are never going to be exactly identical no matter how controlled the polymerization is. These inconsistencies may influence the biological properties of glycopolymers and complicate analysis of lectin-saccharide interactions. Therefore, we have synthesized polymers containing pendant pyridyl disulfide groups that can be reacted with thioglycosides with a simple click reaction. If polymers from the same batch are modified with different saccharides, we can generate glycopolymers with different pendant saccharides while maintaining the same underlying polymer. That is, there is absolutely no difference in the heterogeneity of chain lengths, making the samples directly comparable.

Pyridyl disulfide functional groups are one route towards post-polymerization modification, most popularly through thiol-disulfide exchange. Disulfide exchange can be tracked by the appearance of a byproduct, pyridyl-2-thione, which can be monitored spectrophotometrically (Scheme 5.1). This functional group has been used in a variety of applications, including polymer synthesis and drug delivery.

Their use has been demonstrated as modified polymerization initiators to create a functional chain end for further reactions. This has been shown extensively by the Maynard group to conjugate polymer chains to bovine serum albumin,[117] gold microarrays,,[55] and siRNA.[126] Pyridyl disulfides have also been used to form PEGylated nanoparticles. A polymer with pendant pyridyl disulfides was grafted to poly(ethylene glycol) through thiol-ene and Michael addition. These linkages to PEG created a cross-linked aggregate with a PEG shell.

Polymers with pendant pyridyl disulfides have also been used for delivery applications. Their linkages are cleavable under the mild reducing conditions of the cell cytoplasm environment through the action of glutathione tripeptide, making disulfide groups particularly attractive for intracellular drug delivery. Pyridyl disulfide monomers were copolymerized with methacrylic acid and butyl acrylate to create a polymer that was both pH responsive and membrane disruptive (methacrylic acid component) as well as glutathione reactive (pyridyl disulfide component). The polymer was taken up by macrophages and delivered its peptide payload with no cell toxicity.[127] This work was extended further for use as a nanoparticle vaccine that delivered a protein antigen through the pyridyl disulfide handle.[128]

In this chapter, I describe the synthesis of branched glycopolymers through post-polymerization modification of a branched pyridyl disulfide polymer with thioglycosides to create a library of glycopolymers. More broadly, these polymers can also be used as platforms that can present any thiol containing compounds. For example, tissue engineering applications often require multiple peptide epitopes

for cell binding and signaling. The pyridyl disulfide polymers synthesized in this chapter are modified with thiol-containing integrin binding peptides as a proof of concept demonstration of this method, and tested for their effect on cell adhesion in the following chapter.
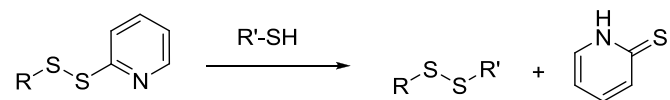
Scheme 5.1: Disulfide exchange with a pyridyl disulfide group results in release of pyridyl-2-thione.

5.2   Synthesis of monomers and thioglycosides

The original vision of this portion of the dissertation was to polymerize pyridyl disulfide ethyl acrylate from a protein macroinitiator and add the sugar component through post-polymerization modification. This scheme was meant as a complement to the protein-glycopolymer conjugates synthesized through direct polymerization as described in Chapter 4. However, proteins have limited solubility and bioactivity in organic solvents so any pyridyl disulfide monomer must be water soluble. The simplest monomer, pyridyl disulfide ethyl acrylate, is poorly water soluble. A pyridyl disulfide PEG macromer, synthesized from the amidification of 2-(pyridyldithio)-ethylamine hydrochloride[129] to polyethylene glycol 526 methacrylate succinate (Scheme 5.2), did not increase water solubility noticeably, despite a report of a water soluble pyridyl disulfide linker using tetraethylene glycol to solubilize the pyridyl disulfide group.[130] A longer PEG tether could help in improving solubility, but would also result in decreased density of saccharide.

Incorporation of protein content with the pyridyl disulfide polymers was abandoned in favor of synthesizing hyperbranched pyridyl disulfide polymers through the copolymerization of pyridyl disulfide ethyl acrylate with ethylene glycol dimethacry-

late as a branching agent. Pyridyl disulfide ethyl acrylate (PDA) was synthesized through disulfide exchange of 2,2'-dipyridyldisulfide with mercaptoethanol to form pyridyl disulfide ethanol followed by acrylation of the alcohol with acryloyl chloride (Scheme 5.2).

Thiogalactoside and thiomannoside were synthesized from the glycosylation of the fully acetylated sugar with thioacetic acid using boron trifluoride as activator followed by deprotection of the O- and S- acetates with sodium methoxide to expose the sugar alcohols and thiol (Scheme 5.3). The molecules were then quenched with Dowex ion exchange resin. Ellman's reagent tests to determine the free thiol content showed that the thioglycosides slowly reacted together into disulfides ($<3\%$ change after 16 hours under ambient conditions at 100 mM). For long term storage, the thioglycosides were incubated over TCEP conjugated resin. If used directly after deprotection, the thioglycosides were used without further purification.

Scheme 5.2: Synthesis of pyridyl disulfide PEG methacrylate macromer and pyridyl disulfide ethyl acrylate monomer.
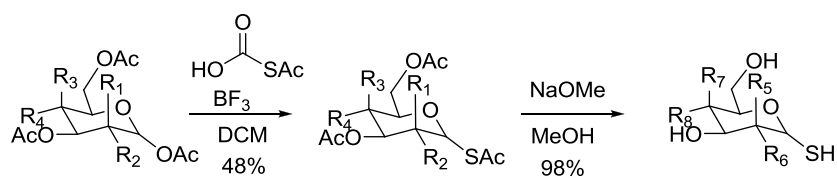
Scheme 5.3: Synthesis of thiomannose (R_1, R_4 = -OAc; R_2, R_3 = -H; R_5, R_8 = -OH; R_6, R_7 = -H), and thiogalactose (R_1, R_4 = -H; R_2, R_3 = -OAc; R_5, R_8 = -H; R_6, R_7 = -OH).

5.3 Synthesis of hyperbranched pyridyl disulfide polymers

Polymerization of pyridyl disulfide polymers was first attempted using ATRP with copper bromide as catalyst, Me_6Tren as ligand, and ethyl 2-bromopropionate (EBP) as initiator. Although ATRP has been used previously to polymerize pyridyl disulfide based monomers,[131] we did not achieve controlled polymerizations. A summary of the pyridyl disulfide polymers generated by ATRP is presented in Table 5.1. High polydispersities can be seen for these linear polymers. The Me_6Tren ligated copper catalyst was observed to precipitate from solution after the addition of pyridyl disulfide monomer, so the lack of control may be attributed to the copper catalyst interacting with the pyridyl group and disrupting the ATRP equilibrium between ligated activated and deactivated catalyst states. Common ATRP ligands such as 2,2'-bipyridine or n-butyl-2-pyridylmethanimine contain pyridines so it is not surprising that the pyridyl disulfide monomer could also have a ligating effect. A report on the ATRP of 4-vinylpyridine used a large excess of ligand to compete with the pyridine monomer and maintain activity of the catalytic system.[132] However, increasing the ratio of the Me_6Tren to catalyst did not result in a significant improvement in polymerization control, and repeating the same experiments with PMDETA as ligand led to no conversion.

Rather than further troubleshooting the ATRP process, reversible addition-fragmentation chain transfer (RAFT) polymerization was used to synthesize the branched pyridyl disulfide polymers. RAFT, like ATRP, is a living radical polymerization technique that results in uniform growth of polymer chains. Control of the polymerization is maintained through an equilibrium of reversible chain-transfer between a monomer and a RAFT chain transfer agent, in this case ethyl 2-(phenylcarbonothioylthio)propionate.

Table 5.1: Summary of data for pyridyl disulfide polymers generated by ATRP.

PDA:EBP:CuBr:Me$_6$Tren	% conversion	M$_w$	M$_n$	PDI
25:1:1:1	35%	9280	4610	2.01
25:1:1:1	94%	15100	6280	2.40
25:1:1:2	86%	19460	9820	1.98
50:1:1:2	58%	4120	2730	1.51

Pyridyl disulfide ethyl acrylate was copolymerized with the branching agent ethylene glycol dimethacrylate (EGDMA) as shown in Scheme 5.4 to synthesize poly(pyridyl disulfide acrylate-*co*-ethyleneglycol dimethacrylate). Molecular weight was roughly controlled by adjusting the ratio of PDA monomer to RAFT CTA. Polymerizations were quenched before reaching high conversion to prevent gelation. EGDMA can also act as a crosslinker and generate bridges between chains at high conversion leading to higher molecular weights and possibly insoluble precipitates. Branching content was adjusted by varying the ratio of EGDMA to RAFT CTA. As expected, increasing the ratio of branching agent to RAFT chain transfer agent corresponded to an increase in molecular weight distribution (Table 5.2)

The GPC traces showed a multi-modal distribution (Figure 5.1), similar to what has been seen previously with RAFT copolymerizations with EGDMA.[133] The higher molecular weight portion of the multi-modal distribution may reflect the population of polymer chains crosslinked together by EGDMA. This distribution may also explain why the GPC determined molecular weights of the entire polymer population are higher than expected.

Table 5.2: Summary of data for pyridyl disulfide polymers generated by RAFT.

PDA:EGDMA:CTA:AIBN	% conversion	M_w	M_n	PDI
60:3:3:1	62%	29710	9850	3.02
100:5:5:1	43%	9860	6960	1.42
100:10:5:1	38%	37170	14000	2.66
198:5:5:1	60%	45950	16480	2.79
198:10:5:1	43%	48470	15350	3.16
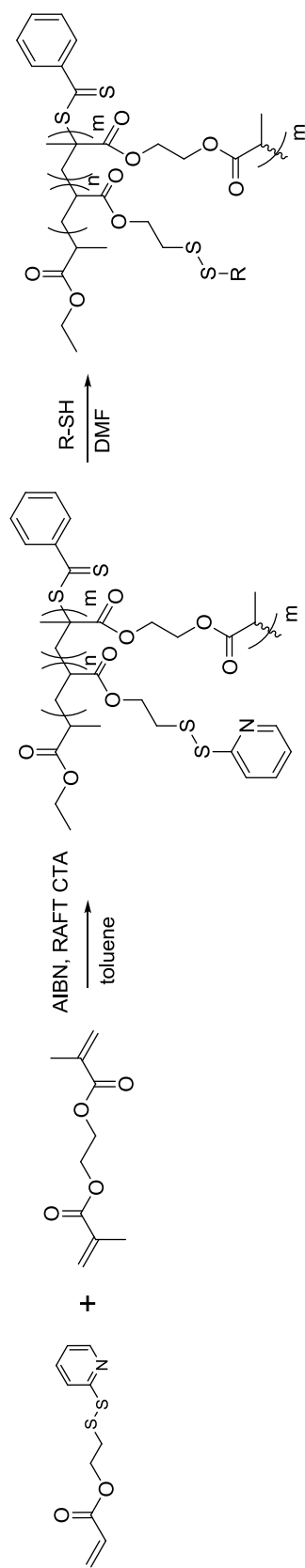
Scheme 5.4: RAFT copolymerization of pyridyl disulfide ethyl acrylate and ethylene glycodimethacrylate leads to branched polymers with pendant pyridyl disulfide groups. Disulfide exchange with thiol containing compounds led to biofunctionalization of the branched polymers. R = thiogalactoside, thiomannoside, or peptide sequence GCGYGRGDSPG.
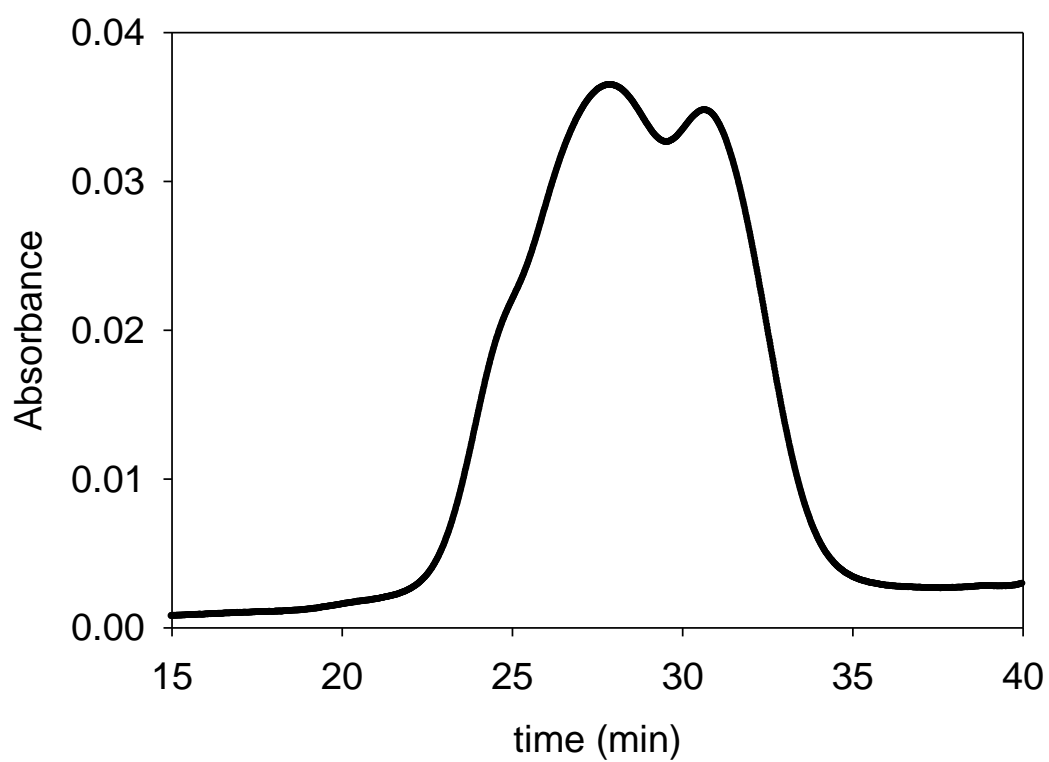
Figure 5.1: GPC trace shows the multi-modal distribution of branched pyridyl disulfide polymer with PDA:EGDMA:CTA:AIBN = 100:10:5:1.

5.4 Disulfide exchange with thioglycosides and CRGDS

We conjugated two classes of thiol-containing biomolecules to the pyridyl disulfide polymers: thioglycosides and a cysteine containing peptide (GCGYGRGDSPG). Preliminary tests of disulfide exchange between thiomannoside and the pyridyl disulfide monomer showed significant Michael addition of the free thiol to the acrylate. Therefore, the pyridyl disulfide monomer must be polymerized prior to exchange of the thiolated compound with pyridyl disulfide.

Disulfide exchange was achieved by dissolving poly(pyridyl disulfide acrylate-*co*-ethyleneglycol dimethacrylate) and the thiol containing biomolecule in dimethylformamide. Disulfide exchange with pyridyl disulfide groups results in pyridyl-2-thione released as a byproduct that can be quantified spectrophotometrically. In our case, we examined UV absorption at 374 nm in DMF (pyridyl-2-thione has a reported molar extinction coefficient of 5,443 M cm^{-1} in DMF[134]) in order to follow the completion of the reaction. The modified polymers became fully water soluble after exchange of the hydrophobic pyridyl group with the hydrophilic saccharide or peptide. Following removal of excess reagent and pyridyl-2-thione through dialysis or centrifugal filtration, ^{1}H NMR analysis showed peaks corresponding to saccharide or peptide, and complete disappearance of pyridine groups (Figure 5.2). Modified polymers were chosen to cover a range of molecular weights and branching density as summarized in Table 5.3.
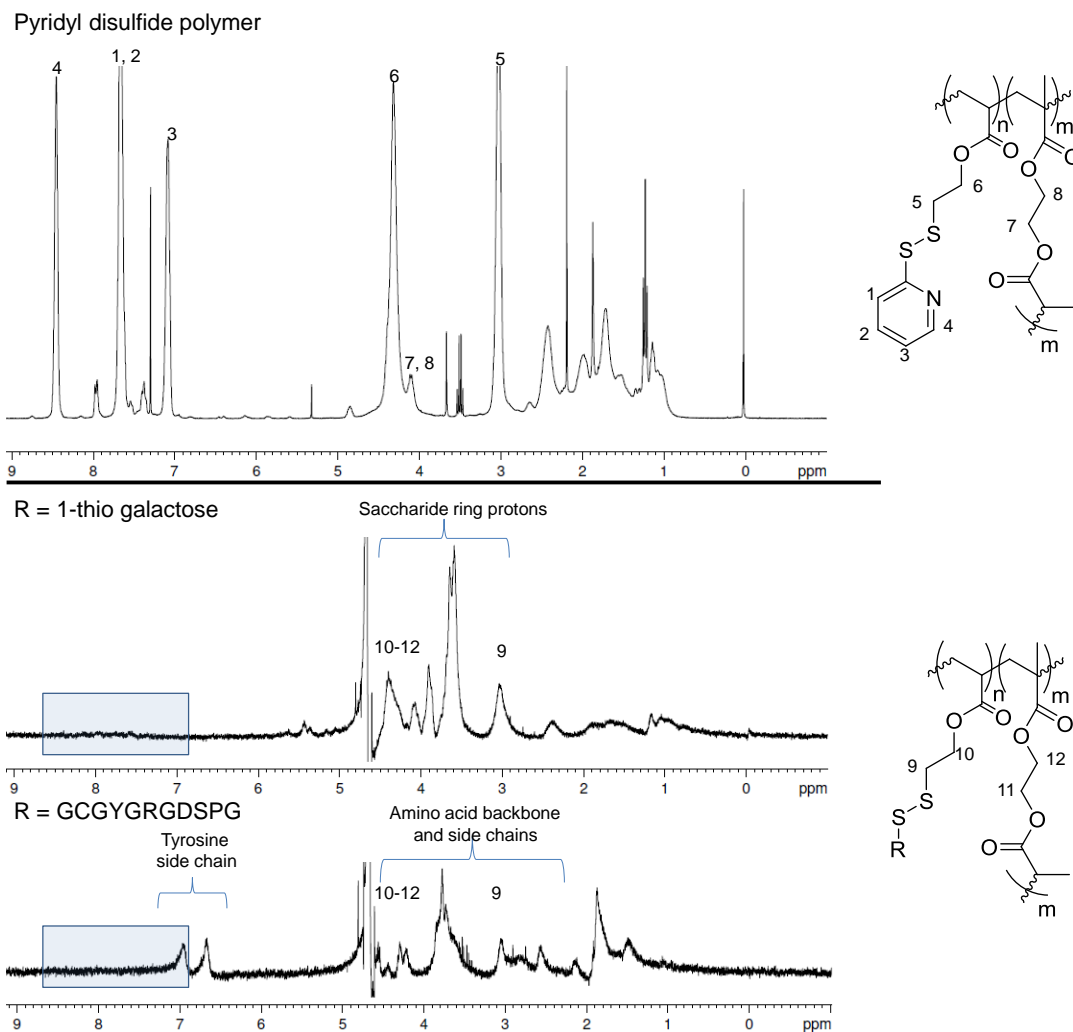
Figure 5.2: ^{1}H NMRs of polymers exchanged with thiol biomolecules show complete disappearance of pyridine groups (7-8.5 ppm) along with peaks corresponding to saccharide ring protons or amino acid side chains and backbone.

Table 5.3: Summary of polymers produced from disulfide exchange with thiol-containing biomolecules.

Biomolecule	PDA:EGDMA:CTA:AIBN	# conjugated[a]
Galactose	100:5:5:1	29
Galactose	100:10:5:1	59
Galactose	198:5:5:1	68
Galactose	198:10:5:1	64
Mannose	198:5:5:1	68
GCGYGRGDSPG	100:5:5:1	29
GCGYGRGDSPG	198:5:5:1	68

a: determined through M_n

5.5 Conclusions

In this chapter, I described the synthesis of branched polymers bearing saccharides or peptides through the post-polymerization modification of a branched pyridyl disulfide polymer. The original polymer, poly(pyridyl disulfide acrylate-*co*-ethyleneglycol dimethacrylate), was synthesized through RAFT rather than ATRP as used in previous chapters of this dissertation. The pyridyl disulfide presenting polymers were exchanged with thioglycosides and a cysteine containing peptide. The effect of these modified polymers on cell adhesion will be tested in Chapter 6.

5.6 Experimentals

5.6.1 Materials

Acetic acid (Mallinckrodt, ACS grade), 2-aminoethanethiol hydrochloride (Acros, 98%), boron trifluoride etherate (Acros, 48%), chloroform (Fisher, HPLC grade), 4-dimethylaminopyridine (Alfa Aesar, 99%), dimethylformamide (BDH, ACS grade), 2,2' dipyridyl disulfide (TCI, 98%), Dowex 50WX8 ion exchange resin (Aldrich, 200-400 mesh), ethyl 2-bromopropionate (Alfa Acros, 99%), 1-ethyl-3-(3-dimethylaminopropyl)carbodiimide (Advanced Chem Tech, 98%), ethyl 2-(phenylcarbonothioylthio)propionate (Sigma Aldrich, 97%), galactose (Fisher, off white to white powder), mannose (Amresco, high purity grade), mercaptoethanol (Sigma Aldrich), peptide Ac-GCGYGRGDSPG-NH$_2$ (GenScript, 95.3%), poly(ethylene glycol) monomethacrylate 525 (Sigma Aldrich), pyridine (J.T. Baker, ACS grade), sodium methoxide (Acros, 30wt% in methanol), succinic anhydride (Alfa Aesar, 99%), and thioacetic acid (Acros, 98%) were used as received. Copper bromide (Acros, 98%) was purified by stirring in glacial acetic acid and then rinsing with ethanol. Acryloyl chloride (Alfa Aesar, 96%), dichloromethane (EMD, ACS grade), ethylene glycol dimethacrylate (Sigma Aldrich, 98%), *N,N,N',N'',N''*-pentamethyldiethylenetriamine (Pfaltz and Bauer, 99%), toluene (Fisher, ACS grade), and triethylamine (Alfa Aesar, 99%) were distilled before use. Azobisisobutyronitrile (Sigma Aldrich, 98%) was recrystallized from methanol. Tris(2-aminoethyl)amine (Me$_6$Tren) was synthesized according to a published procedure.[115] Dialysis tubing with 1000 MWCO (Spectrum Labs) and centrifugal filter units with 3000 MWCO (Amicon Ultra) were used for purification of the disulfide exchanged polymers.

5.6.2 Analytical Techniques

^{1}H NMR spectra (δ ppm) were recorded on Bruker Biospin Ultrashield 300 MHz or 500 MHz NMR spectrometers. Gel permeation chromatography relative to linear poly(methyl methacrylate) standards (GPC_{PMMA}) was conducted on a Waters system equipped with UV/vis absorbance and refractive index detectors and four Waters styragel columns (100-5K, 500-30K, 50-100K, 5K-600K). Tetrahydrofuran (THF) with a flow rate of 1.0 mL/min was used.

5.6.3 Poly(ethylene glycol) monomethacrylate monosuccinate

Poly(ethylene glycol) monomethacrylate 525 (5.0 g, 0.95 mmol) was dissolved in 50 mL chloroform. Succinic anhydride (1.9 g, 1.9 mmol) and 4-dimethylaminopyridine (0.12 g, 0.1 mmol) were added to the solution. The solution was refluxed overnight, washed with 1% HCl (50 mL, 43×), dried over Na_2SO_4, and concentrated to a pale yellow syrup.

^{1}H NMR (300 MHz, $CDCl_3$): δ5.60 (d, H-1), 4.65 (dd, H-3), 4.37 (dd, H-2), 4.31 (dd, H-4), 3.91 (m, 2H, H-6a,b), 3.8 (m, H-5), 1.3-1.57(s, 12H, 4 CH_3).

5.6.4 2-(Pyridyldithio)-ethylamine hydrochloride

2-Aminoethanethiol hydrochloride (2.5 g, 21.6 mmol) in 10 mL methanol was added dropwise to a round bottom flask containing 2,2' dipyridyl disulfide (5 g, 22.7 mmol), acetic acid (0.9 mL), and 30 mL methanol. The solution was stirred for two days and then concentrated to a yellow syrup with a rotary evaporator. The syrup was repeatedly precipitated into cold diethyl ether until no color remained to collect 3.67 g (76%) of a white powder.

^{1}H NMR (300 MHz, $CDCl_3$): δ9.24 (broad, NH_3), 8.69, 7.62, 7.36, 7.23, 3.34 (C_2H_4).

5.6.5 Pyridyl disulfide PEG methacrylate macromer

2-(Pyridyldithio)-ethylamine hydrochloride (0.2 g, 0.9 mmol) and poly(ethylene glycol) monomethacrylate monosuccinate (0.47 g, 0.75 mmol) were dissolved in 5 mL dimethylformamide. After stirring for 15 minutes to allow the 2-(pyridyldithio)-ethylamine hydrochloride to dissolve, 1-ethyl-3-(3-dimethylaminopropyl)carbodiimide (0.35 g, 2.2 mmol) was added and the reaction was stirred overnight. The solution was concentrated to a yellow syrup by rotary evaporation. The syrup was taken up in 30 mL DCM, washed with saturated sodium bicarbonate solution (30 mL, 3×), dried over Na_2SO_4, and concentrated to 0.56 g (79%) of a pale yellow syrup.

^{1}H NMR (300 MHz, $CDCl_3$): δ8.5 (d, 1H), 7.62 (t, 1H), 7.5 (d, 1H), 7.08 (t, 1H), 6.1 (s, CH_2=C), 5.55 (s, CH_2=C), 4.21 (m, PEG), 3.6 (broad, PEG), 3.51 (t, CH_2NH), 2.89 (t, CH_2S), 2.66 (t, CH_2), 2.48 (t, CH_2), 1.9 (s, CH_3).

5.6.6 Pyridyl disulfide ethanol

2,2' Dipyridyl disulfide (10.7 g, 48.6 mmol) and acetic acid (1 mL) were dissolved in 50 mL methanol and placed in a three neck round bottom flask. The solution was left under nitrogen for one hour before adding mercaptoethanol (1.7 mL, 24.3 mmol) dropwise through a septum via a syringe. The solution was stirred overnight before concentrating by rotary evaporation. Vacuum column chromatography was performed to collect 2.4 g (53%) of a pale yellow syrup. Unreacted 2,2' dipyridyl disulfide was also collected and could be reused.

^{1}H NMR (300 MHz, $CDCl_3$): δ8.49 (d), 7.57, 7.39 (d), 7.13, 5.75 (broad, OH), 3.79 (t, CH_2), 2.93 (t, CH_2).

5.6.7 Pyridyl disulfide ethyl acrylate

Pyridyl disulfide ethanol (6.2 g, 33.2 mmol) was dissolved in 50 mL dichloromethane and triethylamine (6.9 mL, 49.8 mmol). The solution was cooled in an ice bath before adding acryloyl chloride (3.5 mL, 43.2 mmol) in 12 mL dichloromethane dropwise. The reaction was stirred overnight before washing the dichloromethane solution with water (50 mL, 3×), dried over Na_2SO_4, and concentrated by rotary evaporation. Vacuum column chromatography was performed to collect 6.2 g (77%) of pyridyl disulfide ethyl acrylate as a pale yellow syrup.

^{1}H NMR (300 MHz, CDCl$_3$): δ8.44 (1H), 7.65 (2H), 7.07 (1H), 6.39(d, 1H, C**H**$_2$=CH), 6.08 (m, CH$_2$=C**H**), 5.83 (d, 1H, C**H**$_2$=CH), 4.4 (s, 2H, CH$_2$), 3.06 (s, 2H, CH$_2$).

5.6.8 Example ATRP of pyridyl disulfide acrylate

CuBr (3.4 mg, 0.024 mmol) was sealed with a septum in a reaction flask, and deoxygenated through argon/vacuum cycles. Me$_6$Tren (18.8 μL, 0.047 mmol) was added and the ligated copper stirred for 15 minutes. Pyridyl disulfide ethyl acrylate (289 mg, 1.19 mmol), ethyl bromopropionate (3.1 μL, 0.024 mmol), and 680 μL toluene was added through the septum with a syringe. The flask contents were degassed through five freeze-pump-thaw cycles and stirred at 70 °C for 20 hours. Contents were passed through an alumina plug and then precipitated into cold diethyl ether to result in 0.19 g (66%) of a yellow oil.

5.6.9 Example RAFT of pyridyl disulfide acrylate

Pyridyl disulfide ethyl acrylate (293 mg, 1.22 mmol), ethylene glycol dimethacrylate (12 mg, 0.061 mmol), ethyl 2-(phenylcarbonothioylthio)propionate (15.4 mg, 0.061 mmol), azobisisobutyronitrile (2 mg, 0.012 mmol), and 1.2 mL toluene were added to a reaction flask. The flask contents were degassed through five freeze-pump-thaw cycles and stirred at 70 °C. After 20 hours, the contents were precipitated into cold diethyl ether to result in 0.21 g (72%) of a red oil.

5.6.10 1-Thio-2,3,4,6-tetraacetate mannopyranose

1,2,3,4,6-Pentaacetate mannopyranose (4.8 g, 12.3 mmol) was dissolved in 20 mL dichloromethane and thioacetic acid (1.7 mL, 24.6 mmol). The solution was cooled in an ice bath before adding boron trifluoride etherate (4.5 mL, 36.9 mmol). The reaction was allowed to warm to room temperature and then stirred for two days. The dichloromethane solution was washed with water (50 mL, 4×), dried over Na_2SO_4, concentrated by rotary evaporation, and crystallized from methanol to collect 2.4 g (48%) of a white powder. ^{1}H NMR (300 MHz, $CDCl_3$): δ5.49 (s, 2H, H-1,H-2), 5.26 (t, H-4), 5.13 (dd, H-3), 4.27 (dd, H-6a), 4.11 (dd, H-6b), 3.82 (ddd, H-5), 1.97-2.36 (s, 12H, CH_3).

5.6.11 1-Thio mannopyranose

1-Thio-2,3,4,6-tetraacetate mannopyranose (100 mg, 0.25 mmol) was dissolved in 500 μL methanol. Sodium methoxide (14.6 mg, 0.27 mmol) was added and the solution stirred until the reaction was complete by TLC. The solution was diluted with an equal volume of water and passed through a short plug of Dowex 50WX8 ion exchange resin and concentrated to collect a 48 mg (98%) of a white powder.

^{1}H NMR (300 MHz, D_2O): δ4.8 (s, H-1), 3.85 (d, H-2), 3.67 (m, 3H, H-3, H-6ab), 3.42 (t, H-4), 3.3 (ddd, H-5).

5.6.12 1-Thio-2,3,4,6-tetraacetate galactopyranose

1-Thio-2,3,4,6-tetraacetate galactopyranose was synthesized in a similar procedure to 1-thio-2,3,4,6-tetraacetate mannopyranose.

^{1}H NMR (300 MHz, CDCl$_3$): δ5.46 (dd, H-4), 5.28 (m, 2H, H-1, H-2), 5.11 (dd, H-3), 4.08 (m, 3H, H-5, H-6ab), 1.98-2.98 (s, 12H, CH$_3$).

5.6.13 1-Thio galactopyranose

1-Thio galactopyranose was synthesized in a similar procedure to 1-thio mannopyranose.

^{1}H NMR (300 MHz, D$_2$O): δ4.45 (d, H-1), 3.9 (d, H-4), 3.68 (m, 3H, H-5,H-6ab), 3.56 (dd, H-3), 3.47 (t, H-2).

5.6.14 Example disulfide exchange with pyridyl disulfide polymer

Poly(pyridyl disulfide acrylate-*co*-ethyleneglycol dimethacrylate) (10 mg, 0.0414 mmol pendant pyridyl disulfides) was dissolved in dimethylformamide (1495 μL) and mixed with a thiogalactoside solution (162 μL of 100 mg/mL in DMF, 0.0828 mmol) and incubated for five hours (absorbance of the solution at 374 nm showed full conversion of pyridyl disulfides). DMF was removed under reduced pressure. The resulting yellow syrup was dissolved in water and dialyzed in 1000 MWCO dialysis tubing against water for 12 hours with three changes of the water solution. The polymer solution was then lyophilized to collect 3.4 mg (51%) of a white powder. Exchange with GCGYGRGDSPG was similar but used centrifugal filter units with 3000 MWCO to remove excess peptide.

CHAPTER 6

Biological interaction of polymers

The experiments described in this chapter elucidate the polymer properties that influence lectin binding, in particular the branching architecture and nature of the branch point (Chapter 3 polymers), and the 3D display of glycans through polymerization from a protein component (Chapter 4 polymers). They also describe the effect of soluble clusters of galactose or RGD on fibroblast adhesion (Chapter 5 polymers).

The glycopolymers described in Chapter 3 are linear with pendant mannoses or branched with mannose, galactose, or no saccharide content at the branch point. The glycopolymers described in Chapter 4 are protein-glycopolymer conjugates containing different ratios and amounts of mannose and galactose. The polymers described in Chapter 5 are branched structures displaying saccharides or RGD peptides. Relevant data for the polymers are shown in Table 6.1, Table 6.2, and Table 6.3.

Table 6.1: Summary of linear and branched glycopolymers from Chapter 3 investigated in Chapter 6.

Linear polymers

Compound	$[M]_0$:[Mannose initiator]$_0$: $[CuBr]$:$[Me_6Tren]$	M_w	M_n	PDI
# mannose = 14	25:1:1:1	6990	5770	1.21
# mannose = 42	50:1:1:1	20480	16820	1.22
# mannose = 75	100:1:1:1	37600	30310	1.24

Branched glycopolymers with mannose at branch point

Compound	$[M]_0$:[Mannose inimer]$_0$: $[CuBr]$:$[Me_6Tren]$	M_w	M_n	PDI
# mannose = 10, $[M]_0$:[Mannose inimer]$_0$ 5:1	125:25:1:1	5780	4050	1.67
# mannose = 14, $[M]_0$:[Mannose inimer]$_0$ 2:1	50:25:1:1	15610	5980	2.61
# mannose = 42, $[M]_0$:[Mannose inimer]$_0$ 2:1	50:25:1:1	37920	17640	2.15
# mannose = 14, $[M]_0$:[Mannose inimer]$_0$ 1:1	25:25:1:1	8600	5750	1.5

Branched glycopolymers without saccharide at branch point

Compound	$[M]_0$:[Inimer]$_0$: $[CuBr]$:$[Me_6Tren]$	M_w	M_n	PDI
# mannose = 18, $[M]_0$:[Inimer]$_0$ 2:1	50:25:1:1	36380	8440	3.12
# mannose = 10, $[M]_0$:[Inimer]$_0$ 1:1	25:25:1:1	10280	5360	1.92

Branched glycopolymers with galactose at branch point

Compound	$[M]_0$:[Galactose inimer]$_0$: $[CuBr]$:$[Me_6Tren]$	M_w	M_n	PDI
# mannose = 13, $[M]_0$:[Galactose inimer]$_0$ 1:1	50:50:1:1	17110	11260	1.52

Table 6.2: Summary of protein-glycopolymers from Chapter 4 investigated in Chapter 6.

Compound	# saccharides/protein
G600	306
G300	184
M1200	360
M600	239
M150	70
MG300300	174

Table 6.3: Summary of branched polymers displaying saccharides or peptides from Chapter 5 investigated in Chapter 6.

Compound	Biomolecule type	#
Gal 198:5:5:1	Galactose	68
RGD 100:5:5:1	GCGYGRGDSPG	29
RGD 198:5:5:1	GCGYGRGDSPG	68

6.1 Introduction

Most biological applications of glycopolymers revolve around their interaction with carbohydrate binding proteins, or lectins. Lectin binding to sugars is primarily dependent on the saccharide identity but in terms of polymer characteristics, lectin binding is also dependent on the chain length/clustering and architecture of the polymer, where chain length/clustering represents the number of sugar repeat units, and architecture describes the polymer's microstructure.

6.1.1 Saccharide identity

Lectins are specific to their corresponding sugars; for example, plant lectins such as peanut agglutinin binds to galactose while concanavalin A (Con A) binds to mannose, but agglutinin does not bind to mannose nor does Con A bind to galactose (Figure 6.1).[135,136] This specificity is related to the orientation of the sugar hydroxyls with mannose having equatorial 3- and 4- hydroxyls while galactose has an equatorial 3- hydroxyl and an axial 4- hydroxyl. Binding specificity has also been demonstrated in human immune system lectins. Haddleton and coworkers synthesized homopolymers and statistical copolymers of mannose and galactose derived monomers and tested their binding with mannose reactive DC-SIGN (dendritic cell specific ICAM-3 grabbing nonintegrin).[68] Binding was not seen with galactose homopolymers, but increased with greater mannose density. Sequence control of the saccharide in the polymer chain had no effect on binding.[69]

6.1.2 Chain length and clustering

Lectins typically bind individual monosaccharides with low affinity but bind polysaccharides with high avidity, where avidity describes the combined synergistic strength of multiple bond interactions. Therefore, lectins must bind multiple saccharides to bind with sufficient strength to trigger the appropriate biological

response. Lectins often have oligomeric structures, reflecting the use of multivalency, where each subunit binds to a separate ligand. A phenomenon commonly known as the cluster glycoside effect has been observed when studying carbohydrate-lectin interactions, where a greater increase in activity is detected with multivalent polysaccharides than an identical molar amount of individual monosaccharides.[9] While in general, larger structures of saccharides have enhanced binding, the effect is more nuanced. In addition to the act of binding, biological activity may also be mediated by clustering of lectins, the rate at which these clusters are formed, and the distance between lectins in the clusters.

The Kiessling group has studied this lectin-saccharide binding differences between various saccharide containing structures such as glycoclusters, glycodendrimers, linear glycopolymers (through controlled or uncontrolled techniques), and glycoproteins.[137] Although there were subtle variations across the different assays used to investigate lectin binding (solid-phase, quantitative precipitation, turbidity, and fluorescence quenching), high molecular weight polymers with the most number of mannoses were the most potent inhibitors of Con A binding. Broad polydispersity polymers bound higher number of Con A but at a slower rate than relatively narrow polydispersity polymers synthesized through ROMP. Furthermore, the distance between Con A tetramers was larger for broad polydispersity polymers than narrow polymers. Inducing biological activity through lectin binding may require a certain threshold of lectin clustering, so these results demonstrate how small changes in polymer structures can change the biological activity.

In another study, the density of binding epitopes was found to have an effect on lectin binding.[67] Glycopolymers with a high density of binding mannose monomers can bind many Con A lectins, but not every saccharide is bound due to steric effects. In comparison, copolymerizing the mannose monomers with non-binding galactose monomers (in order to maintain similar length, polarity, and steric properties of the polymer) results in a glycopolymer with a lower density of binding epitopes that bound fewer Con A but with higher efficiency (fewer mannose per Con A).

6.1.3 Architecture

Polymer architecture refers to the variations in polymer structure due to variations in microstructure, although others have used the term to refer to macromolecules with different linkages. In this thesis, architecture will primarily refer to branching or multivalent display of polymer chains.

Polysaccharide architecture with regards to branching has been shown to influence biological interaction. This is reflected in the different structures of linear and branched natural polysaccharides. For example, glucose is commonly stored in plants as the linear polysaccharide, amylose, but in contrast, animals store glucose as a branched polysaccharide, glycogen. Branching in this case affects the biological properties by providing additional enzyme attachment sites while containing the same amount of overall glucose as a linear starch chain. This arrangement allows for faster release of glucose than compared to a linear starch chain which only has two enzyme attachment sites.[138] Natural β-glucans have been shown to have different immunomodulation potencies depending on their branching complexity, with polysaccharides having degrees of branching between 0.20 and 0.33 as the most potent. This immune activity is hypothesized to be related to the helical conformation and presentation of hydrophilic groups of branched structures.[139,140]

The effect of connectivity is also evident in synthetic oligosaccharide structures. The Seeberger group synthesized a linear trisaccharide and branched trisaccharide, and found different binding results with cyanovirin N between the two despite the same overall number of mannose units.[141]

Glycomimetic branching architecture also affects biological interaction. Reuter found that comb-branched sialic acid glycopolymers were stronger inhibitors of influenza virus than linear glycopolymers and spheroidal glycodendrimers.[142] These binding differences are attributed to the increased binding capacity of branched polymers over their linear counterparts. In the case of the spheroidal glycodendrimer, the rigid size and shape of the dendrimer may have limited its interaction with the virus even though the dendrimer has a large binding capacity similar to the branched polymer. In another study, four arm star glycopolymers had the same bioactivity with Con A as linear polymers.[143]
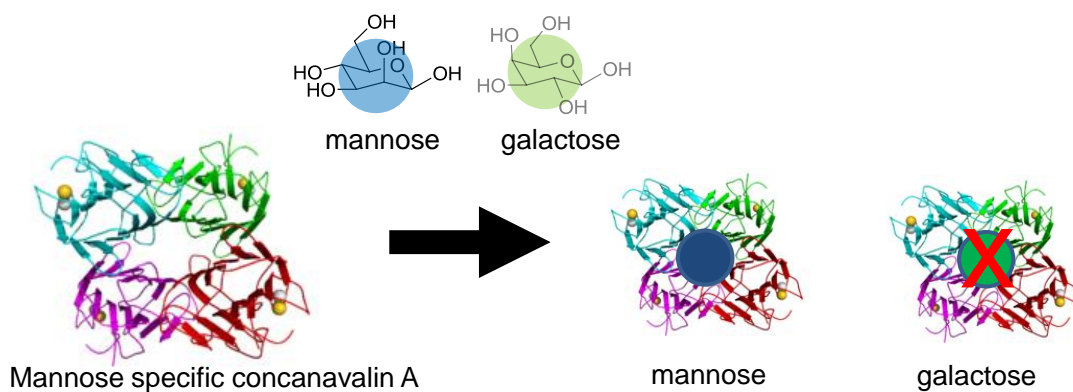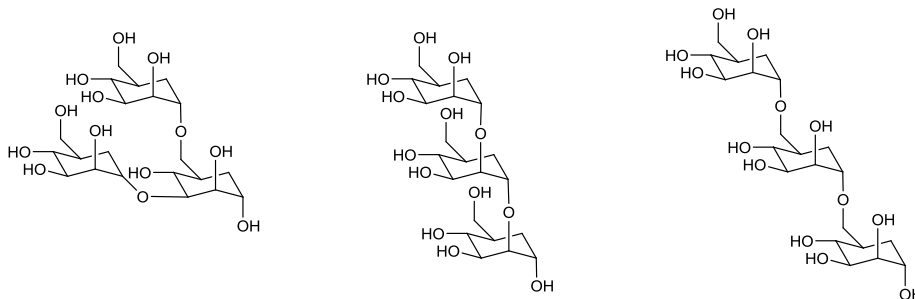
Figure 6.1: Lectin binding with multivalent saccharide structures is sensitive to saccharide identity, polymer chain length, and architecture. Structures of synthetic oligosaccharides are adapted from reference.[141] Concanavalin A structure adapted from the Wikimedia Commons file 3CNA Concanavalin A.png

6.1.4   Mannose binding lectin and complement

Mannose binding lectin's (MBL) primary function in the body is as part of the complement system (although it has also been shown to act directly as an opsonin as well). The complement system is a group of circulating blood proteins that is part of innate immunity, although recent research has linked it to certain aspects of the adaptive immune system as well.[144] Activation of complement results in localized inflammation and recruitment of phagocytes, opsonization of pathogens to enhance their phagocytosis, and lysis of pathogen cell membranes through formation of the membrane attack complex. Activation can occur through three main pathways: the classical pathway from antigen-antibody complexes, the alternative pathway from spontaneous hydrolysis of complement proteins on cells, and the lectin pathway from binding of mannose binding lectin to polysaccharide and glycoprotein elements of pathogens. Mannose binding lectin-associated serine proteases (MASPs) complex with MBL and cleave C4 and C2, much like how C1 acts in the classical pathway. The C4b2a complex is formed resulting in C3 cleavage and the same complement cascade seen with the other pathways.

MBL consists of a sugar binding domain, a neck region, a collagenous region, and a cysteine-rich N-terminal region.[145] The sugar binding domain has three binding sites separated by 54 $\mathring{A}$ that bind sugars typically with equatorial 3- and 4-hydroxyls (e.g. *N*-acetyl glucosamine, mannose, glucose). The spacing of the sugar binding sites requires the lectin to either bind with separate sugar structures on a bacterial membrane or with a large polysaccharide. In contrast, monosaccharides or even short oligosaccharides would not have the correct spacing to sufficiently bind with the lectin. Individual affinity of a sugar to a binding site is rather weak at 10^{-3} M; therefore multiple instances of binding are required for sufficient binding avidity. Native mannose binding lectin circulates as oligomers of protein subunits, with anywhere from two to six subunits clustered together, further reflecting the need for multivalency to generate functional avidity.
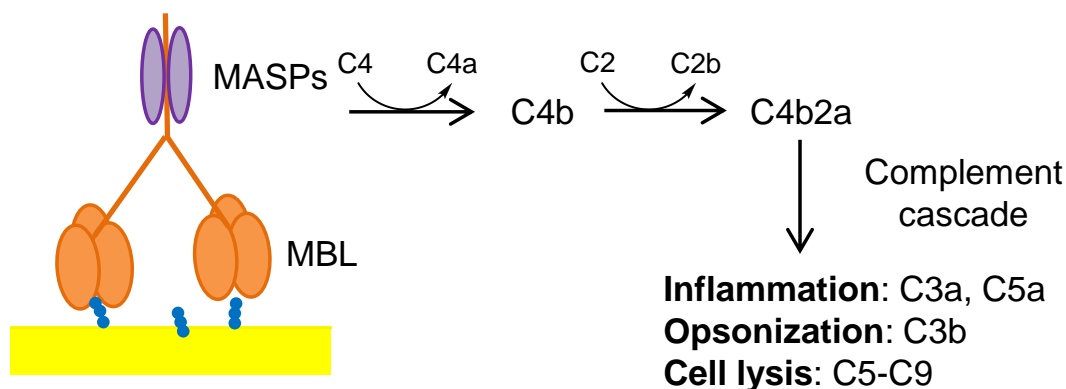
Figure 6.2: Mannose binding lectin binds to mannose or similar saccharides on pathogen surfaces and trigger the complement cascade.

6.2 Biological interaction of linear and branched glycopolymers from Chapter 3

The polymers from Chapter 3 have linear or branched architectures with pendant mannoses. For the branched polymers, the branch point contains mannose, galactose, or no saccharide component. Table 6.1 summarizes the properties of the glycopolymers investigated in this section.

6.2.1 Interaction with Concanavalin A

Biological interaction was first investigated using a turbidimetric assay with concanavalin A (Con A), a plant lectin that binds to mannose. The assay finds the binding ability of the polymers by measuring the absorbance of the solution. As binding occurs, the lectin crosslinks with the polymer, leading to precipitation of the lectin out of solution and an increase in absorbance. An intermediate molecular weight linear polymer was chosen with 25 mannose residues and dissolved to 0.1 mg/mL in a HEPES buffered solution containing Ca^{2+} ions and mixed with an equal volume of 1 μM Con A. No increase in absorbance at 420 nm was seen over 15 minutes. In contrast, a natural polysaccharide, mannan, was tested and

showed a dramatic increase in absorbance as lectin crosslinked and precipitated out of solution. This negative result for Con A and glycopolymer binding was not surprising as the lectin requires binding at the 3-, 4-, and 6- hydroxyls.[146] The synthetic scheme for our glycomonomer and glycoinimer results in the mannose connected to the backbone at the 6 position so binding is therefore not possible.

6.2.2 Interaction with mannose binding lectin

We next studied the ability of human mannose binding lectin to bind with the different glycopolymers. MBL binding is dependent on only the 3- and 4- hydroxyls[75] so in contrast to the Con A experiments, we expect the polymers to exhibit binding activity. MBL binding was first measured using a direct enzyme linked lectin assay (ELLA), an assay similar to the commonly run enzyme linked immunosorbent assay (ELISA). In this assay, the polymer of interest was adsorbed to a plastic plate and checked for binding to lectin in solution. In this set of experiments, human serum was used as a source of MBL. The immunosorbent wells incubated with glycopolymer showed significantly less binding with MBL than positive control wells incubated with mannan (Figure 6.3).

The assay was not sensitive enough to detect differences between polymers with different molecular weight or architecture. This lack of sensitivity may stem from two causes. First, the synthetic glycopolymers are of lower molecular weight compared to mannan resulting in less adsorption to the well. Furthermore, adsorption of the polymers to the plastic may cause conformational changes that mask any binding differences between different polymers.
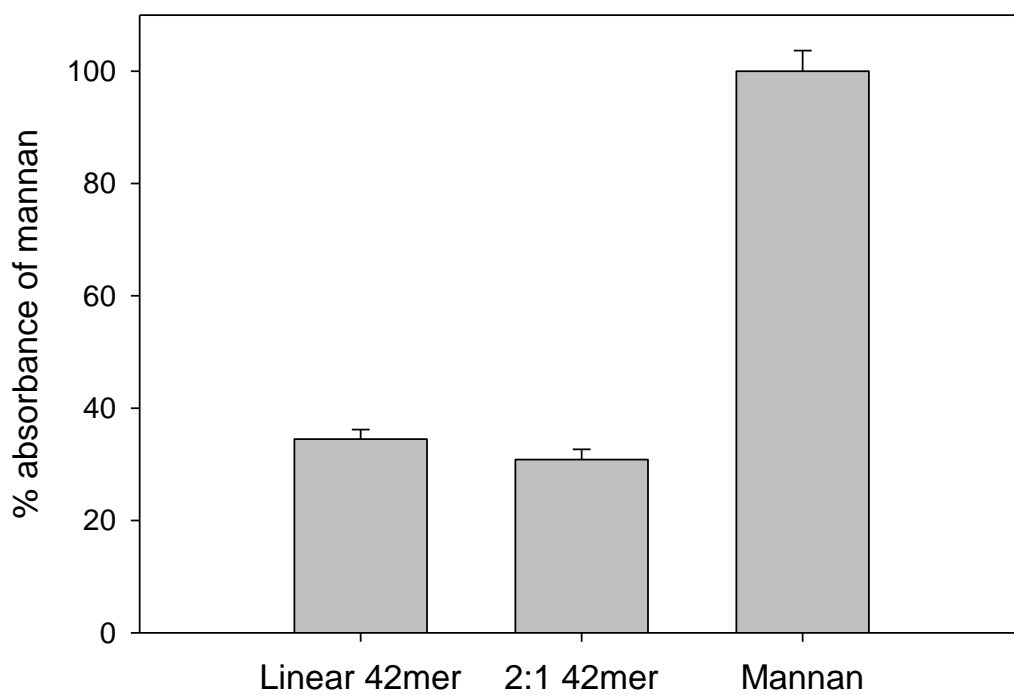
Figure 6.3: Direct enzyme linked lectin assay shows linear and branched glycopolymers glycopolymers interact with mannose binding lectin with much less affinity than the natural polysaccharide mannan. Little difference is seen between the different architectures.

In order to tease out subtle differences in binding activity of glycopolymers, MBL interaction was quantified through an inhibitory enzyme linked lectin assay. The assay relies on a competition between binding of lectin to polymers in solution versus the natural polysaccharide mannan coated on a plate. Polymers with higher inhibition of MBL from mannan can be interpreted as having more interaction and avidity with MBL. Relative potency was determined by comparing the IC_{25} values of monomeric mannose and the polymer rather than the customary IC_{50} values as some of the polymer inhibition curves plateaued before reaching 50% inhibition. This plateau occurs as the bound mannan outcompetes the soluble polymer and is a well known limitation of ELLA.[9] The inhibition values could be artificially increased by decreasing the amount of serum added but would lead to loss of resolution for the higher avidity polymers. Using IC_{25} for relative potency calculations still captures the differences between polymers without leading to any of the magnitude distortions when using IC_{50}. Statistically significant differences between data sets were determined by comparing plotted 95% confidence bands.[147] Two data sets are considered to be significantly different if their confidence bands do not overlap (Figures 6.6, 6.7). Relative potencies of glycopolymers with MBL against free mannose are shown in Table 6.4.

Effect of molecular weight

The cluster glycoside effect was demonstrated with the increased interaction of linear glycopolymers with increasing molecular weight, after normalizing for the concentration of mannose residues. A linear polymer with 42 mannose units (Entry 2) inhibits MBL 80 times better than a linear polymer with 14 mannose units (Entry 1) as seen in Figure 6.4a. This effect tapered off at higher molecular weight with little potency difference between glycopolymers with 42 and 75 mannose units (Entries 2 and 3).

The cluster glycoside effect was also seen with branched glycopolymers when varying the molecular weight but maintaining the comonomer feed ratio (Figure 6.4b). A branched glycopolymer with 42 mannose residues (Entry 5) interacts with MBL ten times better than a branched glycopolymer with 14 mannose residues (Entry 4) with the same apparent branching density.

Effect of branching

The polymer architecture was found to have a significant effect on MBL interaction. A highly branched polymer with 14 mannose residues (Entry 9) has 90 times greater interaction with MBL than a linear polymer with the same number of mannose residues (Entry 6) (Figure 6.4c, black circles versus white triangles). The effect is diminished but still present with higher molecular weight polymers with a branched polymer with 42 mannose residues (Entry 11) inhibiting MBL four times better from mannan than a linear polymer with the same number of mannose residues (Entry 10). This architecture-dependent enhancement in binding avidity can also be attributed to the cluster glycoside effect as the branched glycopolymers offer increased clustering of the mannose units over the linear glycopolymers. This effect has been previously seen with a sialic acid glycopolymer used for influenza virus inhibition,[142] in which linear glycopolymers and spheroidal glycodendrimers were not as effective inhibitors as comb-branched glycopolymers.

Effect of branching density

An increase in the apparent branching density of glycopolymers increases the avidity of the MBL interaction. A branched polymer with higher branching density inhibits MBL three times as well than a branched polymer of the same mannose content but lower branching density (Entry 9 versus Entry 8, Figure 6.4c; black circles versus white circles). Previous work has noted that the increased interaction due to additional branching rapidly diminishes as the excess branches may entangle and limit interaction with the protein or become buried within the polymer and be unavailable for binding.[142] The decrease in interaction with higher branching density is consistent with binding results of natural oligosaccharides with *Apostichopus japonicus* mannose binding lectin. This lectin's hemagglutination activity was inhibited by low-branched oligosaccharides but not by high-branched mannans.[148] Unfortunately, because the glycoinimer could not be homopolymerized, we could not test whether our polymers followed the same trend with the highest theoretical branching density version of our glycopolymer.

Effect of saccharide at the branch point

The presence of mannose at the branch point led to three times as much inhibition compared with a similarly branched polymer without saccharide at the branch point (Figure 6.5a). This result by itself was inconclusive for determining the effect of saccharide at the branch point because these two glycopolymers had a slight difference in the number of mannose residues per chain but similar overall M_n (Entry 12: 10 mannoses with no saccharide in the branch point versus Entry 13: 14 mannoses with mannoses in the branch point). Some of the difference in avidity may be due to differences in the number of mannoses per chain.

Glycopolymers with a lower apparent branching density were also tested. Glycopolymer without mannose at the branch point (Entry 15, 18 mannoses) was tested against glycopolymer with mannose at the branch point (Entry 16, 14 mannoses). If only the number of mannoses is considered, entry 16 should have higher potency. However, there was no significant difference between the two polymers (Figures 6.5b, 6.7). The presence of mannose at the branch point compensated for the lower overall number of mannose units so that the two polymers had similar inhibition profiles.

Placing a saccharide at the branch point will result in changes to the physical properties of the polymer (i.e. more flexible backbone) that could influence lectin binding. Therefore, we tested a branched glycopolymer that used a galactose inimer. Galactose does not bind to MBL and thus allows us to separate the effect of physical properties from the biomimetic properties of placing mannose at the branch point. The glycopolymer that incorporates galactose at the branch point (Entry 14) was three times less potent than a similarly branched glycopolymer with mannose at the branch point (Entry 13), despite both having a similar number of mannoses. In comparison, the galactose containing branched glycopolymer had a similar inhibition profile as Entry 12, a glycopolymer with similar mannose content but with no saccharide content at the branch point, indicating that there was no binding effect from the physical properties of the branch point.

Therefore, we can attribute the increase in MBL avidity to the biomimetic nature of the branched polymers containing the mannose inimer rather than any physical property changes due to the incorporation of saccharide at the branch point. This effect has some precedent: even though MBL typically binds to terminal sugars, a study with natural oligosaccharides suggests that lectins can also interact with backbone or side-chain mannose residues.[148]

131

Table 6.4: Relative potency of glycopolymer interaction with MBL.

Entry	Compound	Relative potency[a]
	Mannose	1
	Effect of MW: Linear polymers[b]	
1	# mannose = 14	1
2	# mannose = 42	80
3	# mannose = 75	60
	Effect of MW: Branched polymers[c]	
4	# mannose = 14, $[M]_0$:[Mannose inimer]$_0$ 2:1	30
5	# mannose = 42, $[M]_0$:[Mannose inimer]$_0$ 2:1	300
	Effect of Architecture[d]	
6	# mannose = 14, linear	1
7	# mannose = 10, $[M]_0$:[Mannose inimer]$_0$ 5:1	3
8	# mannose = 14, $[M]_0$:[Mannose inimer]$_0$ 2:1	30
9	# mannose = 14, $[M]_0$:[Mannose inimer]$_0$ 1:1	90
10	# mannose = 42, linear	80
11	# mannose = 42, $[M]_0$:[Mannose inimer]$_0$ 2:1	300
	Effect of Mannose in Branch Point[e]	
12	# mannose = 10, $[M]_0$:[Inimer]$_0$ 1:1	30
13	# mannose = 14, $[M]_0$:[Mannose inimer]$_0$ 1:1	90
14	# mannose = 13, $[M]_0$:[Galactose inimer]$_0$ 1:1	30
15	# mannose = 18, $[M]_0$:[Inimer]$_0$ 2:1	20
16	# mannose = 14, $[M]_0$:[Mannose inimer]$_0$ 2:1	30

a: $IC_{25mannose}$:$IC_{25compound}$
b: Significant differences between entries 1 and 2, 1 and 3
c: Significant differences between entries 4 and 5
d: Significant differences between entries 6 and 8, 6 and 9, 7 and 8, 7 and 9, 8 and 9, 10 and 11
e: Significant differences between entries 12 and 13, 13 and 14
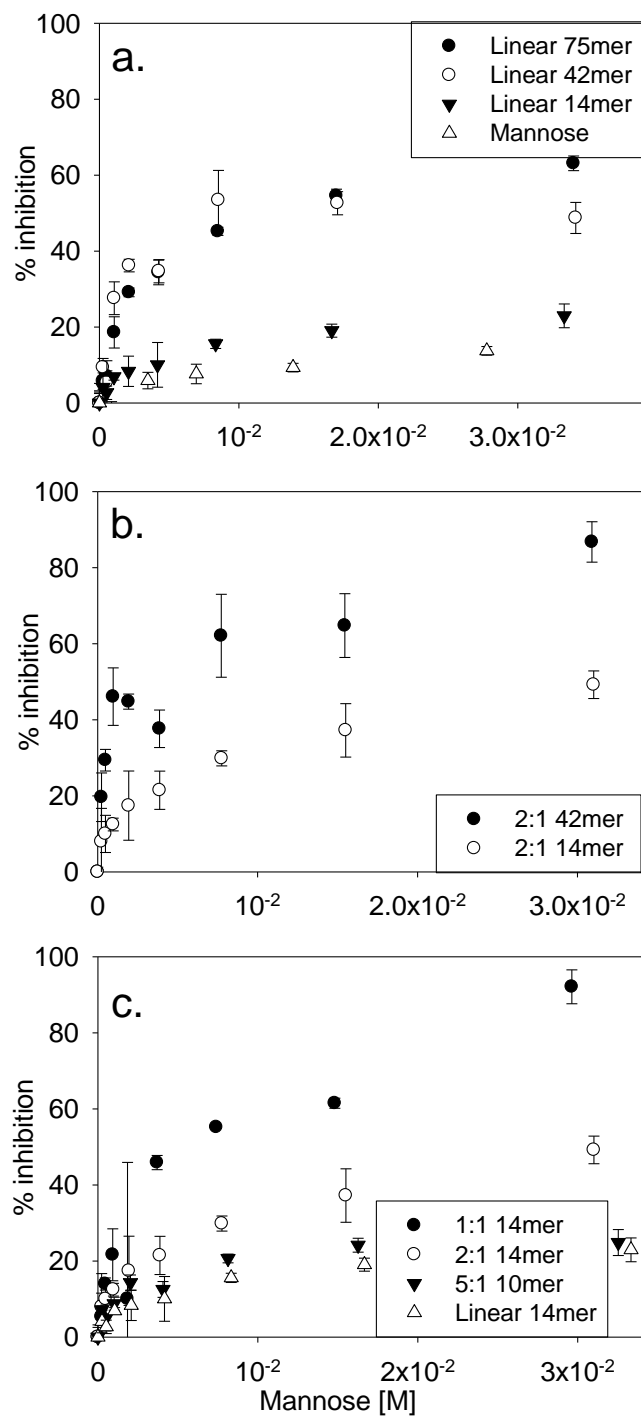
Figure 6.4: Mannose glycopolymers have increased interaction with MBL with (a) increasing linear polymer molecular weight, (b) increasing branched polymer molecular weight, (c) branching architecture, and increasing branching density. The ratios represent the initial polymerization conditions $[M]_0$:[Mannose inimer]$_0$.
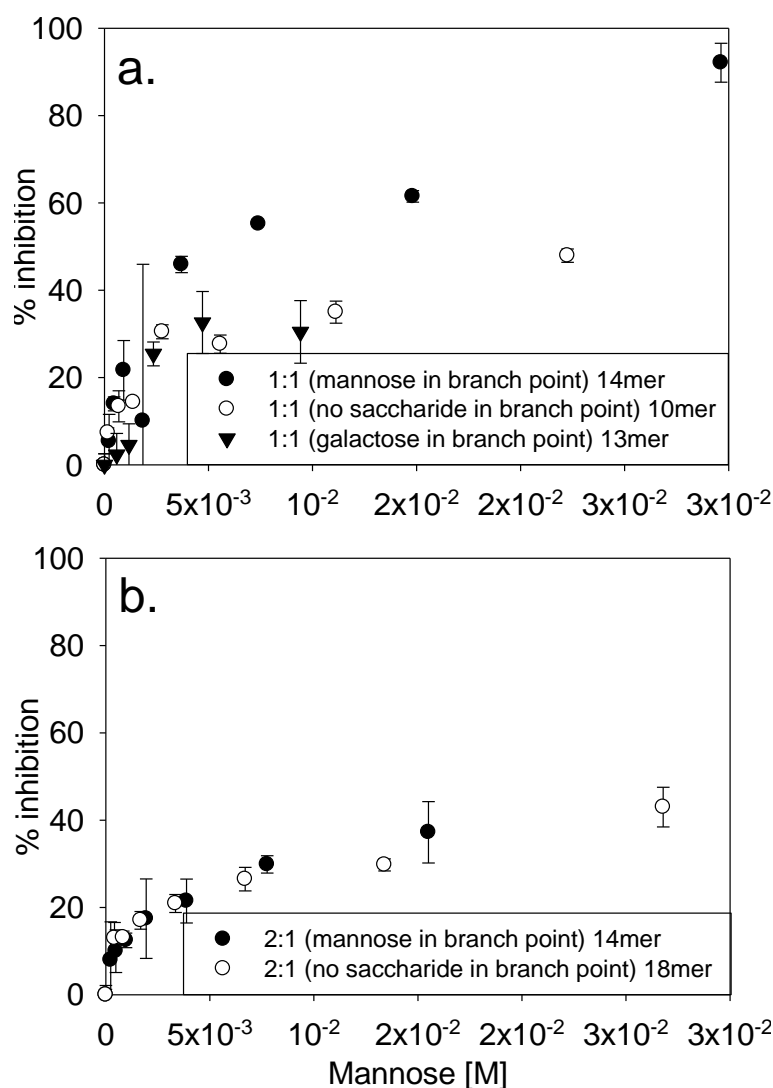
Figure 6.5: Presence of mannose at the branch point of glycopolymers increases interaction with MBL (a) at higher branching density and (b) at lower branching density. The branched polymer with saccharide at the branch point (14 mannose units) has similar inhibition profile as the branched polymer without saccharide at the branch point (18 mannose units). The ratios represent the initial polymerization conditions $[M]_0$:$[Glycoinimer]_0$ (mannose or galactose at branch point) or $[M]_0$:$[Inimer]_0$ (no saccharide at branch point).

134
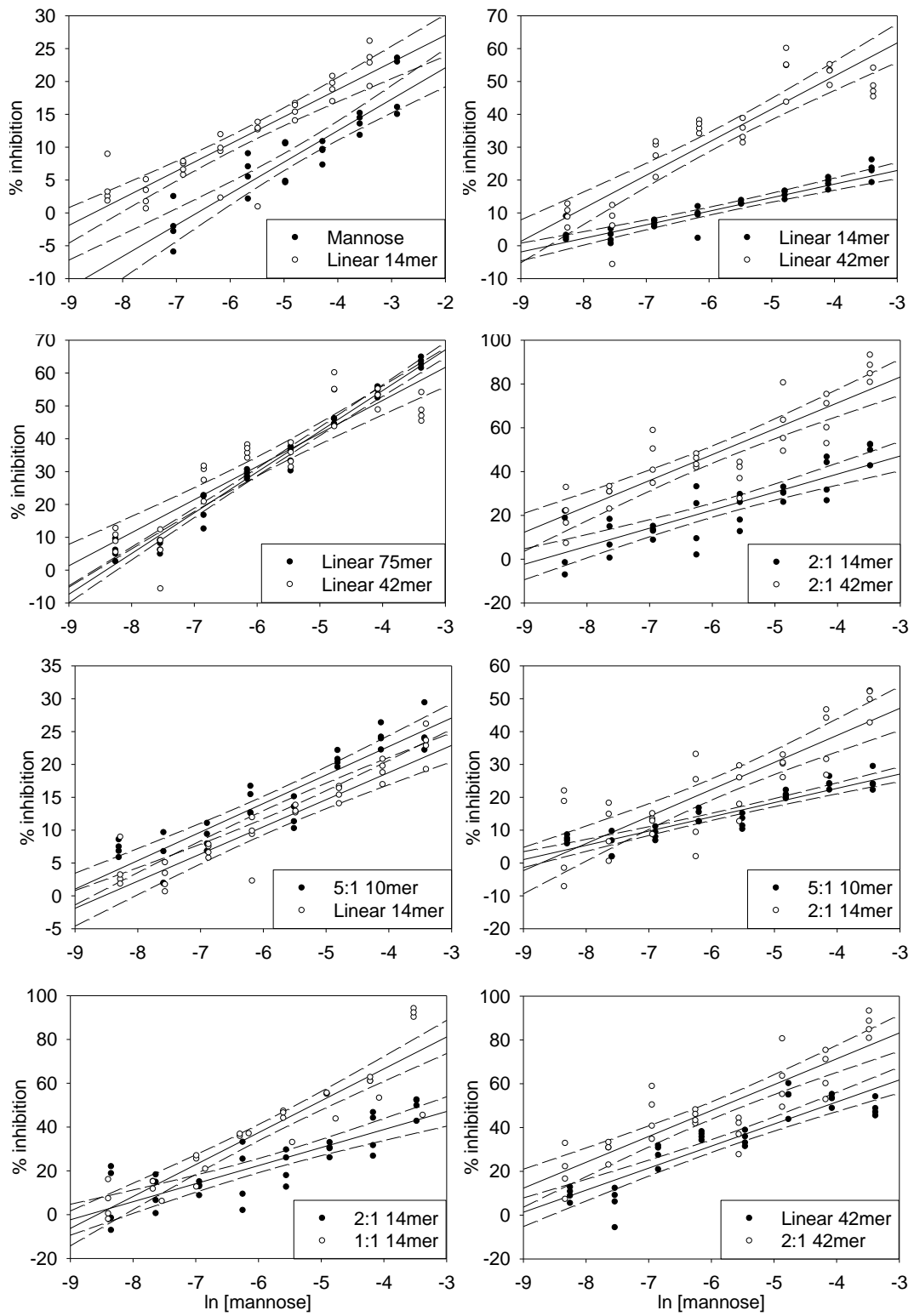
Figure 6.6: Confidence band comparisons of data sets shown in Figure 6.4 to determine significant differences.
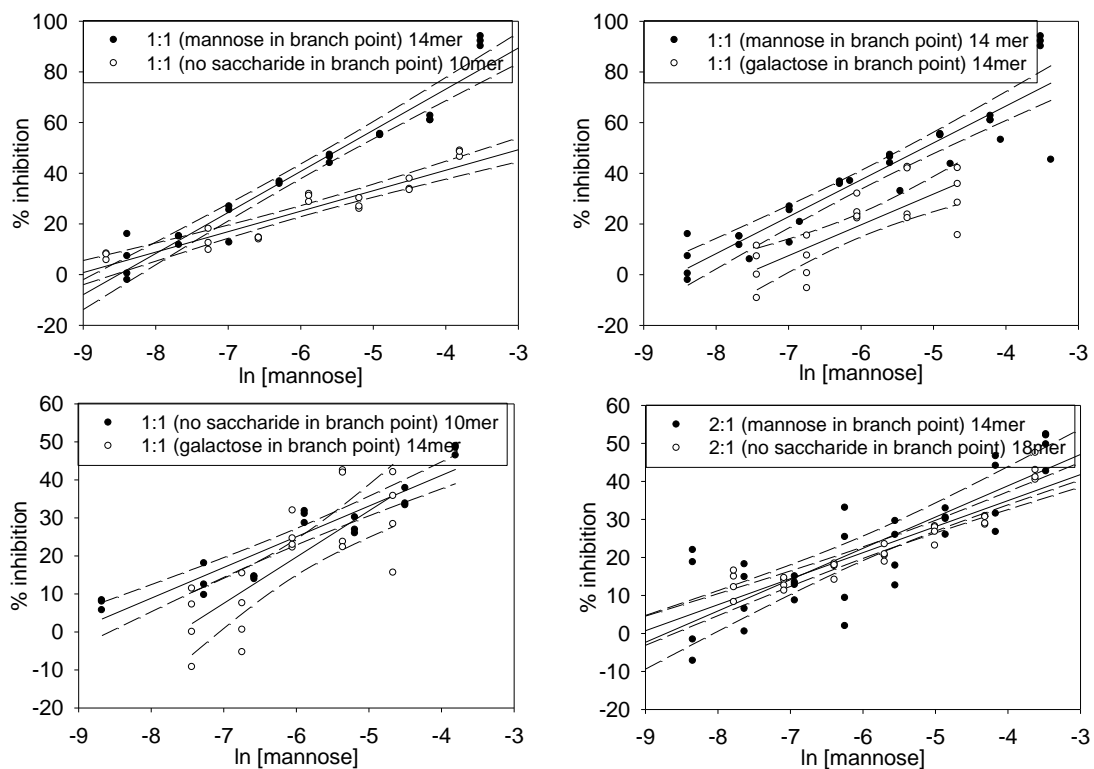
Figure 6.7: Confidence band comparisons of data sets shown in Figure 6.5 to determine significant differences.

6.3 Biological interaction of protein glycopolymers from Chapter 4

The protein-polymers described in Chapter 4 were polymerized directly from bovine serum albumin and are composed of pendant mannose and/or galactose. The number of saccharides per protein (and therefore per chain) were varied along with the composition of mannose and galactose. Table 6.2 summarizes the properties of the glycopolymers investigated in this section.

6.3.1 Interaction with mannose binding lectin

Similar experiments with MBL were conducted on the protein-glycopolymer conjugates as described earlier. The experimental procedures are roughly the same; the largest change is the use of recombinant human mannose binding lectin (rMBL) rather than human serum and a corresponding change in the primary antibody used.

Direct ELLA

Biological interaction was first tested through direct ELLA. Bovine serum albumin (BSA), the BSA macroinitiator, and a BSA-galactose polymer with 184 galactoses all had negligible binding to rMBL when compared to the polysaccharide mannan as seen in Figure 6.8a. When mannose content was incorporated, we observed nearly similar binding as seen with the positive control, mannan, with the greatest interaction seen with the largest polymers, M1200 and M600 with 360 and 239 mannoses respectively (Figure 6.8b). Decreasing mannose content to 70 with M150 led to a statistically significant drop in interaction. MG300300, a mannose/galactose copolymer with 174 total saccharides (87 mannoses assuming even split of mannose and galactose) was not significantly different from M150. These results suggest that the total number of reactive saccharides is the controlling factor in rMBL

binding rather than their distribution, as MG300300 has roughly the same number of reactive mannoses as M150, but they are distributed randomly in a statistical copolymer with galactose.
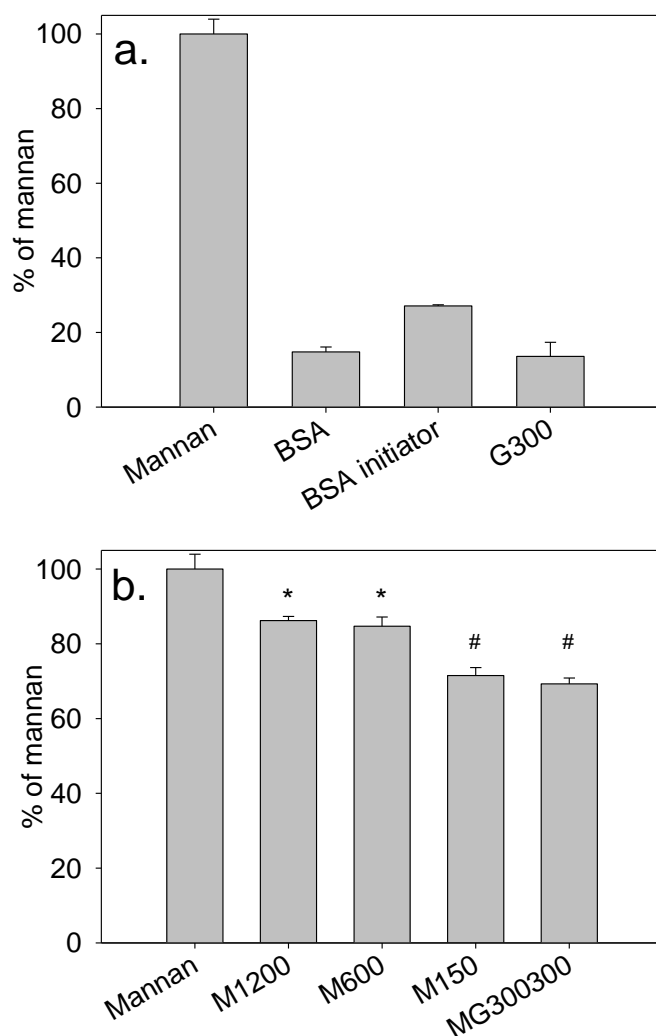
Figure 6.8: Direct enzyme linked lectin assay of protein glycopolymers show (a) BSA, BSA initiator, and BSA-galactose have negligible binding with rMBL and (b) increasing mannose content increases binding. * Denotes statistically significant difference between groups with a * symbol and groups without a * symbol. # denotes statistically significant difference between groups with a # symbol and groups without a # symbol.

Inhibitory ELLA

Although direct ELLA is a good tool for determining binding of the lectin, it may lead to some artifacts because of different levels of adsorption between samples or conformational changes due to adsorption of the protein-glycopolymer to the well plate. Therefore, we also characterized the protein-glycopolymers through inhibitory ELLA to elucidate more subtle differences between the samples. Inhibitory ELLA also allows us to more directly compare these conjugates against glycopolymers with no protein content, as the free glycopolymers may not adsorb to the well plates in a similar fashion.

As expected, unmodified BSA and BSA-macroinitiator had no inhibitory effect on rMBL binding with mannan (Figure 6.9a) and BSA-galactose glycopolymer showed only slight inhibition with an inhibition plateau at 10% (Figure 6.9b). These results demonstrate the assay's specificity for mannose-containing structures and that the protein structure alone has no effect on rMBL binding.

Figure 6.9: Inhibitory enzyme linked lectin assay shows (a) BSA, BSA-Br$_{22}$ do not interact with rMBL and (b) BSA-galactose polymers interact minimally with rMBL.

While a BSA-mannose glycopolymer that bound rMBL and activated complement has been previously synthesized through a grafting-to approach of a *single* polymer chain to BSA's free thiol,[5] no other structures were explored. We studied the effect of mannose content on rMBL interaction as we presented multiple glycopolymer chains and varied the mannose presentation by varying chain length or mannose density.

We increased the mannose chain length by increasing the feed ratio of mannose monomer to BSA-macroinitiator. M600 (239 mannoses per protein) had a relative potency six times higher than M150 (70 mannoses per protein) when comparing IC_{50} values (Figure 6.10, Table 6.5). The increase in potency from M150 to M600 is consistent with the cluster glycoside effect, where multivalent structures of saccharides show enhancement of activity compared to a corresponding amount of monosaccharide.[9] However, when mannose content was increased with M1200 (360 mannoses per protein), there was no statistically significant difference when comparing the IC50 of M1200 with M150 or M600 demonstrating that the cluster glycoside effect tapers off. This tapering behavior was seen previously in the previous work with linear polymers without protein content (Figure 6.4a) The inhibition behavior of M150 may also be near the lower bound of the cluster glycoside effect for this protein-glycopolymer system as M150's individual polymer chains are already at the oligomer scale (three repeat units per chain if polymer grows from all initiating sites).

We decreased the density of pendant mannoses by copolymerizing non-reactive galactose derived monomers. M150 (70 mannoses per protein) exhibits a relative potency 13 times higher than MG300300 (174 saccharides per protein, 87 mannoses per protein) despite having roughly the same number of mannose saccharides (Figure 6.10, Table 6.5). These results directly contradict those seen earlier from direct ELLA of rMBL where there was no difference in binding between M150 and MG300300. However, direct ELLA has limitations due to the adsorption of

protein-polymer to plastic that could mask subtle binding differences from the copolymerization. This decrease in inhibition can be attributed to the increased distance between mannose units leading to decreased avidity of rMBL for the polymer.
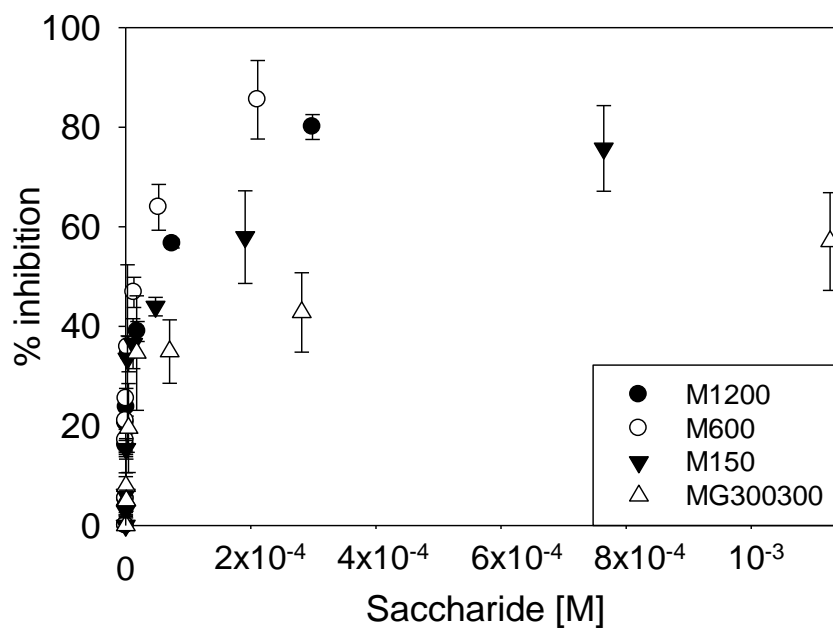
Figure 6.10: Inhibition of rMBL increases with increasing mannose polymer chain length (M150 vs M600) and decreases as galactose content is added (MG300300 vs M150).

We examined the effect of multivalent 3D presentation of the glycopolymer chains from the protein compared to glycopolymers with no protein attachment (synthesized as described in Chapter 3). Inhibition of rMBL binding by a mannose glycopolymer with 75 pendant mannose residues was 260 times weaker than inhibition by M150 with 70 mannoses per protein (Figure 6.11, Table 6.5). These results are even more striking when considering that the average degree of polymerization for M150 is three repeat units if all 22 initiation sites are reactive. In comparison, inhibition curves by a linear glycopolymer with 14 repeat units were no different than monosaccharide mannose.
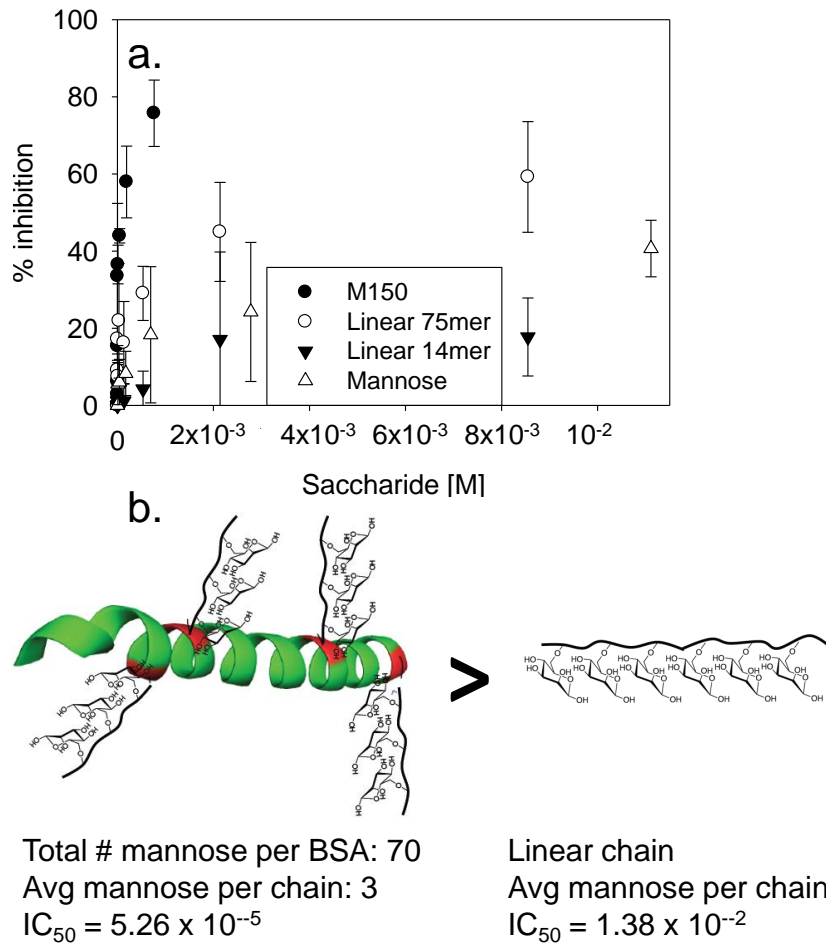
Figure 6.11: (a) M150, a BSA-mannose glycopolymer with 70 mannoses arranged around the protein, inhibits rMBL better than a linear glycopolymer with 75 repeat units. A linear glycopolymer with 14 repeat units has similar inhibition as monomeric mannose. (b) Idealized structures of the protein-polymer conjugate (fragment shown here) compared to the linear polymer.

Table 6.5: Summary of rMBL inhibition data.

Compound	# mannoses/protein	# mannoses per chain	IC_{50}
M1200	360	16	2.35E-05
M600	239	11	8.43E-06
M150	70	3	5.26E-05
MG300300	87	4	6.95E-04
Linear 75mer	N/A	75	1.38E-02
Linear 14mer	N/A	14	N/A
Mannose	N/A	1	N/A

These multivalent 3D presentation results add a new dimension to the traditional view of the cluster glycoside effect as the presence of multiple short mannose chains attached to one protein clearly results in increased interaction between the glycopolymer and rMBL as compared to individual longer polymer chains (Figure 6.11b). The carbohydrate binding activity of most lectins is thought to be mediated through multiple carbohydrate recognition domains (CRDs) comprised of a limited number of amino acids. Lectins from diverse sources lack primary sequence homology but share similarities in their tertiary structure. The similarities in tertiary structure imply that the 3D presentation of multiple CRDs is crucial for lectin-polysaccharide interactions, especially since the per-residue affinity for saccharide-lectin interactions is quite low.

Kiessling has also synthesized a protein with 3D presentation of individual saccharides.[137] Up to ten thiolated mannoses were attached to lysines modified with maleimide groups. The saccharide modified protein inhibited Con A binding 38 times better than αMeMan. In comparison, a 12-mer linear mannose polymer synthesized through ring-opening metathesis polymerization had greater inhibition with 1000 times more binding than αMeMan. We found more inhibition with our protein-saccharide structures versus free linear polymers. Our protein structures differed from Kiessling's structures by having multivalent presentation of saccharides in the form of glycopolymer chains, while having similar 3D presentation of saccharides around the protein.

Another group linked a streptavidin-oligosaccharide conjugate to biotinylated BSA resulting in 11 streptavidins and 140 oligosaccharides bound to BSA on average.[149] The BSA-streptavidin-oligosaccharide conjugate bound Chinese hamster ovary cells 42 times better than individual streptavidin-oligosaccharide structures. These results are not directly comparable to our results due to differences between the assays. However, they do reinforce the importance of both multivalent structures and 3D presentation of polymer chains to promote binding of lectins.

145

We speculate that the attachment of each polymer chain to the central protein component maintains the polymer chains in close proximity and allows for rMBL to more easily span and bind two polymer chains. Further work is still required to elucidate the mechanistic basis behind these enhancements.

6.3.2 Activation of complement

The protein-glycopolymers were tested for their ability to activate complement. The assays described so far only quantify (either directly or indirectly) the amount of MBL bound by the glycopolymers, but do not give any information on whether the lectin binding could support complement activation. We adapted an existing protocol for determining complement activation through the mannose binding lectin pathway.[150] The assay detects the product of the first step of the MBL complement cascade: the cleavage of C4 by MASP. The well was coated with the protein of interest, blocked, and then incubated with human serum to allow binding of MBL and MBL-associated serine proteases (MASP). The MASP complex cleaved supplemented C4 which was detected with an anti-C4 antibody. Any cleavage of C4 by the classical pathway was prevented by using high ionic strength conditions (1 M NaCl) that prevent binding of C1q to antibody and degrades the C1 complex.[151]

Complement binding results revealed that both mannose and galactose protein-polymers were able to activate immune complement (Figure 6.12a). These results do not agree with prior ELLA experiments which showed strong binding of rMBL to mannose polymers but little binding to galactose polymers (Figure 6.9b), as well as commonly understood mechanisms of the MBL pathway. Furthermore, native BSA is not glycosylated and is not expected to trigger any significant activation of complement through the mannose binding lectin pathway. Complement could be activated through the classical pathway due to antibodies reacting against the bovine protein; however, high sodium chloride concentration should prevent activation of the cascade by breaking down any binding of complement proteins

146

to antibody. While complement activation through the alternative pathway is possible due to a chance of increased hydrolysis of C4 by the synthetic polymer component, C4 does not play a role in the alternative pathway.

In order to further explore these results, human serum was depleted of mannose binding lectin through exposure to mannan-agarose. This depletion resulted in near total loss of complement activity against a mannan polysaccharide, but only partial loss of complement activity for the protein-polymers. Mannose polymers had a greater loss of complement activity with MBL depletion than compared to galactose polymers as shown in Figure 6.12b,c for the absolute difference as well as ratio between Abs_{normal} and $\text{Abs}_{depleted}$ although the differences were not statistically significant.

These results suggest that MBL plays a role in directing complement activity against mannose-containing glycopolymer structures, but that there are also unknown pathways that result in continued complement activity against both mannose and galactose protein-polymers, even after MBL depletion from serum. Further studies are warranted to explore these findings.
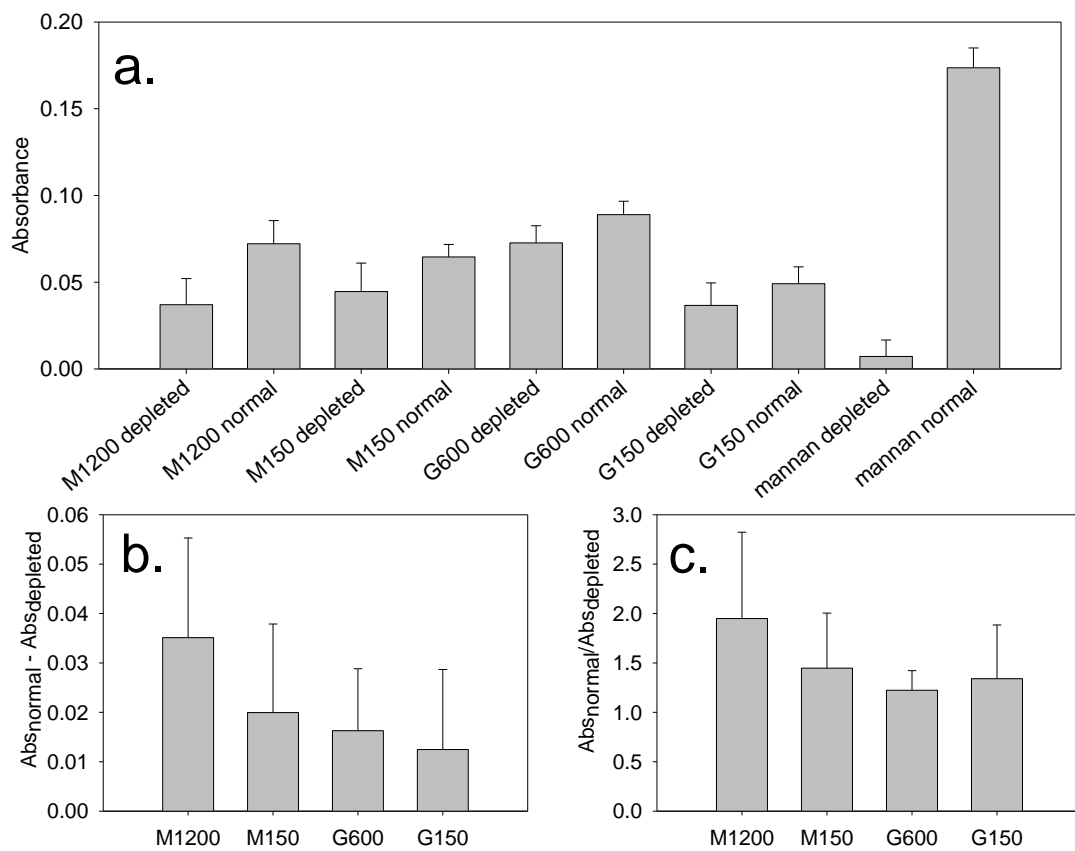
Figure 6.12: Complement is activated against both mannose and galactose protein-polymers through the MBL pathway as well as an unknown pathway. (a) Absorbance values (corrected for a protein control) show activation of complement against protein-glycopolymers and mannan. When serum is depleted of MBL, complement activity is significantly decreased for mannan and to a lesser extent for protein-glycopolymers. Loss of complement activity differs between mannose and galactose protein-polymers when comparing the (b) difference and (c) ratio between Abs_{normal} and $\text{Abs}_{depleted}$.

6.4 Biological interaction of polymers bearing RGD cell binding domain or galactose from Chapter 5

The polymers from Chapter 5 have pendant GCGYG**RGD**SPG peptides or galactoses through post-polymerization modification of pyridyl disulfides. These modified polymers were tested for their effect on cell adhesion. Table 6.3 summarizes the properties of the polymers investigated in this section.

6.4.1 Polymers modified with RGD peptide

Cells bind with extracellular matrix (ECM) proteins such as collagen or fibronectin through integrin mediated adhesion. The specific cell binding domain sequence in the protein has been identified as arginine-glycine-aspartic acid (RGD). This sequence has been incorporated into synthetic peptides in order to promote cell adhesion to tissue engineering surfaces. Conversely, if a peptide containing the RGD sequence is present in solution, it will competitively inhibit cell adhesion to a surface. For 2D polystyrene surfaces used in routine cell culture, cells adhere to the plastic due to hydrophilic and ionic interactions along with integrin-mediated binding due to ECM proteins present in the culture medium.

Competitive inhibition has been demonstrated previously using clusters of 64 RGD peptides on the periphery of polyamidoamine dendrimers.[152] The RGD conjugated dendrimers decreased cell adhesion with a concentration-dependent effect under serum-free conditions. However, there was no difference in cell adhesion compared to control samples with free RGD indicating that there is no clustering effect for the presentation of soluble RGD.

Branched polymers, in comparison to dendrimers, are not as perfectly branched or as densely crowded. Branch points are incorporated statistically rather than through designed syntheses of multiple generations. This architectural change may result in a different effect on cell adhesion. Therefore, we supplemented free

GCGYG**RGD**SPG peptide (referred to simply as RGD peptide from here) or RGD polymer (RGD 198:5:5:1) to the media used to cultivate NIH 3T3 fibroblasts grown on 10% poly(ethylene glycol) diacrylate hydrogels containing 1 mM of tethered RGD.

Within five minutes of adding the free RGD peptide or RGD polymer supplemented media, the fibroblasts had adopted a rounded morphology and began to detach from the hydrogel as the soluble RGD (in both forms) began to compete with tethered RGD for cell binding sites as can be seen in Figure 6.13a and b. After incubating for two hours, the gels were gently washed twice with media to remove detached cells. Cell quantification with Cell Titer-Blue assay showed no significant difference between either RGD polymer or free RGD peptide, although a clear dose-dependent trend was seen, again without a significant difference (Figure 6.13d).

Strong conclusions cannot be made from these results about the efficacy of RGD polymer clustering due to the error introduced from large variability of 2D cell culture on hydrogels. However, it is clear that the presentation of RGD through disulfide exchange with the pyridyl disulfide polymer does not disrupt its biological activity. Furthermore, large multivalent polymers may be advantageous for the removal of cells or generation of cell aggregates.
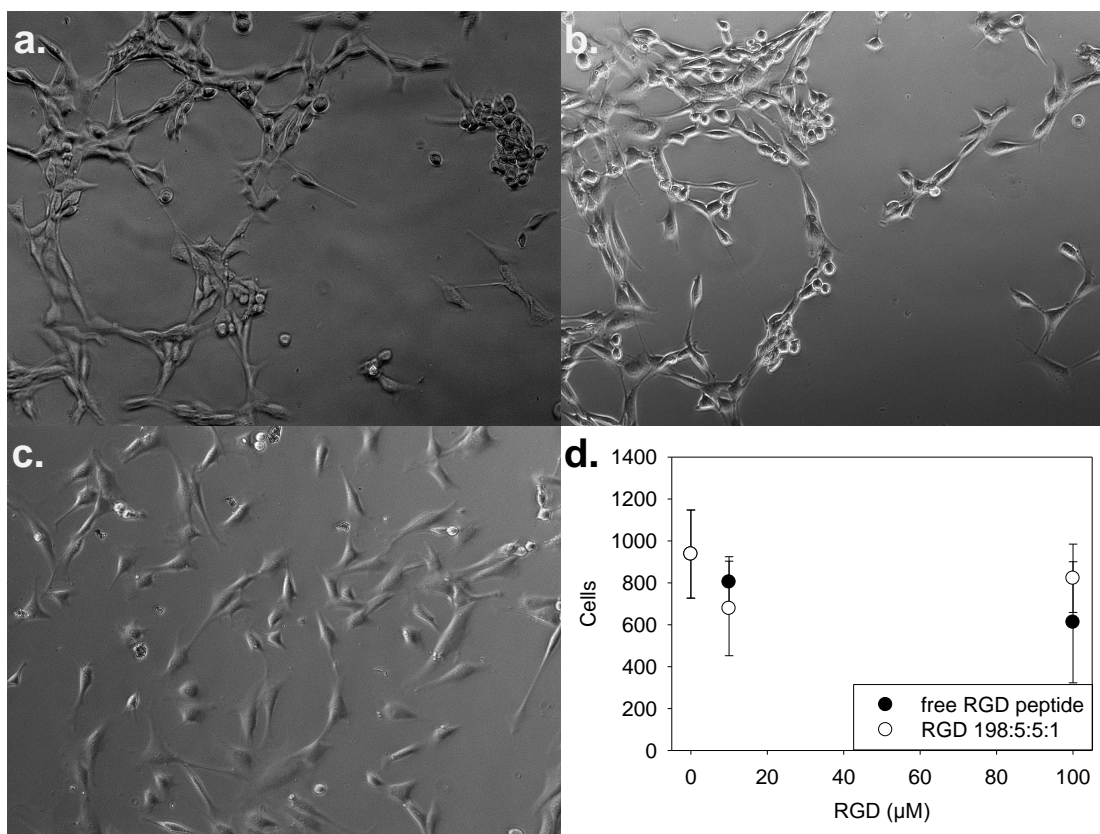
Figure 6.13: 3T3s seeded on 10% PEG hydrogels with 1 mM RGD exhibited rounded morphology and began to detach after five minutes exposure to (a) 100 μM free RGD and (b) RGD 198:5:5:1 with overall 100 μM RGD content, compared to (c) 3T3s cultured in regular media. (d) Cell number was quantified with Cell Titer-Blue and showed no significant difference between RGD presentation methods.

It is interesting to note that when a similar experiment was conducted using 3T3 fibroblasts seeded onto a fibronectin-coated polystyrene surface, the addition of free RGD peptide or RGD polymer (RGD 100:5:5:1 or 198:5:5:1) had no effect on cell adhesion as seen in the DNA quantification results of Figure 6.14 as well as optical micrographs (not shown). We attribute this difference in binding results of PEG-RGD hydrogels and fibronectin coated polystyrene surfaces to binding affinity differences between the short RGD peptide sequence and the full fibronectin sequence, as well as modulus differences between the soft hydrogel and relatively stiff polystyrene surface.
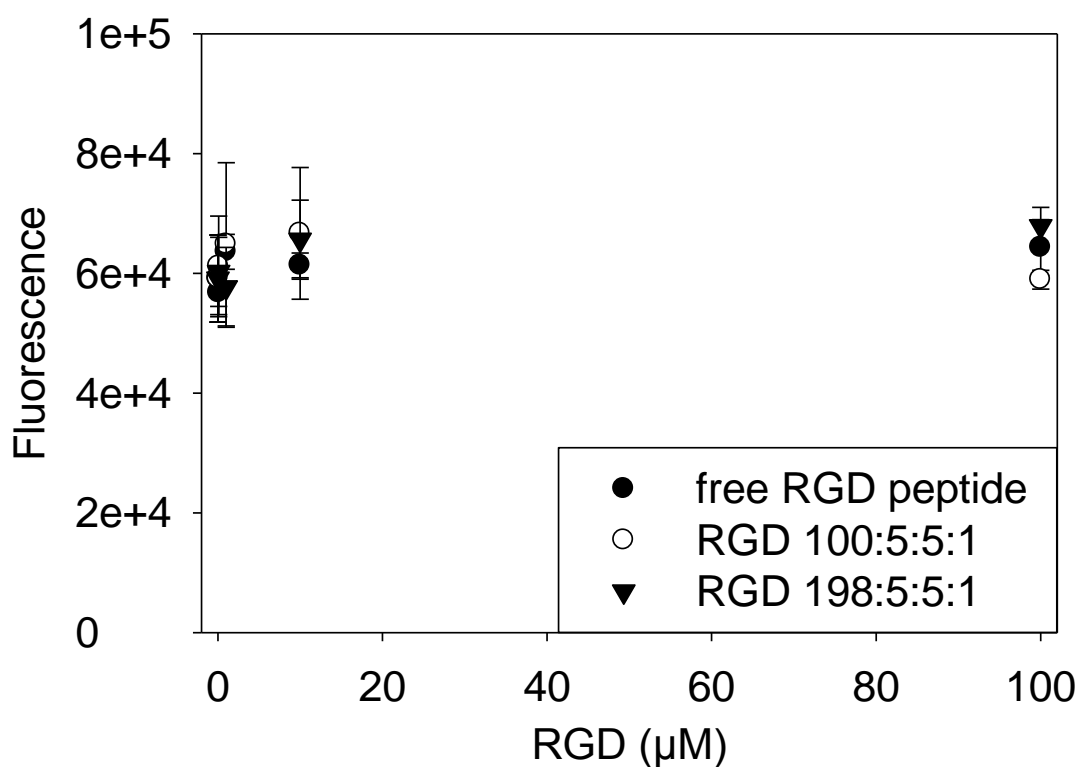
Figure 6.14: DNA quantification shows no effect from free RGD and RGD polymers on cells adhering to a fibronectin coated surface.

6.4.2 Polymers modified with galactose

Saccharides may also play a role in cell adhesion. For example, liver tissue enginer-
ing often relies on surfaces modified with galactose to bind with the asiaglycoprotein
receptor (ASGPR) on hepatocytes. ASGPR binding reduces integrin mediated
signalling and avoids the loss of hepatocyte phenotype. Aside from liver tissue
engineering, much of the research with biomimetic ECMs has ignored the promi-
nent role sugars have between cells and the natural ECM due to glycosylated
proteins (e.g. chondroitin sulfate on aggrecan) and polysaccharides (hyaluronic
acid). Instead, biomimetic ECMs used in tissue engineering have been composed
of proteins and protein derived compounds.

A related pilot project in our lab incorporated galactose monomers into PEG
hydrogel networks to see if cell adhesion could be mediated by saccharide containing
structures. In this work, NIH 3T3 fibroblasts were found to adhere to 10%
PEG hydrogels when the PEG diacrylate was photopolymerized with 6-acryloxy
galactopyranose (20 to 100 mole % with respect to PEG) as shown in Scheme 6.1.
PEG hydrogels with no galactose content and no added cell-binding domains had
minimal cell adhesion, with cells adopting a rounded morphology (Figure 6.15).
Cells were similarly sparse on the 20 mole % galactose gels, but adopted a more
extended morphology. There were dense regions of cells with extended morphology
on the 50 mole % gels. When galactose content was increased to 100 mole %,
some regions were very dense while others had very little adhesion, possibly due to
delamination as a result of overgrowth. Picogreen DNA quantification confirmed
the visual results as well (Figure 6.16).

We hypothesize that galectins in solution may bind to the hydrogel's galactose polymer chains and in turn, mediate fibroblast adhesion to the hydrogel.[153] However, our results were somewhat inconsistent, possibly due to varying levels of galectin produced by the fibroblasts or in the cultivation serum, or to distribution of monovalent residues throughout the gel.
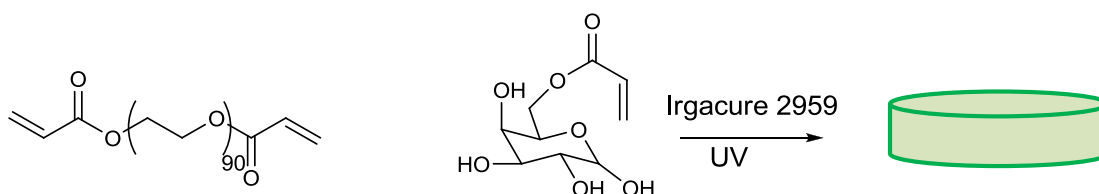
Scheme 6.1: Hydrogels with galactose content were created through UV initiated polymerization of poly(ethylene glycol 4000) diacrylate with 6-acryloxy galactopyranose.
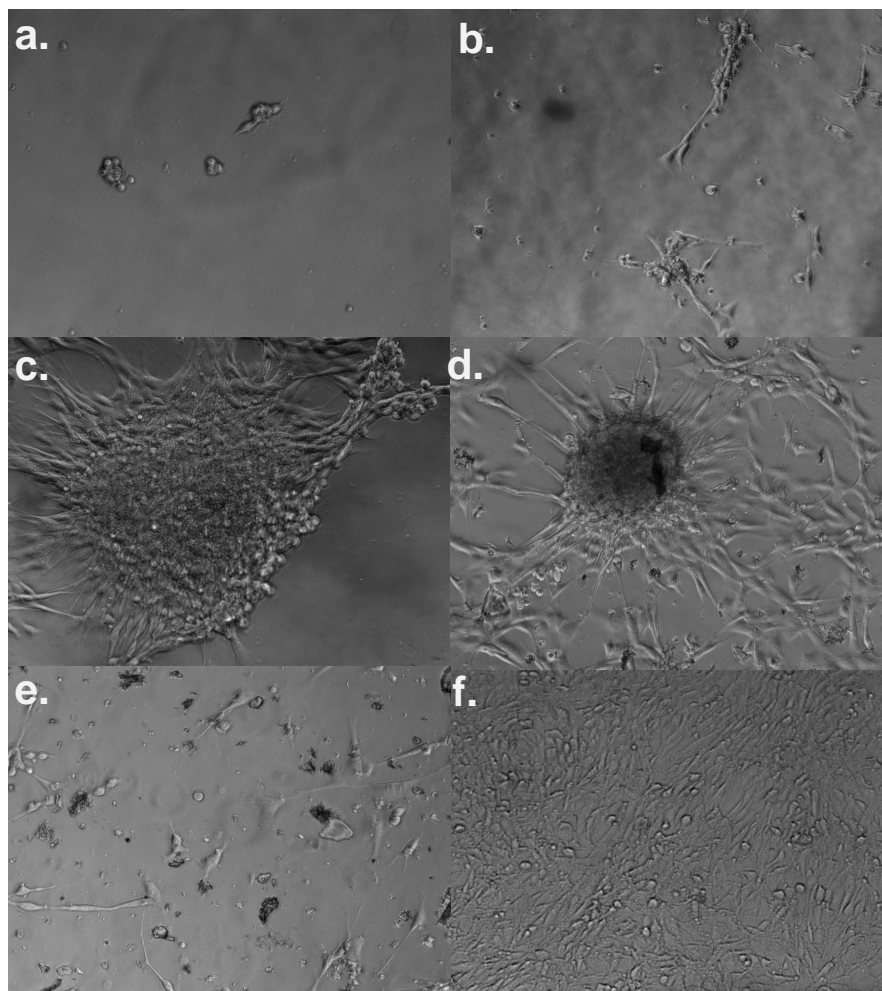
Figure 6.15: 3T3s seeded on 10% PEG hydrogels of different compositions exhibited varying morphologies: (a) PEG 4K gels with no galactose content, (b) 20 mole % galactose (c) 50 mole % galactose (d)100 mole % galactose with high cell adhesion (e) and 100 mole % galactose with low cell adhesion. Cells were also seeded directly on (f) tissue culture plates for comparison.
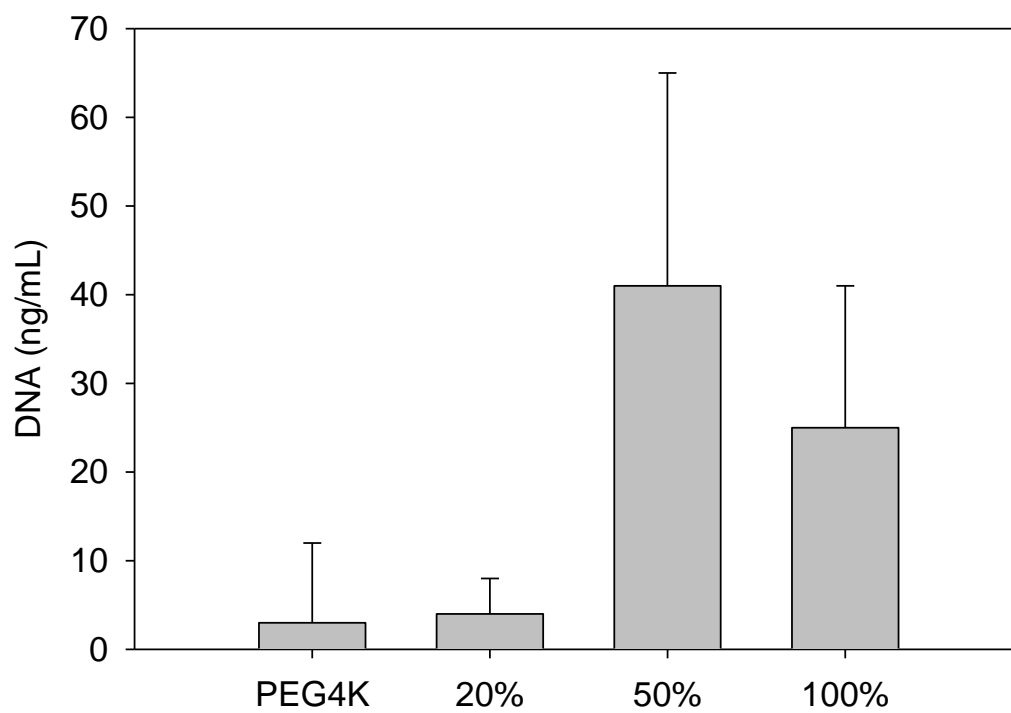
Figure 6.16: Picogreen quantification of DNA showed more cells on hydrogels with high galactose content (50 and 100 mole %), roughly correlating with the visual results.

We wanted to verify the results above by using soluble galactose polymers to competitively inhibit cell adhesion, similar to the RGD cell adhesion experiments in the previous section. If soluble galactose could disrupt cell adhesion, it would give further support towards the ability of tethered galactose to help mediate cell adhesion.

3T3s were cultured on 10% PEG hydrogels with 1 mM tethered RGD and exposed to media supplemented with free galactose or galactose glycopolymer. Much like the RGD experiment, the fibroblasts became rounded and also aggregated together (Figure 6.17a and b), indicating that soluble galactose of both presentation types can also interfere with cell adhesion albeit at a much higher concentration. After a two hour incubation and media wash, cell quantification showed a dose-dependent effect of galactose on cell adhesion, but no significant difference between free galactose and clustered galactose polymer (Figure 6.17d).

While these specific results do not indicate any increase in activity due to polymer clustering versus monomeric galactose for cell adhesion, they do reinforce the notion that galactose mediated cell adhesion is possible for other cell lines beyond hepatocytes. Taken together with the behavior of 3T3s cultured with tethered galactose polymers on PEG hydrogels, these results justify further investigation into the use of glycopolymers as extracellular matrix mimics for cell adhesion.
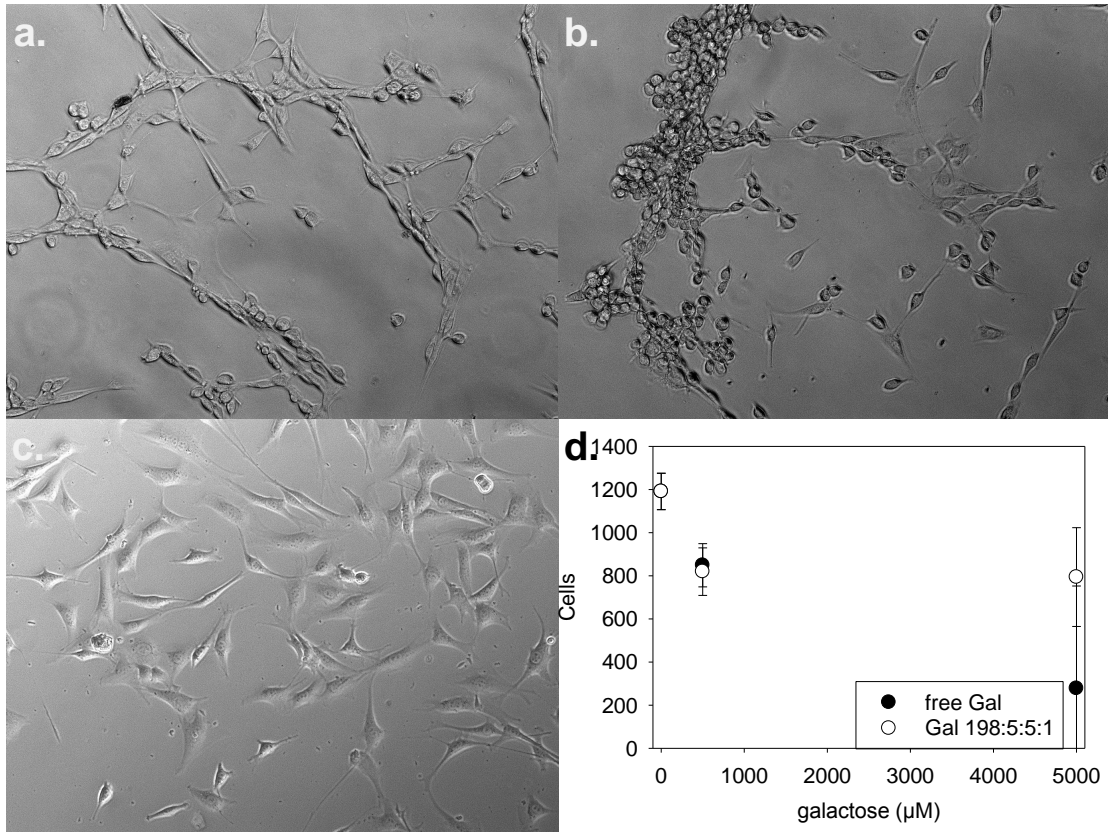
Figure 6.17: 3T3s seeded on 10% PEG hydrogels with 1 mM RGD exhibited round morphology and began to detach after five minutes exposure to (a) 5000 μM free galactose and (b) Gal 198:5:5:1 with overall 5000 μM galactose content, compared to (c) 3T3s cultured in regular media. (d) Cell number was quantified with Cell Titer-Blue and showed no significant difference between galactose presentation methods.

6.5   Conclusions

These binding results of the glycopolymers described in Chapters 3 and 4 provide more information on the structure-property relationships of glycopolymers and lectin binding, and can guide the design and synthesis of potential glycomimetic drugs for immune applications.

For the glycopolymers described in Chapter 3, their biological interaction with mannose binding lectin increased with longer chain length. Glycopolymers with branched architectures also increased their biological interaction with MBL. 90 times greater inhibition was seen when the architecture of glycopolymer was changed from linear to branched, with higher apparent branching density increasing the interaction with MBL. Mannose at the branch point was also found to increase inhibition of MBL to mannan as compared to similar structures with galactose or no saccharide content at the branch point.

Bovine serum albumin glycopolymers from Chapter 4 were also tested for their interaction with MBL. Increasing number and density of mannose resulted in more interaction with MBL. More significantly, 3D presentation of multiple polymer chains had superior interaction with MBL than compared to linear glycopolymer chains with the same number of mannoses but without 3D presentation. These enhanced binding results with small quantities of saccharides arranged in a multi-valent 3D presentation can have profound impact in how glycopolymer conjugates are constructed, particularly when using compounds available in short supply. The combination of this saccharide presentation method with a protein component could potentially lead to materials with enzymatic activity combined with lectin binding properties.

The polymers described in Chapter 5 were tested for their ability to inhibit cell adhesion. Both RGD and galactose containing polymers could inhibit adhesion, but neither had any difference in 3T3 fibroblast adhesion when compared to monomeric

159

RGD or galactose. These results show, in contrast to the binding results with MBL, that there is no improvement in activity because of ligand clustering. Nevertheless, the galactose adhesion results suggest that galactose plays a role in fibroblast adhesion to tissue engineering surfaces.

6.6   Experimentals

6.6.1   Materials

Human serum (Lonza, 12001-814), mouse anti-mannan binding lectin (Pierce Biotechnology, HYB1311402), goat anti-mouse HRP (Invitrogen, 62-6520), recombinant human mannose binding lectin (US Biological, M2250), mouse anti-mannose binding lectin (US Biological, M2245), C4 (Sigma, C8195), sheep anti-C4 HRP (Abcam, AB80051), mannan-agarose (Sigma), and TMB (Acros, 98%) were used as received. Nunc Maxisorp 96 well plates were used for adsorbing compounds. The NIH 3T3 cell line was obtained from ATCC.

The following buffers were used:

- HEPES buffer: 10 mM HEPES, 150 mM NaCl, 1 mM $CaCl_2$

- Coating buffer: 15 mM Na_2CO_3, 35 mM $NaHCO_3$, pH 9.6

- Blocking buffer: 5 mg/mL BSA, 10 mM TrisCl, 145 mM NaCl, pH 7.4

- Washing buffer: 100 mM TrisCl, 0.9% NaCl, 0.05% Tween 20 and 5 mM $CaCl_2$, pH 7.5

- Lectin binding buffer: 20 mM TrisCl, 1 M NaCl, 0.05% Triton X-100, 10 mM $CaCl_2$, 1 mg/mL BSA, pH 7.4

6.6.2 Binding assays of linear and branched glycopolymers from Chapter 3

Turbidimetric assay

The polymer of interest (synthetic polymer or mannan) was dissolved to 0.1 mg/mL in HEPES buffer and mixed with an equal volume of 1 μM concanavalin A. The solution was placed in a cuvette and absorbance at 420 nm was recorded for 15 minutes.

Direct enzyme linked lectin assay

100 μL of 10 μg/mL polymer of interest (synthetic polymer or mannan) in coating buffer was incubated at room temperature overnight in immunosorp wells. The solution was removed and replaced with blocking buffer for two hours at 37 °C. Human serum diluted 1:1500 was added to the wells and incubated overnight at 4 °C. The wells were then washed three times with washing buffer and then 100 μL of mouse anti-MBL diluted 1:250 in washing buffer was added to each well and incubated for two hours at room temperature. Wells were washed again then 100 μLof HRP Goat anti-mouse diluted 1:1500 in washing buffer was added to each well and incubated for two hours at room temperature. Following a final wash, 100 μL of TMB was added to each well and developed for 25 minutes before stopping with 2 M sulfuric acid and read at 450 nm on a plate reader.

Inhibitory enzyme linked lectin assay

100 μL of 10 μg/mL mannan in coating buffer was incubated at room temperature overnight in immunosorp wells. The solution was removed and replaced with blocking buffer for two hours at 37 °C. While wells were blocking, the inhibitor (glycopolymer of interest) was dissolved in lectin binding buffer to 16 mg/mL, and then serially diluted. Equal volume of human serum solution was added to result in overall serum dilution of 1:1500 and concentrations of inhibitor from 8 mg/mL to 0.06 mg/mL. For the no inhibitor solutions, a 1:750 dilution of human serum was diluted with equal volume lectin binding buffer. Inhibitor and serum was pre-incubated for 30 minutes at room temperature. The wells were washed three times with washing buffer and then 100 μL of pre-incubated inhibitor and serum were added and incubated overnight at 4 °C. Wells were washed with washing buffer then 100 μL of mouse anti-MBL diluted 1:250 in washing buffer was added to each well and incubated for two hours at room temperature. Wells were washed again then 100 μL HRP Goat anti-mouse diluted 1:1500 in washing buffer was added to each well and incubated for two hours at room temperature. Following a final wash, 100 μL of TMB was added to each well and developed for 25 minutes before stopping development with 2 M sulfuric acid and read at 450 nm on plate reader. % inhibition was calculated as $100\text{-}100\times\text{Abs}_{inhibitor}/\text{Abs}_{noinhibitor}$. Relative potency was determined through the ratio of mannose concentration needed for 25% inhibition for the polymer of interest versus monomeric mannose.

6.6.3 Binding assays of protein-glycopolymers from Chapter 4

Direct enzyme linked lectin assay

A similar protocol for direct ELLA as above was used for the protein-glycopolymers. Recombinant MBL at a final concentration of 5 μg/mL (1:2000 dilution) was used rather than human serum. Mouse anti-recombinant MBL diluted 1:5000 was used rather than mouse anti-MBL.

MBL depletion from human serum

2 mL of human serum was adjusted to 10 mM calcium with $CaCl_2$ and incubated for 16 hours at 4 °C with mannan agarose (500 μL slurry adjusted with TBS:1 mL 10 mM TrisHCl, 150 mM NaCl, 10 mM $CaCl_2$, pH 7.4). The serum-agarose suspension was passed through a short column of additional mannan-agarose (also adjusted with TBS) to collect the depleted serum. MBL depletion was validated with MBL ELLA against normal serum that was diluted a corresponding amount with TBS.

Inhibitory enzyme linked lectin assay

A similar protocol for inhibitory ELLA as above was used for the protein-glycopolymers. Inhibitor (protein-glycopolymer) was diluted from 1 mg/mL to 0.008 mg/mL with respect to protein content. Recombinant MBL at a final concentration of 5 μg/mL (1:2000 dilution) was used rather than human serum. Mouse anti-recombinant MBL diluted 1:5000 was used rather than mouse anti-MBL. Sample analysis accounted for the different saccharide concentrations of each compound.

Complement binding assay

100 μL of 10 μg/mL compound of interest (BSA-Br$_{22}$, BSA-polymer, or mannan) in coating buffer was incubated at room temperature overnight in immunosorp wells. The solution was removed and replaced with blocking buffer for two hours at 37 °C. Human serum (normal or MBL depleted) was added to the wells and incubated overnight at 4 °C. The wells were then washed three times with washing buffer then 5 μg/mL C4 in washing buffer was incubated for two hours at 37 °C. The wells were washed again and then 100 μL of anti-C4 HRP diluted 1:250 in washing buffer was added to each well and incubated for two hours at room temperature. Following a final wash, 100 μL of TMB was added to each well and developed for 25 minutes before stopping development with 2 M sulfuric acid and read at 450 nm on a plate reader.

6.6.4 Cell adhesion experiments of exchanged polymers from Chapter 5

PEG4000 diacrylate

Polyethylene glycol 4000 (10 g, 2.5 mmol) was dissolved in dichloromethane (50 mL) and triethylamine (1 mL, 7.5 mmol) and cooled in an ice bath prior to drop wise addition of acryloyl chloride (470 μL, 5.82 mmol) in dichloromethane (10 mL). The solution was stirred overnight followed by evaporation of dichloromethane by rotary evaporation. The solution was re-suspended in acetone to precipitate the triethylamine salts which were filtered by a silica plug. Acetone was removed by rotary evaporation and the solution was again suspended in a minimal amount of dichloromethane before being precipitated slowly into vigorously stirring cold ether (100 mL/g). Precipitate was filtered to yield 9.8 g (98%) of a white powder.

Experiments with competitive 3T3 adhesion between soluble cell adhesion molecules and PEG hydrogels with RGD

PEG4000 diacrylate (150 mg) and GCGYGRGDSPG peptide (1.6 mg) were dissolved in PBS (600 μL, 100 mM, pH 8) and allowed to react for 30 minutes. Irgacure 5929 photoinitiator (150 μL of a 0.5% w/v solution, final concentration 0.05% w/v) and PBS (750 μL, 100 mM, pH 7) were then added to make the pre-polymer solution. The hydrogel disks were formed by placing the solution between two glass slides separated by rubber spacers to ensure a thickness of 2 mm. Hydrogels were cured under the UV-lamp for 10 minutes. The resulting gels were cut into 5 mm discs and then left to swell in water overnight. Gels were sterilized by five 20 minutes washes with 70% ethanol followed by five 20 minute washes with sterile phosphate buffer saline (supplemented with calcium and magnesium) followed by incubation overnight in 3T3 growth medium.

NIH 3T3 cells was cultured in Dulbecco's Modified Eagle Medium (DMEM) with 10% bovine calf serum. Cells were seeded at a density of 2,000 cells per cm^2 and allowed to settle for two hours. Gels were washed gently with media once before media with supplemented cell adhesion molecules at different concentrations (RGD and RGD 198:5:5:1 at 100 and 10 μM, galactose and 198:5:5:1 at 5000 and 500 μM) was added. Gels were incubated with modified media for two hours before quantification.

Hydrogels were fabricated with varying concentrations of galactose acrylate: 0, 20, 50 and 100 mole percent with respect to PEG4000 diacrylate. Each solution was prepared by dissolving PEG4000 diacrylate (10% w/v) in water, followed by addition of Irgacure 5929 photoinitiator (final concentration 0.05% w/v) and the appropriate amount of galactose acrylate monomer. The hydrogel disks were formed by placing the solution between two glass slides separated by rubber spacers to ensure a thickness of 2 mm. Hydrogels were cured under the UV-lamp. Minimum amount of time for curing was 10 minutes, corresponding to the gels without galactose, and maximum was 35 minutes, corresponding to the highest volume of galactose. The resulting gels were cut into 10 mm discs and then left to swell in water overnight. Gels were sterilized by five 20 minute washes with 70% ethanol followed by five 20 minute washes with sterile phosphate buffer saline (supplemented with calcium and magnesium) followed by incubation overnight in 3T3 growth medium.

NIH 3T3 cells was cultured in Dulbecco's Modified Eagle Medium (DMEM) with 10% bovine calf serum. In a typical experiment, cells were seeded at a density of 2,000 cells per cm^2 and allowed to settle for at least 12 hours before any quantification or manipulation.

Quantification of cell adhesion

Images of hydrogels were taken on an optical microscope or quantified through Picogreen assay or Cell Titer-Blue assay. Before cell quantification, the wells were gently washed twice with media to remove detached cells.

For Picogreen, media was aspirated from the well and replaced with a 0.1% Triton X solution and incubated for 30 minutes at room temperature before addition of 0.1% BSA solution for another 30 more minutes. 10 μL from each sample was combined with 90 μL TE buffer and 100 μL Picogreen solution in a black fluorescent plate and read with Ex: 485 nm, Em: 535 nm.

For Cell Titer-Blue assay, media was aspirated from the well and replaced with media containing Cell Titer-Blue reagent and incubated for four hours in the incubator. 100 μL of the solution was transferred to a black fluorescent plate and read with Ex: 535 nm, Em: 595 nm.

CHAPTER 7

Conclusions and future directions

7.1   Project conclusions

This dissertation describes new synthetic methods for creating glycopolymers that bridge the gap between natural glycan structures and synthetic glycopolymers. Branched glycopolymers were synthesized using a glycoinimer that incorporated saccharide content at the branch point. These glycopolymers with pendant mannoses and mannose at the branch point were shown to interact with mannose binding lectin using enzyme linked lectin assays. MBL interaction with glycopolymers increases with increasing mannose content and with increasing branching. Most significantly, mannose at the branch point increases the polymer's interaction with MBL compared to similar structures with galactose or no saccharide content at the branch point.

Protein-glycopolymers were polymerized directly from a protein macroinitiator using a grafting-from approach, in contrast to previous efforts towards protein-glycopolymers that used a grafting-to approach. These protein-glycopolymers were shown to interact with recombinant MBL. Increasing mannose number (controlled through the polymer chain length) and density (controlled through the comonomer feed ratio of mannose versus galactose) results in increased interaction with MBL. The 3D presentation of multiple glycopolymer chains around the protein enhances its interaction with MBL more than simply clustering glycoresidues in a linear polymer chain.

Finally, branched polymers with pendant pyridyl disulfide groups were synthesized as a facile route towards incorporating thiolated biomolecules. Thiogalactoside and cysteine-containing cell adhesion peptide were exchanged onto the polymer and tested for their ability to competitively inhibit cell adhesion to PEG hydrogels with tethered RGD. The clustered presentation of these biomolecules in the form of polymers did not have an effect on cell adhesion relative to freely associated galactose or RGD. However, in our preliminary experiments, it may prove to be useful in other applications such as cell aggregation.

Overall, this dissertation has described synthetic techniques for creating biomimetic glycopolymers that were used to study structure-property relationships between polymers and lectins (Figure 7.1). Previous studies have provided abundant evidence towards the enhancement of protein binding due to multivalency. The current research found that subtle changes in polymer architecture (with regard to branching) and 3D presentation can also lead to dramatic enhancement of protein binding. These findings can direct the design of glycomimetic drugs for various biomedical applications.
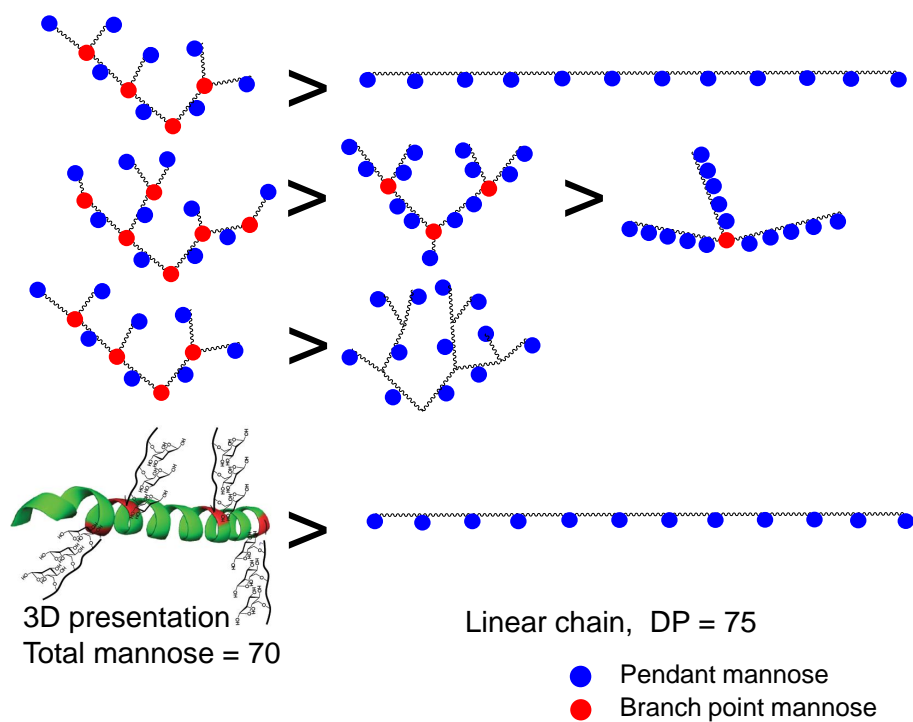
Figure 7.1: Structure-property relationships found in this dissertation are summarized: Branched glycopolymers with saccharide at the branch point and were shown to have superior interaction with MBL compared to linear glycopolymers of similar mannose content. Higher branching density and mannose at the branch point were also found to increase MBL interaction. Mannose glycopolymers were also synthesized from protein macroinitiators. The 3D presentation of polymer chains was found to significantly increase MBL interaction.

7.2 Future directions

The results of this dissertation provide a glimpse of how sugars can be harnessed for urgent biomedical needs. Before these needs can be addressed, further synthetic work must be conducted to be able to fully understand the structure-property relationships of branching and 3D presentation with lectin binding (Figure 7.2). The synthetic schemes can be expanded to include charged monosaccharides or disaccharides (including the repeat units of various glycosaminoglycans) in the branch point (Chapter 3 glycopolymers). The synthesis of disaccharide inimers may be challenging so synthesis of glycomimetics containing these disaccharides can also be pursued through post-polymerization modification (Chapter 5 glycopolymers).

More complex polymer architectures can also be incorporated with protein-glycopolymers. All previous examples of protein-glycopolymers have had linear architectures, in contrast to the diverse architectures of natural glycoproteins. Branching architecture can be introduced by using a glycoinimer similar to that seen in Chapter 3, or by using a simple divinyl monomer as seen in Chapter 5. Protein-glycopolymers can be expanded to include proteins with active biological properties such as immune reactivity or enzymatic activity (Chapter 4 glycopolymers). Glycopolymers can be used to target enzymes or shield them from degradation, although further work must be done to ensure that synthesis of the initiator or the polymerization process does not destroy or inhibit enzymatic activity. Improved methods for specifically controlling the placement of the polymer chain, regardless of grafting technique, would help tremendously in that regard. 3D presentation of glycopolymer chains can also be explored without a protein component by, for example, polymerizing monomers from the surface of nanoparticles.
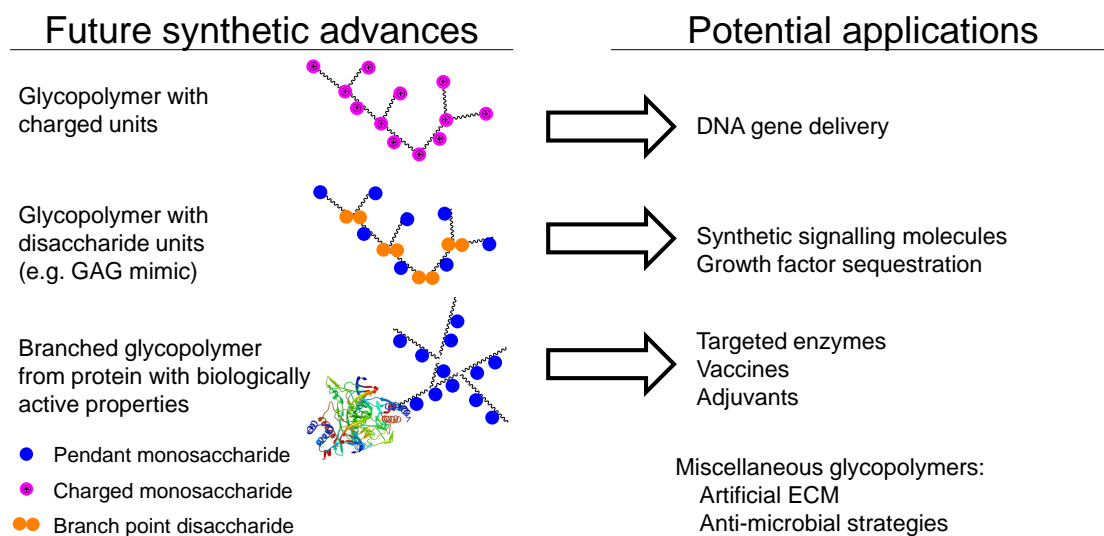
Figure 7.2: Future synthetic advances include: glycopolymers with charged or disaccharide units that also incorporate branching architecture, and branched glycopolymers from proteins with biologically active properties. These synthetic advances would allow us to pursue various therapies.

With these synthetic advances, glycopolymers can be applied to solve biomedical problems. For example, gene delivery is one avenue where glycopolymers can be applied as shown by Reineke and other's work.[106] Branched glycopolymers with charged monosaccharides such as glucosamine as pendant groups or in the branch point can be used to complex and deliver DNA with potentially less cytotoxic effects. The effect of glycopolymer structure on gene delivery efficiency and cytotoxicity can be studied with a library of these branched charged glycopolymers.

Glycopolymers that incorporate the disaccharide repeat units of glycosaminoglycans can create mimics of their source polysaccharide. These mimics can be used in some cases as synthetic signalling molecules. For example, a hyaluronic acid micmic glycopolymer with a repeat unit of glucuronic acid and N-acetylglucosamine can be used to promote signalling with the CD44 receptor through the same route as natural hyaluronic acid. Glycopolymers with the correct saccharide composition can also be used to stabilize growth factors, similarly to how fibroblast growth factor 2 is stabilized by heparin.

Glycopolymers can also be used as artificial ECM mimics. Pilot experiments described in Chapter 6 demonstrated that glycopolymers can mediate fibroblast adhesion to hydrogel surfaces. This research can be expanded to fully understand how glycopolymer structure (glycoside identity, chain length, distribution) affects cell adhesion, proliferation, migration, and differentiation (in the case of stem cells). The glycopolymers with glycosaminoglycan derived disaccharides can also be incorporated into the hydrogels to create niches with localized growth factor sequestration.

Protein-glycopolymers can be applied towards vaccination if proteins with more potent immune reactivity are used as macroinitiators and saccharides associated with pathogens are used as glycomonomers. Saccharides are poor immunogens by themselves and often require a carrier protein to generate a lasting immune response. Glycopolymers have been recently explored for vaccination to replace traditional

lower valency vaccines, but either did not include a protein component,[79] or used a "grafting-from" method to attach the glycopolymer.[6] Different glycomonomers can also be incorporated into the protein glycopolymer in order to present multiple vaccination antigens in one compound. This strategy has been explored using glycoclusters of multiple saccharide cancer antigens on one synthetic backbone to provide broad spectrum immunization against heterogeneous cancers.[154] A logical next step would be to create co-glycopolymers with several cancer antigens displayed either as statistical or block mixtures. This *multiblock* and *multivalent* glycopolymer vaccine design could generate a more robust immune response and subsequent improvement in clinical responses.

Finally, glycopolymers can be used to study bacteria pili binding and eventually be used as a method to prevent bacterial adhesion to a surface and subsequent biofilm formation. Preliminary work with Professor Gerard Wong's group (not described in this dissertation) has shown that mannose glycopolymers can bind to *V. cholera*. We can further study the attachment profiles of *V. cholera* as a solution's mannose content increases and competitively binds with bacteria pili and prevents adhesion to a surface. Alternatively, we can capture bacteria by promoting bacteria adhesion through a mannose glycopolymer coated surface. This in-depth study would shed further light into the mechanistic aspects of bacteria pili-saccharide interaction and provide further insight for strategies to inhibit bacteria adhesion.

References

[1] S. Muthukrishnan, G. Jutz, X. André, H. Mori, and A. H. E. Müller. Synthesis of Hyperbranched Glycopolymers via Self-Condensing Atom Transfer Radical Copolymerization of a Sugar-Carrying Acrylate. *Macromolecules*, 38(1):9–18, 2005.

[2] S. Muthukrishnan, H. Mori, and A. H. E. Müller. Synthesis and Characterization of Methacrylate-Type Hyperbranched Glycopolymers via Self-Condensing Atom Transfer Radical Copolymerization. *Macromolecules*, 38(8):3108–3119, 2005.

[3] M. Semsarilar, V. Ladmiral, and S. Perrier. Highly Branched and Hyperbranched Glycopolymers via Reversible Addition-Fragmentation Chain Transfer Polymerization and Click Chemistry. *Macromolecules*, 43(3):1438–1443, 2010.

[4] M. Ahmed, B. F. L. Lai, J. N. Kizhakkedathu, and R. Narain. Hyperbranched Glycopolymers for Blood Biocompatibility. *Bioconjugate Chemistry*, 23(5):1050–1058, 2012.

[5] J. Geng, G. Mantovani, L. Tao, J. Nicolas, G. Chen, R. Wallis, D. A. Mitchell, B. R. G. Johnson, S. D. Evans, and D. M. Haddleton. Site-directed conjugation of "clicked" glycopolymers to form glycoprotein mimics: binding to mammalian lectin and induction of immunological function. *Journal of the American Chemical Society*, 129(49):15156–15163, 2007.

[6] T. Lipinski, P. I. Kitov, A. Szpacenko, E. Paszkiewicz, and D. R. Bundle. Synthesis and immunogenicity of a glycopolymer conjugate. *Bioconjugate Chemistry*, 22(2):274–281, 2011.

[7] R. Narain. Tailor-made protein glycopolymer bioconjugates. *Reactive and Functional Polymers*, 66(12):1589–1595, 2006.

[8] R. J. Mancini, J. Lee, and H. D. Maynard. Trehalose Glycopolymers for Stabilization of Protein Conjugates to Environmental Stressors. *Journal of the American Chemical Society*, 134(20):8474–8479, 2012.

[9] J. J. Lundquist and E. J. Toone. The cluster glycoside effect. *Chemical Reviews*, 102(2):555–578, 2002.

[10] K. Hedlund, D. Coyne, D. Sanford, and J. Huddelson. The heparin recall of 2008. *Perfusion*, 28(1):61–5, 2013.

[11] D. R. Mootoo, P. Konradsson, U. Udodong, and B. Fraser-Reid. Armed and disarmed *n*-pentenyl glycosides in saccharide couplings leading to oligosaccharides. *Journal of the American Chemical Society*, 110(16):5583–5584, 1988.

[12] Z. Zhang, I. R. Ollmann, X.-S. Ye, R. Wischnat, T. Baasov, and C.-H. Wong. Programmable One-Pot Oligosaccharide Synthesis. *Journal of the American Chemical Society*, 121(4):734–753, 1999.

[13] T. K.-K. Mong, H.-K. Lee, S. G. Duron, and C.-H. Wong. Reactivity-based one-pot total synthesis of fucose GM1 oligosaccharide: a sialylated antigenic epitope of small-cell lung cancer. *Proceedings of the National Academy of Sciences of the United States of America*, 100(3):797–802, 2003.

[14] O. J. Plante, E. R. Palmacci, and P. H. Seeberger. Automated solid-phase synthesis of oligosaccharides. *Science*, 291(5508):1523–1527, 2001.

[15] O. Calin, S. Eller, and P. H. Seeberger. Automated polysaccharide synthesis: assembly of a 30mer mannoside. *Angewandte Chemie (International ed. in English)*, 52(22):5862–5, 2013.

[16] T. J. Boltje, C. Li, and G.-J. Boons. Versatile set of orthogonal protecting groups for the preparation of highly branched oligosaccharides. *Organic Letters*, 12(20):4636–9, 2010.

[17] L. Manzoni and R. Castelli. Synthesis of the Lewis a trisaccharide based on an anomeric silyl fluorous tag. *Organic Letters*, 6(23):4195–4198, 2004.

[18] G. Park, K. S. Ko, A. Zakharova, and N. L. Pohl. Mono-vs. di-fluorous-tagged glucosamines for iterative oligosaccharide synthesis. *Journal of Fluorine Chemistry*, (10):978–982, 2008.

[19] J. Van Der Vlist, M. Palomo Reixach, M. Van Der Maarel, L. Dijkhuizen, A. J. Schouten, and K. Loos. Synthesis of Branched Polyglucans by the Tandem Action of Potato Phosphorylase and Deinococcus geothermalis Glycogen Branching Enzyme. *Macromolecular Rapid Communications*, 29(15):1293–1297, 2008.

[20] J. Van Der Vlist, I. Schönen, and K. Loos. Utilization of glycosyltransferases for the synthesis of a densely packed hyperbranched polysaccharide brush coating as artificial glycocalyx. *Biomacromolecules*, 12(10):3728–32, 2011.

[21] T. Murata. Enzymatic Synthesis of Important Oligosaccharide Units Involved in N- and O-linked glycans. *Trends In Glycoscience And Glycotechnology*, 12(65):161–174, 2000.

[22] Y. Ichikawa, G. C. Look, and C. H. Wong. Enzyme-catalyzed oligosaccharide synthesis. *Analytical Biochemistry*, 202(2):215–238, 1992.

[23] G. Perugino, A. Trincone, M. Rossi, and M. Moracci. Oligosaccharide synthesis by glycosynthases. *Trends in Biotechnology*, 22(1):31–37, 2004.

[24] L. F. Mackenzie, Q. Wang, R. A. J. Warren, and S. G. Withers. Glycosynthases - Mutant Glycosidases for Oligosaccharide Synthesis. *Journal of the American Chemical Society*, 120(22):5583–5584, 1998.

[25] J. F. Tolborg, L. Petersen, K. J. Jensen, C. Mayer, D. L. Jakeman, R. A. J. Warren, and S. G. Withers. Solid-phase oligosaccharide and glycopeptide synthesis using glycosynthases. *The Journal of Organic Chemistry*, 67(12):4143–4149, 2002.

[26] S. D. Burke, Q. Zhao, M. C. Schuster, and L. L. Kiessling. Synergistic Formation of Soluble Lectin Clusters by a Templated Multivalent Saccharide Ligand. *Journal of the American Chemical Society*, 122(18):4518–4519, 2000.

[27] D. Pagé and R. Roy. Synthesis and biological properties of mannosylated starburst poly(amidoamine) dendrimers. *Bioconjugate Chemistry*, 8(5):714–723, 2000.

[28] S. André, P. J. Ortega, M. A. Perez, R. Roy, and H. J. Gabius. Lactose-containing starburst dendrimers: influence of dendrimer generation and binding-site orientation of receptors (plant/animal lectins and immunoglobulins) on binding properties. *Glycobiology*, 9(11):1253–1261, 1999.

[29] W. B. Turnbull and J. F. Stoddart. Design and synthesis of glycodendrimers. *Journal of Biotechnology*, 90(3-4):231–255, 2002.

[30] R. Roy. A Decade of Glycodendrimer Chemistry. *ChemInform*, 35(34):291–310, 2004.

[31] K. Godula, D. Rabuka, K. T. Nam, and C. R. Bertozzi. Synthesis and microcontact printing of dual end-functionalized mucin-like glycopolymers for microarray applications. *Angewandte Chemie International Edition*, 48(27):4973–4976, 2009.

[32] F. A. M C Garcia-Oteiza M Sanchez-Chaves. Poly(vinyl alcohol) having amino sugar as the pendant group: synthesis, characterization and binding of Concanavalin A. *Macromolecular Chemistry And Physics Makromolekulare Chemie*, 198(7):2237–2247, 1997.

[33] G. Pasparakis, A. Cockayne, and C. Alexander. Control of bacterial aggregation by thermoresponsive glycopolymers. *Journal of the American Chemical Society*, 129(36):11014–11015, 2007.

[34] S. Slavin, J. Burns, D. M. Haddleton, and C. Remzi Becer. Synthesis of glycopolymers via click reactions. *European Polymer Journal*, 47(4):435–446, 2011.

[35] J. Kumar, L. McDowall, G. Chen, and M. H. Stenzel. Synthesis of thermo-responsive glycopolymers via copper catalysed azide alkyne 'click' chemistry for inhibition of ricin: the effect of spacer between polymer backbone and galactose. *Polymer Chemistry*, 2(8):1879–1886, 2011.

[36] H. Paulsen, Z. Györgydeák, and M. Friedmann. Konformationsanalyse, III.exo-Anomerer Effekt und Circulardichroismus von Glycopyranosylaziden. *Chemische Berichte*, 107(5):1568–1578, 1974.

[37] T. Tanaka, H. Nagai, M. Noguchi, A. Kobayashi, and S.-I. Shoda. One-step conversion of unprotected sugars to beta-glycosyl azides using 2-chloroimidazolinium salt in aqueous solution. *Chemical Communications*, 3(23):3378–3379, 2009.

[38] J. Luis, J. Blanco, J. Manuel, A. Gadelle, and J. Defaye. A mild one-step selective conversion of primary hydroxyl groups into azides in mono- and oligo-saccharides. *Carbohydrate Research*, 303:367–372, 1997.

[39] J. Geng, J. Lindqvist, G. Mantovani, and D. M. Haddleton. Simultaneous copper(I)-catalyzed azide-alkyne cycloaddition (CuAAC) and living radical polymerization. *Angewandte Chemie International Edition*, 47(22):4180–4183, 2008.

[40] G. Mantovani, V. Ladmiral, L. Tao, and D. M. Haddleton. One-pot tandem living radical polymerisation-Huisgens cycloaddition process ("click") catalysed by N-alkyl-2-pyridylmethanimine/Cu(I)Br complexes. *Chemical Communications*, (16):2089–2091, 2005.

[41] Q. Yang, Z.-K. Xu, Z.-W. Dai, J.-L. Wang, and M. Ulbricht. Surface Modification of Polypropylene Microporous Membranes with a Novel Glycopolymer. *Chemistry of Materials*, 17(11):3050–3058, 2005.

[42] L. Renaudie, C. L. Narvor, E. Lepleux, and P. Roger. Functionalization of poly(ethylene terephthalate) fibers by photografting of a carbohydrate derivatized with a phenyl azide group. *Biomacromolecules*, 8(2):679–685, 2007.

[43] K. Kobayahi, H. Sumitomo, and Y. Ina. Synthesis and functions of polystyrene derivatives having pendant oligosaccharides. *Polymer Journal*, 17(4):567–575.

[44] M. Okada. Molecular design and syntheses of glycopolymers. *Progress in Polymer Science*, 26(1):67–104, 2001.

[45] A. J. Varma, J. F. Kennedy, and P. Galgali. Synthetic polymers functionalized by carbohydrates: a review. *Carbohydrate Polymers*, 56(4):429–445, 2004.

[46] Y. Miura. Synthesis and biological application of glycopolymers. *Journal of Polymer Science Part A: Polymer Chemistry*, 45(22):5031–5036, 2007.

[47] S. R. S. Ting, G. Chen, and M. H. Stenzel. Synthesis of glycopolymers and their multivalent recognitions with lectins. *Polymer Chemistry*, 1(9):1392, 2010.

[48] S. Pearson, G. Chen, and M. H. Stenzel. Synthesis of Glycopolymers. In R. Narain, editor, *Engineered CarbohydrateBased Materials for Biomedical Applications*, chapter 1, pages 1–118. John Wiley & Sons, 2011.

[49] W. Jakubowski and K. Matyjaszewski. Activator Generated by Electron Transfer for Atom Transfer Radical Polymerization. *Macromolecules*, 38(10):4139–4146, 2005.

[50] K. Ohno, Y. Tsujii, and T. Fukuda. Synthesis of a well-defined glycopolymer by atom transfer radical polymerization. *Journal of Polymer Science Part A: Polymer Chemistry*, 36(14):2473–2481, 1998.

[51] R. Narain and S. P. Armes. Synthesis of low polydispersity, controlled-structure sugar methacrylate polymers under mild conditions without protecting group chemistry. *Chemical Communications*, (23):2776–2777, 2002.

[52] M. Kohri, M. Sato, F. Abo, T. Inada, M. Kasuya, T. Taniguchi, and T. Nakahira. Preparation and lectin binding specificity of polystyrene particles grafted with glycopolymers bearing S-linked carbohydrates. *European Polymer Journal*, 47(12):2351–2360, 2011.

[53] T. Taniguchi, M. Kasuya, Y. Kunisada, T. Miyai, H. Nagasawa, and T. Nakahira. Surface modification of polymer latex particles by AGET ATRP of a styrene derivative bearing a lactose residue. *Colloids and Surfaces, B: Biointerfaces*, 71(2):194–199, 2009.

[54] A. M. Granville, D. Quémener, T. P. Davis, C. Barner-Kowollik, and M. H. Stenzel. Chemo-enzymatic Synthesis and RAFT Polymerization of 6-O-Methacryloyl Mannose: A Suitable Glycopolymer for Binding to the Tetrameric Lectin Concanavalin A? *Macromolecular Symposia*, 255(1):81–89, 2007.

[55] V. Vázquez-Dorbatt, Z. P. Tolstyka, C.-W. Chang, and H. D. Maynard. Synthesis of a pyridyl disulfide end-functionalized glycopolymer for conjugation to biomolecules and patterning on gold surfaces. *Biomacromolecules*, 10(8):2207–2212, 2009.

[56] R. M. Broyer, G. M. Quaker, and H. D. Maynard. Designed amino acid ATRP initiators for the synthesis of biohybrid materials. *Journal of the American Chemical Society*, 130(3):1041–1047, 2008.

[57] S. Sen Gupta, K. S. Raja, E. Kaltgrad, E. Strable, and M. G. Finn. Virus-glycopolymer conjugates by copper(I) catalysis of atom transfer radical polymerization and azide-alkyne cycloaddition. *Chemical Communications*, 34(34):4315–4317, 2005.

[58] V. Vázquez-Dorbatt and H. D. Maynard. Biotinylated glycopolymers synthesized by atom transfer radical polymerization. *Biomacromolecules*, 7(8):2297–2302, 2006.

[59] V. Ladmiral, L. Monaghan, G. Mantovani, and D. M. Haddleton. alpha-Functional glycopolymers: New materials for (poly)peptide conjugation. *Polymer*, 46(19):8536–8545, 2005.

[60] M. Ejaz, K. Ohno, Y. Tsujii, and T. Fukuda. Controlled Grafting of a Well-Defined Glycopolymer on a Solid Surface by Surface-Initiated Atom Transfer Radical Polymerization. *Macromolecules*, 33(8):2870–2874, 2000.

[61] S. Muthukrishnan, F. Plamper, H. Mori, and A. H. E. Muller. Synthesis and Characterization of Glycomethacrylate Hybrid Stars from Silsesquioxane Nanoparticles. *Macromolecules*, 38(26):10631–10642, 2005.

[62] J. E. Raynor, T. A. Petrie, K. P. Fears, R. A. Latour, A. J. García, and D. M. Collard. Saccharide polymer brushes to control protein and cell adhesion to titanium. *Biomacromolecules*, 10:748–755, 2009.

[63] S. Pétursson. Protecting Groups in Carbohydrate Chemistry. *Journal of Chemical Education*, 74(11):1297, 1997.

[64] Z.-C. Li, Y.-Z. Liang, G.-Q. Chen, and F.-M. Li. Synthesis of amphiphilic block copolymers with well-defined glycopolymer segment by atom transfer radical polymerization. *Macromolecular Rapid Communications*, 21(7):375–380, 2000.

[65] Y. Miura, T. Ikeda, and K. Kobayashi. Chemoenzymatically synthesized glycoconjugate polymers. *Biomacromolecules*, 4(2):410–415, 2003.

[66] S. Warwel. An efficient method for lipase-catalysed preparation of acrylic and methacrylic acid esters. *Biotechnology Techniques*, 10(4):283–286, 1996.

[67] C. W. Cairo, J. E. Gestwicki, M. Kanai, and L. L. Kiessling. Control of multivalent interactions by binding epitope density. *Journal of the American Chemical Society*, 124(8):1615–1619, 2002.

[68] C. R. Becer, M. I. Gibson, J. Geng, R. Ilyas, R. Wallis, D. A. Mitchell, and D. M. Haddleton. High-affinity glycopolymer binding to human DC-SIGN and disruption of DC-SIGN interactions with HIV envelope glycoprotein. *Journal of the American Chemical Society*, 132(43):15130–15132, 2010.

[69] Q. Zhang, J. Collins, A. Anastasaki, R. Wallis, D. A. Mitchell, C. R. Becer, and D. M. Haddleton. Sequence-Controlled Multi-Block Glycopolymers to Inhibit DC-SIGN-gp120 Binding. *Angewandte Chemie International ed in English*, pages 4435–4439, 2013.

[70] O. León, A. Muñoz Bonilla, V. Bordegé, M. Sánchez-Chaves, and M. Fernández-García. Amphiphilic block glycopolymers via atom transfer radical polymerization: Synthesis, self-assembly and biomolecular recognition. *Journal of Polymer Science Part A: Polymer Chemistry*, 49(12):2627–2635, 2011.

[71] X.-H. Dai and C.-M. Dong. Synthesis, self-assembly and recognition properties of biomimetic star-shaped poly(ϵ-caprolactone)- b -glycopolymer block copolymers. *Journal of Polymer Science Part A: Polymer Chemistry*, 46(3):817–829, 2008.

[72] Y.-M. Chen and G. Wulff. ABA and Star Amphiphilic Block Copolymers Composed of Polymethacrylate Bearing a Galactose Fragment and Poly(caprolactone). *Macromolecular Rapid Communications*, 23(1):59–63, 2002.

[73] S. Muthukrishnan, M. Zhang, M. Burkhardt, M. Drechsler, H. Mori, and A. H. E. Müller. Molecular Sugar Sticks: Cylindrical Glycopolymer Brushes. *Macromolecules*, 38(19):7926–7934, 2005.

[74] S. Qiu, H. U. I. Huang, X.-h. Dai, W. E. I. Zhou, and C.-m. Dong. Star-Shaped Polypeptide/Glycopolymer Biohybrids: Synthesis, Self-Assembly, Biomolecular Recognition, and Controlled Drug Release Behavior. *Polymer*, 47(8):2009–2023, 2009.

[75] W. K. E. Ip, K. Takahashi, R. A. Ezekowitz, and L. M. Stuart. Mannose-binding lectin and innate immunity. *Immunological Reviews*, 230(1):9–21, 2009.

[76] E.-H. Song, M. J. Manganiello, Y.-H. Chow, B. Ghosn, A. J. Convertine, P. S. Stayton, L. M. Schnapp, and D. M. Ratner. In vivo targeting of alveolar macrophages via RAFT-based glycopolymers. *Biomaterials*, 33(28):6889–97, 2012.

[77] V. Verez-Bencomo, V. Fernández-Santana, E. Hardy, M. E. Toledo, M. C. Rodríguez, L. Heynngnezz, A. Rodriguez, A. Baly, L. Herrera, M. Izquierdo, A. Villar, Y. Valdés, K. Cosme, M. L. Deler, M. Montane, E. Garcia, A. Ramos, A. Aguilar, E. Medina, G. Toraño, I. Sosa, I. Hernandez, R. Martínez, A. Muzachio, A. Carmenates, L. Costa, F. Cardoso, C. Campa, M. Diaz, and R. Roy. A synthetic conjugate polysaccharide vaccine against Haemophilus influenzae type b. *Science*, 305(5683):522–525, 2004.

[78] G. Toraňo, M. E. Toledo, A. Baly, V. Fernandez-Santana, F. Rodriguez, Y. Alvarez, T. Serrano, A. Musachio, I. Hernandez, E. Hardy, A. Rodríguez, H. Hernandez, A. Aguilar, R. Sánchez, M. Diaz, V. Muzio, J. Dfana, M. C. Rodríguez, L. Heynngnezz, and V. Verez-Bencomo. Phase I clinical evaluation of a synthetic oligosaccharide-protein conjugate vaccine against Haemophilus influenzae type b in human adult volunteers. *Clinical and Vaccine Immunology*, 13(9):1052–6, 2006.

[79] A. L. Parry, N. A. Clemson, J. Ellis, S. S. R. Bernhard, B. G. Davis, and N. R. Cameron. Multicopy Multivalent Glycopolymer-Stabilized Gold Nanoparticles as Potential Synthetic Cancer Vaccines. *Journal of the American Chemical Society*, page 130617075225007, 2013.

[80] T. Furuike, S. Aiba, T. Suzuki, T. Takahashi, Y. Suzuki, K. Yamada, and S.-I. Nishimura. Synthesis and anti-influenza virus activity of novel glycopolymers having triantennary oligosaccharide branches. *Journal of the Chemical Society, Perkin Transactions 1*, (17):3000–3005, 2000.

[81] S.-k. Choi, M. Mammen, and G. M. Whitesides. Generation and in Situ Evaluation of Libraries of Poly(acrylic acid) Presenting Sialosides as Side Chains as Polyvalent Inhibitors of Influenza-Mediated Hemagglutination. *Journal of the American Chemical Society*, 119(8):4103–4111, 1997.

[82] K. Totani, T. Kubota, T. Kuroda, T. Murata, K. I.-P. J. Hidari, T. Suzuki, Y. Suzuki, K. Kobayashi, H. Ashida, K. Yamamoto, and T. Usui. Chemoenzymatic synthesis and application of glycopolymers containing multivalent sialyloligosaccharides with a poly(L-glutamic acid) backbone for inhibition of infection by influenza viruses. *Glycobiology*, 13(5):315–326, 2003.

[83] A. Tsuchida, K. Kobayashi, N. Matsubara, T. Muramatsu, T. Suzuki, and Y. Suzuki. Simple synthesis of sialyllactose-carrying polystyrene and its binding with influenza virus. *Glycoconjugate Journal*, 15(11):1047–1054, 1998.

[84] A. Vetere, I. Donati, C. Campa, S. Semeraro, A. Gamini, and S. Paoletti. Synthesis and characterization of a novel glycopolymer with protective activity toward human anti-alpha-Gal antibodies. *Glycobiology*, 12(4):283–290, 2002.

[85] Q. Yang, C. Kaul, and M. Ulbricht. Anti-nonspecific protein adsorption properties of biomimetic glycocalyx-like glycopolymer layers: effects of glycopolymer chain density and protein size. *Langmuir: the ACS Journal of Surfaces and Colloids*, 26(8):5746–5752, 2010.

[86] D. Rabuka, R. Parthasarathy, G. S. Lee, X. Chen, J. T. Groves, and C. R. Bertozzi. Hierarchical assembly of model cell surfaces: synthesis of mucin

mimetic polymers and their display on supported bilayers. *Journal of the American Chemical Society*, 129(17):5462–5471, 2007.

[87] D. Rabuka, M. B. Forstner, J. T. Groves, and C. R. Bertozzi. Noncovalent cell surface engineering: incorporation of bioactive synthetic glycopolymers into cellular membranes. *Journal of the American Chemical Society*, 130(18):5947–5953, 2008.

[88] M. D. Disney, J. Zheng, T. M. Swager, and P. H. Seeberger. Detection of bacteria with carbohydrate-functionalized fluorescent polymers. *Journal of the American Chemical Society*, 126(41):13343–13346, 2004.

[89] M. D. Disney and P. H. Seeberger. The use of carbohydrate microarrays to study carbohydrate-cell interactions and to detect pathogens. *Chemistry & Biology*, 11(12):1701–1707, 2004.

[90] B. Mukhopadhyay, M. Martins, R. Karamanska, D. Russell, and R. Field. Bacterial detection using carbohydrate-functionalised CdS quantum dots: a model study exploiting E. coli recognition of mannosides. *Tetrahedron Letters*, 50(8):886–889, 2009.

[91] N. P. Pera, A. Kouki, S. Haataja, H. M. Branderhorst, R. M. J. Liskamp, G. M. Visser, J. Finne, and R. J. Pieters. Detection of pathogenic Streptococcus suis bacteria using magnetic glycoparticles. *Organic and Biomolecular Chemistry*, 8(10):2425–2429, 2010.

[92] Q. Yang, M. Strathmann, A. Rumpf, G. Schaule, and M. Ulbricht. Grafted glycopolymer-based receptor mimics on polymer support for selective adhesion of bacteria. *ACS Applied Materials Interfaces*, 2(12):3555–3562, 2010.

[93] S.-G. Lee, J. M. Brown, C. J. Rogers, J. B. Matson, C. Krishnamurthy, M. Rawat, and L. C. Hsieh-Wilson. End-functionalized glycopolymers as mimetics of chondroitin sulfate proteoglycans. *Chemical Science*, 1(3):322–325, 2010.

[94] D. Grande, S. Baskaran, C. Baskaran, Y. Gnanou, and E. L. Chaikof. Glycosaminoglycan-Mimetic Biomaterials. 1. Nonsulfated and Sulfated Glycopolymers by Cyanoxyl-Mediated Free-Radical Polymerization. *Macromolecules*, 33(4):1123–1125, 2000.

[95] D. Grande, S. Baskaran, and E. L. Chaikof. Glycosaminoglycan Mimetic Biomaterials. 2. Alkene- and Acrylate-Derivatized Glycopolymers via Cyanoxyl-Mediated Free-Radical Polymerization. *Macromolecules*, 34(6):1640–1646, 2001.

[96] S. Baskaran, D. Grande, X.-L. Sun, A. Yayon, and E. L. Chaikof. Glycosaminoglycan-mimetic biomaterials. 3. Glycopolymers prepared from

alkene-derivatized mono- and disaccharide-based glycomonomers. *Bioconjugate Chemistry*, 13(6):1309–1313, 2002.

[97] X.-L. Sun, K. M. Faucher, M. Houston, D. Grande, and E. L. Chaikof. Design and synthesis of biotin chain-terminated glycopolymers for surface glycoengineering. *Journal of the American Chemical Society*, 124(25):7258–7259, 2002.

[98] R. Guan, X.-L. Sun, S. Hou, P. Wu, and E. L. Chaikof. A glycopolymer chaperone for fibroblast growth factor-2. *Bioconjugate Chemistry*, 15(1):145–151, 2004.

[99] S.-H. Kim, M. Goto, C.-S. Cho, and T. Akaike. Specific adhesion of primary hepatocytes to a novel glucose-carrying polymer. *Biotechnology Letters*, 22(Lee 1992):1049–1057, 2000.

[100] S.-H. Kim, J.-H. Kim, and T. Akaike. Regulation of cell adhesion signaling by synthetic glycopolymer matrix in primary cultured hepatocyte. *FEBS Letters*, 553(3):433–439, 2003.

[101] C. Yin, L. Ying, P.-C. Zhang, R.-X. Zhuo, E.-T. Kang, K. W. Leong, and H.-Q. Mao. High density of immobilized galactose ligand enhances hepatocyte attachment and function. *Journal of Biomedical Materials Research Part A*, 67(4):1093–1104, 2003.

[102] L. Zhang, J. Bernard, T. P. Davis, C. Barner-Kowollik, and M. H. Stenzel. Acid-Degradable Core-Crosslinked Micelles Prepared from Thermosensitive Glycopolymers Synthesized via RAFT Polymerization. *Macromolecular Rapid Communications*, 29(2):123–129, 2008.

[103] F. Suriano, R. Pratt, J. P. K. Tan, N. Wiradharma, A. Nelson, Y.-Y. Yang, P. Dubois, and J. L. Hedrick. Synthesis of a family of amphiphilic glycopolymers via controlled ring-opening polymerization of functionalized cyclic carbonates and their application in drug delivery. *Biomaterials*, 31(9):2637–2645, 2010.

[104] X.-Q. Zhang, X.-L. Wang, P.-C. Zhang, Z.-L. Liu, R.-X. Zhuo, H.-Q. Mao, and K. W. Leong. Galactosylated ternary DNA/polyphosphoramidate nanoparticles mediate high gene transfection efficiency in hepatocytes. *Journal of Controlled Release*, 102(3):749–763, 2005.

[105] K. Roy, H. Q. Mao, S. K. Huang, and K. W. Leong. Oral gene delivery with chitosan–DNA nanoparticles generates immunologic protection in a murine model of peanut allergy. *Nature Medicine*, 5(4):387–391, 1999.

[106] T. M. Reineke. Poly (glycoamidoamine)s: Cationic Glycopolymers. *Polymer*, 44:6895–6908, 2006.

[107] M. Ahmed and R. Narain. The effect of polymer architecture, composition, and molecular weight on the properties of glycopolymer-based non-viral gene delivery systems. *Biomaterials*, 32(22):5279–90, 2011.

[108] C. Pugh, B. Raveendra, A. Singh, R. Samuel, and G. Garcia. Design and Regioselective Synthesis of (2-Bromo-2-alkoxycarbonyl)ethyl Acrylates as Inimers for Hyperbranched (Co)Polyacrylates. *Synlett*, (13):1947–1950, 2010.

[109] C. Pugh, A. Singh, R. Samuel, and K. M. Bernal Ramos. Synthesis of Hyperbranched Polyacrylates by a Chloroinimer Approach. *Macromolecules*, 43(12):5222–5232, 2010.

[110] A. H. E. Müller, D. Yan, and M. Wulkow. Molecular Parameters of Hyperbranched Polymers Made by Self-Condensing Vinyl Polymerization. 1. Molecular Weight Distribution. *Macromolecules*, 30(23):7015–7023, 1997.

[111] W. Burchard. Solution Properties of Branched Macromolecules. *Polymer*, 143:113–194, 1999.

[112] A. M. Kasko, S. R. Grunwald, and C. Pugh. Effect of End Groups on the Thermotropic Behavior of Linear Poly[11-(4'-cyanophenyl-4"-phenoxy)undecyl acrylate]s Prepared by ATRP and Their Topological Blends. *Macromolecules*, 35(14):5466–5474, 2002.

[113] A. M. Kasko and C. Pugh. Solution Behavior of Topological Isomers of Poly[11-(4'-cyanophenyl-4"-phenoxy)undecyl acrylate]s Prepared by Atom Transfer and Conventional Radical Polymerizations. *Macromolecules*, 37(13):4993–5001, 2004.

[114] K. Chaicharoen, M. J. Polce, A. Singh, C. Pugh, and C. Wesdemiotis. Characterization of linear and branched polyacrylates by tandem mass spectrometry. *Analytical and Bioanalytical Chemistry*, 392(4):595–607, 2008.

[115] M. Ciampolini and N. Nardi. Five-Coordinated High-Spin Complexes of Bivalent Cobalt, Nickel, and Copper with Tris(2-dimethylaminoethyl)amine. *Inorganic Chemistry*, 5(1):41–44, 1966.

[116] M. Schmidt, L. W. Riley, and I. Benz. Sweet new world: glycoproteins in bacterial pathogens. *Trends in Microbiology*, 11(12):554–561, 2003.

[117] D. Bontempo, K. L. Heredia, B. A. Fish, and H. D. Maynard. Cysteine-reactive polymers synthesized by atom transfer radical polymerization for conjugation to proteins. *Journal of the American Chemical Society*, 126(47):15372–3, 2004.

[118] D. Bontempo and H. D. Maynard. Streptavidin as a macroinitiator for polymerization: in situ protein-polymer conjugate formation. *Journal of the American Chemical Society*, 127(18):6508–9, 2005.

[119] C. K. Riener, G. Kada, and H. J. Gruber. Quick measurement of protein sulfhydryls with Ellman's reagent and with 4,4'-dithiodipyridine. *Analytical and Bioanalytical Chemistry*, 373(4-5):266–76, 2002.

[120] B. S. Lele, H. Murata, K. Matyjaszewski, and A. J. Russell. Synthesis of uniform protein-polymer conjugates. *Biomacromolecules*, 6(6):3380–7, 2005.

[121] W. Wang, H. Cao, G. Zhu, and P. Wang. A facile strategy to modify TiO_2 nanoparticles via surface-initiated ATRP of styrene. *Journal of Polymer Science Part A: Polymer Chemistry*, 48(8):1782–1790, 2010.

[122] K. L. Heredia, D. Bontempo, T. Ly, J. T. Byers, S. Halstenberg, and H. D. Maynard. In situ preparation of protein-"smart" polymer conjugates with retention of bioactivity. *Journal of the American Chemical Society*, 127(48):16955–60, 2005.

[123] B. Zhu, D. Lu, J. Ge, and Z. Liu. Uniform polymer-protein conjugate by aqueous AGET ATRP using protein as a macroinitiator. *Acta Biomaterialia*, 7(5):2131–2138, 2011.

[124] T. Masuko, A. Minami, N. Iwasaki, T. Majima, S.-I. Nishimura, and Y. C. Lee. Carbohydrate analysis by a phenol-sulfuric acid method in microplate format. *Analytical Biochemistry*, 339(1):69–72, 2005.

[125] P. Ascenzi, M. Gioia, G. Fanali, M. Coletta, and M. Fasano. Pseudo-enzymatic hydrolysis of 4-nitrophenyl acetate by human serum albumin: pH-dependence of rates of individual steps. *Biochemical and Biophysical Research Communications*, 424(3):451–5, 2012.

[126] K. L. Heredia, T. H. Nguyen, C.-W. Chang, V. Bulmus, T. P. Davis, and H. D. Maynard. Reversible siRNA-polymer conjugates by RAFT polymerization. *Chemical Communications*, 28:3245–3247, 2008.

[127] V. Bulmus. A new pH-responsive and glutathione-reactive, endosomal membrane-disruptive polymeric carrier for intracellular delivery of biomolecular drugs. *Journal of Controlled Release*, 93(2):105–120, 2003.

[128] J. T. Wilson, S. Keller, M. J. Manganiello, C. Cheng, C.-C. Lee, C. Opara, A. Convertine, and P. S. Stayton. pH-Responsive nanoparticle vaccines for dual-delivery of antigens and immunostimulatory oligonucleotides. *ACS Nano*, 7(5):3912–25, 2013.

[129] G. T. Zugates, D. G. Anderson, S. R. Little, I. E. B. Lawhorn, and R. Langer. Synthesis of poly(beta-amino ester)s with thiol-reactive side chains for DNA delivery. *Journal of the American Chemical Society*, 128(39):12726–34, 2006.

[130] J. D. Thomas and T. R. Burke. Application of a water-soluble pyridyl disulfide amine linker for use in Cu-free click bioconjugation. *Tetrahedron Letters*, 52(33):4316–4319, 2011.

[131] S. Ghosh, S. Basu, S. Thayumanavan, and S. Thayumanavan*. Simultaneous and Reversible Functionalization of Copolymers for Biological Applications. *Macromolecules*, 39(17):5595–5597, 2006.

[132] D. Li, Q. He, Y. Cui, and J. Li. Fabrication of pH-Responsive Nanocomposites of Gold Nanoparticles/Poly(4-vinylpyridine). *Chemistry of Materials*, 19(3):412–417, 2007.

[133] B. Liu, A. Kazlauciunas, J. T. Guthrie, and S. Perrier. One-Pot Hyperbranched Polymer Synthesis Mediated by Reversible Addition Fragmentation Chain Transfer (RAFT) Polymerization. *Macromolecules*, 38(6):2131–2136, 2005.

[134] L. Wong, C. Boyer, Z. Jia, H. M. Zareie, T. P. Davis, and V. Bulmus. Synthesis of versatile thiol-reactive polymer scaffolds via RAFT polymerization. *Biomacromolecules*, 9(7):1934–44, 2008.

[135] J. U. Baenziger and D. Fiete. Structural determinants of concanavalin A specificity for oligosaccharides. *Journal of Biological Chemistry*, 254(7):2400–2407, 1979.

[136] V. Sharma, V. R. Srinivas, P. Adhikari, M. Vijayan, and A. Surolia. Molecular basis of recognition by Gal/GalNAc specific legume lectins: Influence of Glu 129 on the specificity of peanut agglutinin (PNA) towards C2-substituents of galactose. *Glycobiology*, 8(10):1007–1012, 1998.

[137] J. E. Gestwicki, C. W. Cairo, L. E. Strong, K. A. Oetjen, and L. L. Kiessling. Influencing receptor-ligand binding mechanisms with multivalent ligand architecture. *Journal of the American Chemical Society*, 124(50):14922–14933, 2002.

[138] R. Meléndez, E. Meléndez-Hevia, and E. I. Canela. The fractal structure of glycogen: A clever solution to optimize cell metabolism. *Biophysical Journal*, 77(3):1327–32, 1999.

[139] J. A. Bohn and J. N. BeMiller. (1-3)-β-d-Glucans as biological response modifiers: a review of structure-functional activity relationships. *Carbohydrate Polymers*, 28(1):3–14, 1995.

[140] G. C.-F. Chan, C. W. Keung, and S. D. Man-Yuen. The effects of β-glucan on human immune and cancer cells. *Journal of Hematology & Oncology*, 2, 2009.

[141] D. M. Ratner, E. W. Adams, J. Su, B. R. O'Keefe, M. Mrksich, and P. H. Seeberger. Probing protein-carbohydrate interactions with microarrays of synthetic oligosaccharides. *ChemBioChem*, 5(3):379–382, 2004.

[142] J. D. Reuter, A. Myc, M. M. Hayes, Z. Gan, R. Roy, D. Qin, R. Yin, L. T. Piehler, R. Esfand, D. A. Tomalia, and J. R. Baker. Inhibition of viral adhesion and infection by sialic-acid-conjugated dendritic polymers. *Bioconjugate Chemistry*, 10(2):271–278, 1999.

[143] Y. Chen, G. Chen, and M. H. Stenzel. Synthesis and Lectin Recognition of Glyco Star Polymers Prepared by "Clicking" Thiocarbohydrates onto a Reactive Scaffold. *Macromolecules*, 43(19):8109–8114, 2010.

[144] M. C. Carroll. The complement system in regulation of adaptive immunity. *Nature Immunology*, 5(10):981–6, 2004.

[145] M. Turner. The role of mannose-binding lectin in health and disease. *Molecular Immunology*, 40(7):423–429, 2003.

[146] I. J. Goldstein, C. M. Reichert, A. Misaki, and P. A. Gorin. An "extension" of the carbohydrate binding specificity of concanavalin A. *Biochimica et biophysica acta*, 317(2):500–504, 1973.

[147] J.-B. du Prel, G. Hommel, B. Röhrig, and M. Blettner. Confidence interval or p-value?: part 4 of a series on evaluation of scientific publications. *Deutsches Ärzteblatt international*, 106(19):335–9, 2009.

[148] A. A. Bulgakov, M. G. Eliseikina, I. Y. Petrova, E. L. Nazarenko, S. N. Kovalchuk, V. B. Kozhemyako, and V. A. Rasskazov. Molecular and biological characterization of a mannan-binding lectin from the holothurian Apostichopus japonicus. *Glycobiology*, 17(12):1284–1298, 2007.

[149] Y. Hashimoto, M. Suzuki, P. R. Crocker, and A. Suzuki. A streptavidin-based neoglycoprotein carrying more than 140 GT1b oligosaccharides: quantitative estimation of the binding specificity of murine sialoadhesin expressed on CHO cells. *Journal of Biochemistry*, 123(3):468–478, 1998.

[150] S. Petersen, S. Thiel, L. Jensen, R. Steffensen, and J. Jensenius. An assay for the mannan-binding lectin pathway of complement activation. *Journal of Immunological Methods*, 257(1-2):107–116, 2001.

[151] H. R. Colten, T. Borsos, and H. J. Rapp. Reversible loss of activity of the first component of complement (C'1) as a function of ionic strength. *Journal of Immunology*, 100(4):799–807, 1968.

[152] H. Yang and W. J. Kao. Synthesis and characterization of nanoscale dendritic RGD clusters for potential applications in tissue engineering and drug delivery. *International Journal of Nanomedicine*, 2(1):89–99, 2007.

[153] N. L. Perillo, M. E. Marcus, and L. G. Baum. Galectins: versatile modulators of cell adhesion, cell proliferation, and cell death. *Journal of Molecular Medicine*, 76(6):402–412, 1998.

[154] G. Ragupathi, F. Koide, P. O. Livingston, Y. S. Cho, A. Endo, Q. Wan, M. K. Spassova, S. J. Keding, J. Allen, O. Ouerfelli, R. M. Wilson, and S. J. Danishefsky. Preparation and evaluation of unimolecular pentavalent and hexavalent antigenic constructs targeting prostate and breast cancer: a synthetic route to anticancer vaccine candidates. *Journal of the American Chemical Society*, 128(8):2715–2725, 2006.